MOBILIZATION OF OXYANION FORMING TRACE ELEMENTS FROM FLY ASH
BASED GEOPOLYMER CONCRETE

by

Olanrewaju Abdur-Rahman Sanusi

A dissertation submitted to the faculty of
The University of North Carolina at Charlotte
in partial fulfillment of the requirements
for the degree of Doctor of Philosophy in
Infrastructure and Environmental Systems

Charlotte

2012

Approved by:

_____
Dr. Vincent Ogunro

_____
Dr. John Daniels

_____
Dr. Brett Tempest

_____
Dr. Miguel Pando

_____
Dr. Ertunga Ozelkan

_____
Dr. Carlos Orozco

ABSTRACT

OLANREWAJU ABDUR-RAHMAN SANUSI. Mobilization of oxyanion forming trace elements from fly ash based geopolymer concrete (Under the direction of Dr. VINCENT OGUNRO)

The suitability of fly ash based geopolymer concrete as a replacement for ordinary Portland cement (OPC) concrete depends on the mobility of elements from the material. Due to the alkaline nature of geopolymer concrete, there is a potential for the release of oxyanion forming elements such as As, Cr and Se which are characterized by their high mobility in the alkaline environment. In this study, geopolymer concretes were produced with varying amount of hydrated lime and subjected to tests that include pH dependence test, Dutch availability test, tank test, water leach test, mineralogical, microstructural analysis and geochemical modeling using PHREEQC/PHREEPLOT. The results of this study confirmed that As and Se and other oxyanion forming elements exhibit higher mobility in the alkaline pH. Further investigation using the Dutch availability and tank test showed that As have the highest mobility from all the geopolymer concretes. It also reveals that the mobility of As and Se reduces with time as the element becomes depleted in the matrix. Mobility of the two elements was observed to be lowest in the geopolymer concrete with 1% hydrated lime which suggest that the addition of 1% hydrated lime lead to reduction in the mobility of As and Se. Cr on the other hand have the same low mobility from all the geopolymer, this suggest that hydrated lime addition has no effect on the mobility the element. Finally, PHREEQC/PHREEPLOT identifies species of leached elements as As (5), Se (6) and Cr (6). These species of As and Se have low toxicity whereas the species of Cr is of the more toxic form, but it is released in level far below the Maximum Concentration Level (MCL) set by EPA for drinking water.

DEDICATION

This dissertation is dedicated to my parents, siblings and friends.

ACKNOWLEDGMENTS

My sincere gratitude goes to my advisor, Dr. Vincent Ogunro for his guidance, valuable suggestions and encouragement throughout my doctoral studies. I would like to extend my appreciation to members of my committee – Drs. Brett Tempest, John Daniels, Miguel Pando, Ertunga Ozelkan and Carlos Orozco – for their time, support and constructive comments.

A big thank you to Marge Galvin-Karr of Duke Energy laboratory for her assistance in analyzing all leachates from my leaching tests. Many thanks to Claire Chadwick for giving me the freedom to impose on her for assistance with analysis of samples and use of instruments at the department of Geography and Earth Sciences. Special thanks to Mike Moss for his help in various ways in the workshop. I would also like to thank Alec Martin for teaching me how to use the XRD and SEM. Sincere appreciation to Elizabeth Scott and Erin Morant for their assistance with various administrative tasks related to my study.

My deepest appreciation is due to my parents, siblings (Diran, Titi, Tope, Tayo, Iyabo, Latifah and Gary), lab buddies (Yogesh and Ari), friends (Onyewuchi, Femi, Appolo, Ayoola, Amanda, Toyin) and others too numerous to mention. Thank you all for having confidence and believing in me. Finally, I acknowledge the support of the department of civil and environmental engineering and the graduate school for awarding me the graduate assistant support plan (GASP) fellowship.

TABLE OF CONTENTS

LIST OF FIGURES

LIST OF TABLES

LIST OF ABBREVIATIONS

AMSCD	American mineralogist crystal structure database
ANC	acid neutralization capacity
As	arsenic
ASTM	American society for testing and materials
BNC	base neutralization capacity
CA	coarse aggregate
CASH	calcium aluminosilicate hydrate
Cd	cadmium
CFA	coal fly ash
Cr	chromium
Cs	cesium
CSH	calcium silicate hydrate
Cu	copper
De	effective diffusion coefficient
DI	deionized water
DL	detection limit
EDX	energy dispersive x-ray spectroscopy
ELT	equilibrium leach test
EP Tox	extraction procedure toxicity test
FA	fine aggregate
Fe	iron
Gt	gigaton

Hg	mercury
IC	ion chromatography
ICP-AES	inductively coupled plasma atomic emission spectrometer
ICP-MS	inductively coupled plasma mass spectrometer
L/S	liquid to solid ratio
LOI	loss on ignition
LX	leachability index
MCL	maximum contaminant level
MEP	multiple extraction procedure
Mo	molybdenum
MPa	megapascal
Mt	megaton
NEN	Netherlands standardization institute
OPC	ordinary Portland cement
Pb	lead
ppm	part per million
PS	polysialate
PSD	particle size distribution
PSDS	polysialate disiloxo
PSS	polysialate siloxo
RCA	recycled concrete aggregate
Sb	antimony
SCM	supplementary cementitious materials

Se	selenium
SEM	scanning electron microscope
SF	silica fume
SI	saturation index
SPLP	synthesis precipitation leach procedure
TCLP	toxicity characteristics leaching procedure
USEPA	united states environmental protection agency
V	vanadium
W	tungsten
WLT	water leach test
XRD	x-ray diffraction
XRF	x-ray fluorescence
Zn	zinc

CHAPTER 1: INTRODUCTION

This chapter presents the main research problem addressed in this PhD dissertation together with the main research objectives and hypotheses. The chapter starts with a brief background section related to concrete and geopolymer concrete to provide the reader with the right context used to formulate the problem statement and associated objectives, hypotheses and work plan.

1.1   Background

Concrete is the most widely used material in the world after water (van Oss and Padovani, 2002; Hardjito and Rangan, 2005; Damtoft et al., 2008), and a very important construction material used in many civil engineering applications such as buildings, sidewalks, bridges, dams and industrial plants. The material is typically manufactured from components that include approximately 65% to 80% aggregates (fine and coarse), between 10% to 12% cement, a maximum of 21% water and between 0.5% to 8% air content (van Oss and Padovani, 2003; Quiroga and Fowler, 2004). All these components are in percentage by weight of the total. Cement is the major component of concrete because it is the binding agent holding the aggregates together thereby giving the conglomerate its characteristic strength and durability. Fine aggregates utilized in concrete are typically natural sand or fine crushed stones with particle size that range from 150 µm to a maximum of 4.75 mm while coarse aggregates are typically natural

gravel or granitic stones with a minimum particle size of 4.75 mm (Badur and Chaudhary, 2008).

Aggregates are a very important component of the concrete mix that has a great effect on the resulting concrete physical properties. In order to obtain concrete of specific characteristics, other components such as superplasticizers and retarders can be added during the mixing process to respectively improve the workability and reduce the setting time of the concrete (Badur and Chaudhary, 2008). Ordinary Portland Cement (OPC) is the most commonly used type of cement; it sets and hardens in the presence of water due to hydration reaction. In making construction grade concrete, cement usage can typically be either 100% OPC or a mixture of OPC and other supplementary cementitious materials (SCM) such as steel slag and fly ash (Struble and Godfrey, 2004).

Manufacturing of OPC involves mining limestone and shale, heating the mixture (limestone and shale) in a rotary kiln to convert the limestone into lime via a process known as calcination, and finally grinding the resulting cement clinker with gypsum (Struble and Godfrey, 2004). This production process is very energy intensive and involves the release of greenhouse gases such as CO_2 and N_2O into the atmosphere. For every metric ton of cement produced, there is approximately 0.8 metric ton CO_2 released to the atmosphere (Gartner, 2004). An estimated 80.2 megatons (Mt) CO_2 per year were generated from cement production in the United States between 1996-2000 (van Oss and Padovani, 2002). Apart from the emission of CO_2, other environmental issues associated with cement production are dust, noise, and vibration.

One way of reducing CO_2 emission associated with concrete usage is to reduce the amount of cement utilized in making concrete by increasing the use of SCM

(Bremner, 2001). There have been up to 35% replacement of OPC in concrete with SCM such as fly ash (Tempest, 2010), which is a pozzolan that reacts with $Ca(OH)_2$ from OPC hydration to form additional calcium silicate hydrate (CSH) gel thereby improving the later day strength of concrete (Hardjito and Rangan, 2005). Most of the fly ash used as SCM in concrete comes from coal fired power plants. According to the American Coal Ash Association, about 72 million tons of coal fly ash is produced in the United States annually, with only 44% being re-utilized in various applications and the remaining disposed in landfills (ACAA, 2008). This huge abundance of fly ash created an opportunity for achieving high replacement of OPC in concrete with the material.

Coal fly ash (CFA) is a highly heterogeneous material that is enriched with major elements such as silicon (Si), aluminum (Al), calcium (Ca) and iron (Fe) accounting for nearly 90% of the fly ash composition (Jankowski et al., 2006; Jegadeesan et al., 2008; Izquierdo and Querol, 2011). Other elements present in CFA include trace elements such as antimony (Sb), arsenic (As), boron (B), cadmium (Cd) chromium (Cr), cobalt (Co), lead (Pb), selenium (Se), nickel (Ni), zinc (Zn) and copper (Cu) which account for a small percentage of the bulk composition (Dogan and Kobya, 2006; Izquierdo and Querol, 2011). The composition of elements present in CFA varies greatly mainly due to the coal source, particle size of the coal, combustion process and type of ash collector (Jankowski et al., 2006; Jegadeesan et al., 2008). The presence of the high content of Si, Al and Ca makes coal fly ash a suitable SCM and source aluminosilicate material for synthesis of alkali activated binder. But the presence of trace elements that are susceptible to leaching from the material into the environment may impact the suitability of coal fly ash for beneficial reuse (Jegadeesan et al., 2008).

In the 1970s, Prof Davidovits pioneered the development of a new binder termed "geopolymer" (Davidovits, 1991) which can completely replace Portland cement in concrete. This new binder is an inorganic three-dimensional (3D) polymeric material made from the reaction of any material rich in silica and alumina (aluminosilicate) with a strong alkaline solution (activator) that contains sodium silicate and or sodium hydroxide (Duxson et al., 2007; Komnitsas and Zaharaki, 2007; Provis and van Deventer, 2009). Aluminosilicate materials such as metakaolin, kaolinite, steel slag, coal fly ash and rice husk ash also have been successfully used in the production of geopolymer (Nazari et al., 2011).

Studies have shown that geopolymer possesses excellent properties that include high compressive strength, acid and heat resistance, low shrinkage and the potential or ability to immobilize hazardous contaminants within its matrix (Davidovits, 1991; Komnitsas and Zaharaki, 2007; Tempest, 2010), making it a suitable replacement for cement in concrete and waste stabilization. In the past years, there has been rapid progress in the development of geopolymer from coal fly ash, research groups from Curtin University of Technology and the University of Melbourne in Australia which are leading in this area of research. Hardjito and Rangan (2005) from Curtin University of Technology pioneered the production of concrete specimens using fly ash based geopolymer as binder instead of OPC. In 2008, our materials research team at the University of North Carolina at Charlotte led by Dr. Brett Tempest with support of Drs. Janos Gergely and Vincent Ogunro started work on fly ash based geopolymer concrete. The majority of the work to date completed focused on engineering characterization of

geopolymer concrete for structural components like columns, reinforced beams, and large scale girders (Tempest, 2010).

Most of the research that has been done on geopolymer paste, mortar and concrete to date has been extensively on understanding their chemistry and reaction mechanism, curing conditions, durability, mineralogy, microstructure and other engineering properties. In contrast, there has been very little environmental related characterization such as the leaching of potentially hazardous elements.

1.2   Problem Description

The limited environmental characterization conducted on geopolymer have shown that potentially toxic elements can leach out when the material is exposed to aqueous environment (Bankowski et al., 2004; Xu et al., 2006; Izquierdo et al., 2009), which might be harmful to human and the environment when released in high concentrations. The majority of these environmental characterization have focused primarily on cationic elements (Xu et al., 2006; Izquierdo et al., 2009) such as lead (Pb), copper (Cu), mercury (Hg), cesium (Cs), zinc (Zn), cadmium (Cd) and iron (Fe), and very limited study on elements that form oxyanionic species (Bankowski et al., 2004; Izquierdo et al., 2010) such as arsenic (As), selenium (Se), chromium (Cr), vanadium (V), antimony (Sb), molybdenum (Mo), and tungsten (W) which are characterized by their high mobility at neutral to alkaline pH.

Due to the alkaline nature of geopolymer, and the known high mobility of oxyanion forming elements (As, Cr, Se) at high pH, their potential release from geopolymer make them elements of great environmental concern. In order to demonstrate the suitability of fly ash based geopolymer concrete as an everyday construction material,

there is a need to minimize the mobility of these elements during the service life and at end of life of a geopolymer concrete product.

1.3   Significance and Benefit of the Study

Oxyanion forming trace elements (e.g As, Cr, Se) are toxic at very low concentration thereby making their potential immobilization or decreased mobility through addition of lime an important factor in the determination of geopolymer as a safe alternative to cement in construction and waste stabilization. The success of this research would add to the knowledge of reducing any concern regarding potential environmental impact of geopolymer which has not been sufficiently investigated by many researchers, and would produce important parameters for life cycle analysis that could important in selecting the most environmentally responsible manner of utilizing the product.

1.4   Research Goal and Objectives

The overall goal of the research is to assess/characterize the leaching mechanisms of oxyanion forming trace elements from coal fly ash based geopolymer concrete/mortar and investigate the effect of additives such as lime on reduction of element mobility from the geopolymer concrete by rendering the element partially insoluble. The specific objectives of the research are:

1. To determine the release of oxyanion elements (As, Cr, Se) from fly ash based geopolymer concrete under service life (monolithic) and end of service life (granular) conditions using appropriate tests.

2. To assess the potential to decrease mobility, or even total immobilization of oxyanion elements (As, Cr, Se) in geopolymer concrete by means of using hydrated lime as an admixture.

3. To determine the maximum amount of oxyanion forming elements that would be released under the worst case scenario when the material is pulverized.

4. To determine if there is formation of calcium containing mineral phases, calcium precipitates or calcium metalates in the produced geopolymer concrete.

5. To identify probable mechanisms responsible for immobilization of the oxyanion forming elements (if there is any immobilization).

6. To determine the species of the oxyanion elements (As, Cr, Se) released from fly ash based geopolymer concrete and their potential environmental impacts.

1.5   Research Hypotheses

In conducting this study, the following hypotheses were formulated to address the goal and specific objectives of the research:

1. Oxyanion elements (As, Cr, Se) are present in leachates from fly ash based geopolymer concrete.

2. Oxyanion forming trace elements exhibit different leaching behavior than other elements that are leached from the alkaline fly ash based geopolymer.

3. Standard leaching test methods conducted at a neutral pH are adequate for predicting the leaching of oxyanion forming elements.

4. Calcium containing mineral phases such as ettringite, hydrocalumite, monosulfoaluminate, calcium metalates and calcium silicate hydrates (CSH) are effective for immobilizing oxyanion forming elements via ion substitution.

5. Leaching of these oxyanion forming elements can be mitigated by the addition of extra calcium in the form of lime during the geopolymer synthesis, which would lead to the formation of oxyanion substituted calcium containing mineral phases

in addition to the geopolymer phase without affecting the durability of the geopolymer.

1.6   Scope of Work

This dissertation focuses mainly on geopolymer concrete produced from class F fly ash (low calcium), silica fume (as the additional silica source), hydrated lime $(Ca(OH)_2)$ as source of additional calcium and aggregates that make up not more than 70% of the concrete mix that has a target 28 days compressive strength of 41 MPa (6000 psi). The study was based solely on laboratory investigation that focuses on the service life condition (monolith state) and end of life condition (granular state) of the geopolymer. Laboratory speciation analysis was not performed to determine the species of the elements leached from the geopolymer concrete. Geochemical modeling using PHREEQC/PHREEPLOT was employed in predicting the species of the elements in the leachates.

1.7   Organization of the Dissertation

The dissertation is organized into nine chapters. Chapter 1 describes the impetus for the study of the mobility of oxyanion forming trace elements from fly ash based geopolymer concrete. Chapter 2 presents review of relevant literature on geopolymer and leaching of elements. Topics covered in this chapter include the historical development of geopolymer as an alternative binder, source material used for geopolymer synthesis, and mobility/immobilization of the oxyanion forming trace elements.

Chapter 3 describes the research approach used, the starting materials, summary of the experimental methods, preliminary investigation completed, procedures for quality assurance and quality control, and statistical tools employed for data analysis.

Geopolymer concrete synthesis is presented in Chapter 4. The chapter also describes sample preparation methods used in the study. Chapter 5 focuses on materials characterization such as particle size distribution (PSD), X-Ray fluorescence (XRF) analysis, and acid/base neutralization capacity (ANC/BNC). The entire laboratory leaching test methods employed and results obtained are presented in Chapter 6.

Chapter 7 contains the mineralogical and microstructural characterization of the starting materials and produced geopolymer concrete samples using X-Ray diffraction (XRD) and scanning electron microscope (SEM)/energy dispersive spectroscopy (EDX) analysis. Chapter 8 describes the application of PHREEQC/PHREEPLOT to predict the speciation of oxyanion elements from the geopolymer concrete leachates. The last chapter of the dissertation, Chapter 9 presents the conclusions drawn from this investigation and presents recommendations for future research work.

CHAPTER 2: LITERATURE REVIEW

2.1   Historical Development of Geopolymer as Alternative Binder

Portland cement has been the dominant binder used in concrete and mortar since it was developed by Joseph Aspdin in the early 19th century. It is the most abundant building material due to its versatility and economic values, with annual worldwide production estimated to be around 3 gigatons (Gt) (Juenger et al., 2010). However, there are environmental issues such as huge energy consumption, particulate emission and enormous release of CO_2 arising from the manufacturing of this binder. Infact, it is considered one of the largest industrial emitter of CO_2, a greenhouse gas that causes global warming (van Oss and Padovani, 2002). With the growing concern about threats posed by increased release of CO_2 to the atmosphere, attempts have been made at reducing the percentage of cement used in making concrete by replacing them with SCM such as coal fly ash, ground blast furnace slag and silica fume in the hope of reducing the overall environmental impact (Juenger et al., 2010). Researchers also seek to find alternative binders with reduced energy use and low CO_2 emission that can completely replace cement which led to the development of alkali activated binders.

Alkali activated binders were considered as an alternative binder due to their durability, low energy and reduced CO_2 emission, hence resulting in reduced environmental impacts. These binders are sometimes referred to as inorganic polymer, geopolymer, alkali activated cement, geocement and soil silicate, with geopolymer being

the most commonly used name (Duxson et al., 2007; Komnitsas and Zaharaki, 2007; Juenger et al., 2010). They are produced from the reaction of aluminosilicate raw materials with an alkaline solution.

Although the term geopolymer was coined by Joseph Davidovits in the 1970s to describe an alkali activated binder developed from metakaolin with the hope of producing a fire resistant plastic material (Davidovits, 1991), similar alkali activated binders have been described earlier by Purdon in the 1940s and Glukhovsky in the 1950s (Roy, 1999; Komnitsas and Zaharaki, 2007; Škvára, 2007; Pacheco-Torgal et al., 2008b). The aluminosilicate source material used by most of the earlier researchers was ground blast furnace slag. It was reported that activation of blast furnace slag led to an alkali activated systems that contains both calcium silicate hydrate gel (CSH) and aluminosilicate phase since the blast furnace slag is rich in calcium (Komnitsas and Zaharaki, 2007), while the activation of metakaolin produced only a zeolite-like aluminosilicate phase (Sakulich, 2009).

2.2   Basic Concept of Geopolymer

As discussed in the previous section, geopolymer is a generic name used to describe all alkali activated binders synthesized from the reaction of an aluminosilicate source with a strong alkali activating solution that contains a mixture of Na_2SiO_3 and NaOH or KOH solution (Pacheco-Torgal et al., 2008a). The aluminosilicate material is dissolved by the alkali solution which also provides additional silicate required for the geopolymerization process. Silica fume is sometimes used instead of Na_2SiO_3 as the source of additional reactive silica (Tempest, 2010). Geopolymer gel formation is achieved by the application of mild heat at a temperature less than $100^{\circ}C$.

Many curing regime have been implemented for geopolymer, Kong and Sanjayan (2010) cured geopolymer specimens at ambient temperature for 24 hours before oven curing at 80°C for additional 24 hours. Similar curing regime was employed by Tempest (2010) but the temperature of the oven was set to 75°C. Perera at al. (2007) used a curing schedule that involves oven curing of several specimens at 22°C, 40°C, 60°C, and 80°C in order to investigate the effect of temperature on geopolymerization and reported that at higher temperature, the chemical reactions are accelerated leading to the formation of higher strength geopolymer concrete. The optimal curing temperature for the formation of geopolymer was reported to be 75°C (Pacheco-Torgal et al., 2008a).

2.2.1   Source Materials for Geopolymer Synthesis

Metakaolin, granulated blast furnace slag, and coal fly ash are the most commonly used source materials in geopolymer synthesis. Metakaolin is obtained by the calcination of kaolinite at high temperature (Cioffi et al., 2003) while blast furnace slag is a byproduct of iron production. Coal fly ash on the other hand is obtained as a byproduct of the combustion process in coal fired power plants.

Komnitsas and Zaharaki (2007) reported that geopolymer made from metakaolin are too soft for construction purposes due to high porosity as a result of high water requirement, thereby hindering further use of this starting material.

Blast furnace slag based geopolymer on the other hand have been reported as containing calcium silicate hydrates (CSH) and calcium aluminosilicate hydrates (CASH) in addition to the geopolymer phase as a result of the high content of calcium in the starting material (Pacheco-Torgal et al., 2008b).

Fly ash based geopolymer provides significant advantage over other alternative binders (Provis et al., 2009) due to the cheaper cost associated with coal fly ash when compared to other source material like metakaolin which resulted in porous and soft geopolymer.

In recent years, many researchers have focused on using coal fly ash as the main aluminosilicate source for geopolymer synthesis due to its high silica content and its abundance as a waste product. But due to variability of fly ash as a result of characteristics such as their amorphous content, chemical composition, fineness, calcium content and unburned organic content, producing geopolymer of consistent and acceptable quality might be a big challenge (Tempest, 2010). These led to the investigation of coal fly ash characteristics that can make them suitable for producing geopolymer of acceptable quality. Khale and Chaudhary (2007) reported that fineness is one important characteristic that affect strength development in geopolymer. Tempest (2010) stated that loss on ignition (LOI), chemical composition, calcium and amorphous content of the coal fly ash are also important characteristics that contribute to the quality of the produced geopolymer. It is thus necessary to select coal fly ash that possessed these characteristics that would lead to an acceptable geopolymer.

Coal fly ash is classified based on chemical composition as either Class F and Class C ash (ASTM, 2008) as shown in TABLE 2-1. Class C ash are referred to as high calcium ash because they contain more than 20% CaO, a minimum of 50% $SiO_2 + Al_2O_3$ $+Fe_2O_3$ and self-cementing properties while Class F ash are referred to as low calcium ash due to the low content of CaO (<10%), a minimum of 70% $SiO_2 + Al_2O_3 + Fe_2O_3$ and non self-cementing properties (ASTM, 2008). Class F fly ash is mostly used in the

production of geopolymer due to higher content of silica and alumina and low amount of CaO since the amount of CaO in the starting material significantly affect the properties of hardened geopolymer (Diaz et al., 2010). Higher content of CaO contained in Class C fly ash would alter the microstructure of the produced geopolymer leading to formation of more hydration products such as CSH instead of the geopolymer phase (Temuujin et al., 2009). TABLE 2-2 shows the typical chemical composition of the two main types of coal fly ash. For comparison purpose, this table also shows composition of Portland cement

TABLE 2-1: Chemical requirement for fly ash classification (% mass)

	Class F	Class C
$SiO_2 + Al_2O_3 + Fe_2O_3$, (min %)	70	50
SO_3, (max %)	5.0	5.0
Moisture content, (max %)	3.0	3.0
Loss on ignition (LOI), (max %)	6.0	6.0
Available alkali as Na_2O, (max%)	1.5	1.5

Source: ASTM (2008)

TABLE 2-2: Typical chemical composition of coal fly ash and cement (%)

	SiO_2	Al_2O_3	Fe_2O_3	CaO	MgO	SO_3
Class F	55	26	7	9	2	1
Class C	40	17	6	24	5	3
Portland cement	23	4	2	64	2	2

Source: ACAA (2003)

The total amount of some trace elements found in typical coal fly ash is presented in TABLE 2-3.

TABLE 2-3: Typical total amount of some trace elements present in CFA

element	mg/kg
As	136.2
B	900
Be	13.4
Cd	0.78
Co	50
Cr	198.2
Cu	112.8
Ni	120.6
Pb	68.2
Sb	6
Se	10.26
V	295.7
Zn	210

Source: Iwashita et al. (2007)

2.2.2   Chemistry and Reaction Mechanisms

Irrespective of the aluminosilicate source, activating solution or the curing conditions used during geopolymer synthesis, it is believed that the reaction mechanism involved in geopolymer formation is the same. This reaction mechanism can be grouped into three separate but interrelated stages that include dissolution of the aluminosilicate source by the high alkaline solution (MOH) where M^+ is the alkali metal such as Na^+ or

K^+, followed by reorientation/reorganization of the dissolved species and later polycondensation to form the hardened geopolymer (Xu and Van Deventer, 2000; Tempest, 2010). FIGURE 2-1 shows a simplified representation of the reaction mechanisms involved in geopolymer synthesis.

Dissolution of the aluminosilicate is believed to be initiated by the presence of hydroxyl ion (OH^-) from the alkali hydroxide, leading to the production of aluminate and silicate monomers (Komnitsas and Zaharaki, 2007). Production of these monomers is strongly dependent on the reactivity of the source aluminosilicate material, type and amount of the alkali hydroxide used. Reactivity of aluminosilicate material used in geopolymer synthesis decreases in the following order: metakaolin > slag> fly ash> kaolin (Panagiotopoulou et al., 2007; Tempest, 2010). According to Komnitsas and Zaharaki (2007), higher amount of hydroxyl ions facilitate the production of different silicates and aluminate species which would lead to further geopolymerization.

During the reorientation stage, free aluminate and silicate monomers in addition to silicate present in the activation solution come together to form oligomers of varying polymeric structure. These polymeric units then undergo polycondensation reaction in which they are joined together by oxygen bond formed from the reaction of adjacent hydroxyl ions, leading to the formation of the rigid oxygen bonded silica and alumina tetrahedral structure of geopolymer.

The reaction mechanism revealed that the alkali hydroxide (NaOH or KOH) act as catalyst that aid the dissolution and condensation stages. Most of the water is expelled during the high temperature curing since they are not actually involved in geopolymer formation (Khale and Chaudhary, 2007).
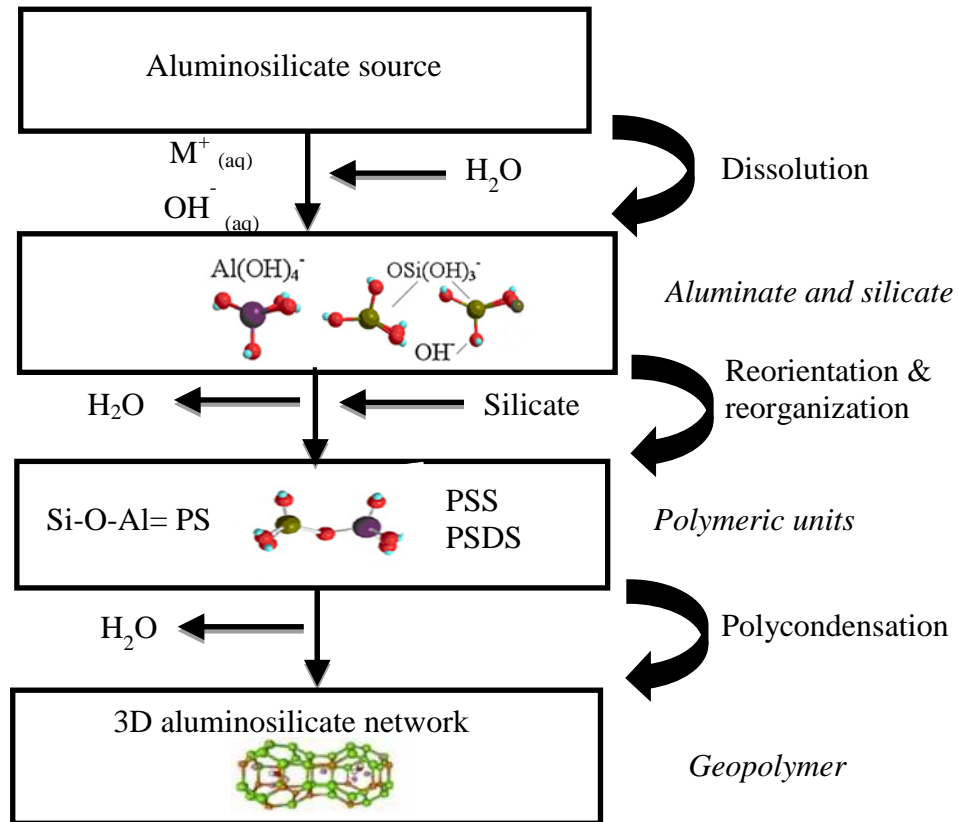
FIGURE 2-1: Simplified representation of geopolymer reaction mechanism.
Adapted from Duxson et al. (2007) and Yao et al. (2009)

2.2.3   Structure of Geopolymer

Geopolymer structure as suggested by Davidovits is a poly(sialate) network consisting of silica (SiO_2) and alumina (Al_2O_3) tetrahedral connected together by sharing oxygen atoms (FIGURE 2-2). Sialate is an abbreviation for silicon-oxo-aluminate (Si-O-Al) which form the basic polymeric precursor (Komnitsas and Zaharaki, 2007). Structure of the polymeric precursor formed depends on the ratio of silica to alumina (Si/Al) in the starting materials and can be classified according to this ratio. FIGURE 2-2 shows an illustration of the three polymeric structures that form geopolymers.
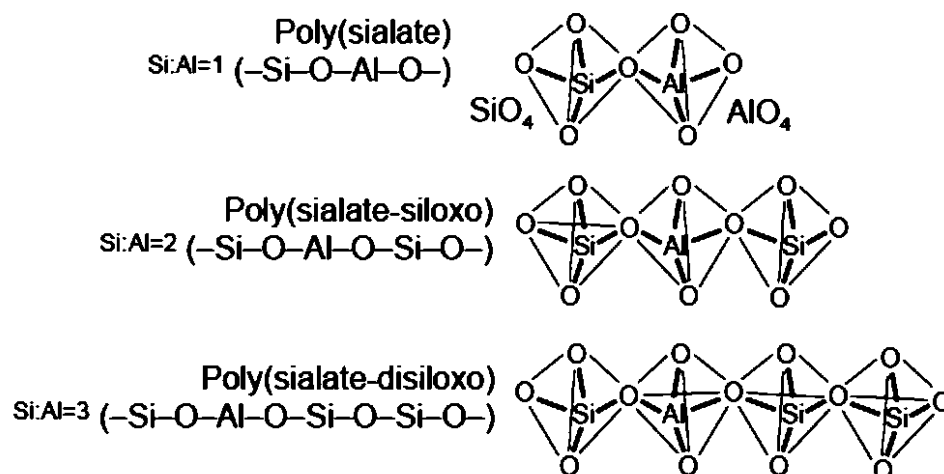
FIGURE 2-2: Polymeric precursor that form geopolymers.(Škvára, 2007)

Higher amount of silicate is required to form the higher order poly(sialate-siloxo) and poly(sialate-disiloxo) structure. Increase in the Si/Al ratio can be achieved by the addition of extra reactive silica using Na_2SiO_3 or silica fume in order to form these precursors. The polymeric precursors form chain and ring network united by Si-O-Al bridges with the silicon and aluminum atoms in 4-fold coordination with oxygen. Metallic cations such as K and Na help keep the formed geopolymer structure neutral by balancing the charge of Al atoms present in the structure. FIGURE 2-3 shows the conceptual model of sodium-poly(sialate-siloxo) (Na-PSS) geopolymer.

Equation 2.1 shows the empirical formula that can be used to characterize the formed geopolymer structure (Komnitsas and Zaharaki, 2007; Pacheco-Torgal et al., 2008a).

$$M_n [-(SiO_2)_z-AlO_2]_n .wH_2O \qquad (2.1)$$

Where M is the alkali cation, n is the degree of polycondenation, z is 1, 2 or 3, and $w \leq 3$.
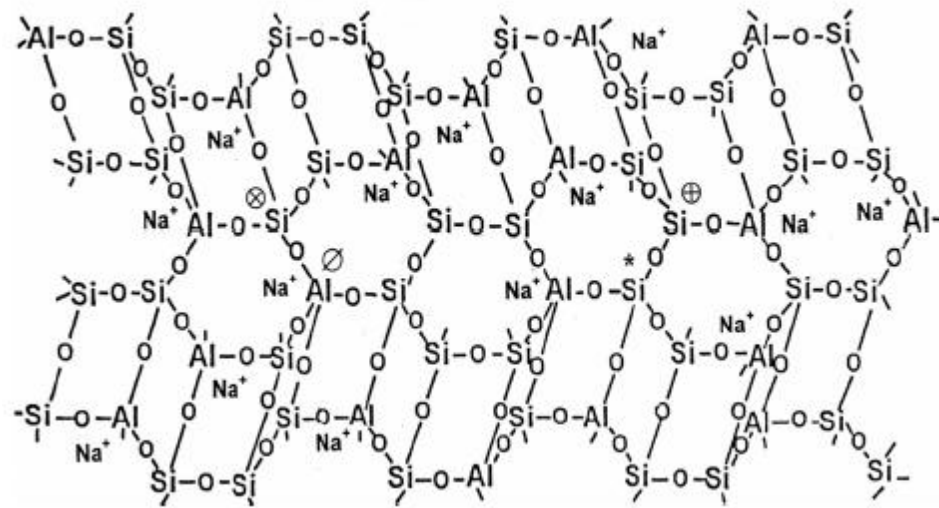
FIGURE 2-3: Conceptual structure of Na-PSS geopolymer (Škvára, 2007)

2.4   Characteristics and Application of Geopolymer

A lot of researchers have extensively studied the physical and mechanical properties of geopolymer such as compressive strength, creep, freeze-thaw resistance, permeability, thermal stability and shrinkage (Subaer, 2004; Hardjito and Rangan, 2005; Rangan, 2009; Tempest, 2010) that make the material a viable alternative in a wide application area. According to some studies, geopolymer concrete can reach 28 days compressive strengths ranging between 70 MPa (10,000 psi) to 100 MPa (14,000psi) (Komnitsas and Zaharaki, 2007; Zhang et al., 2008; Tempest, 2010). Somna et al. (2011) observed that the compressive strength of the material increases with age which is similar to the strength development in Portland cement. Result of creep and shrinkage test performed to assess the long term performance of geopolymer showed that the material undergo low creep and very little drying shrinkage of about 100 microstrain (μstrain) after one year (Khale and Chaudhary, 2007; Rangan, 2008), and can withstand heat of up to 800°C (Hardjito and Tsen, 2008). Sun (2005) observed that geopolymer does not show

any mass loss after about 300 freeze-thaw cycles, thus having a better freeze-thaw performance than Portland cement. Permeability of the material was found to be between $10^{-9} - 10^{-12}$ cm/s (Giannopoulou and Panias, 2007) which happens to be a very low value when compared to other cementitious material.

Due to the excellent properties possessed by geopolymer, the material has been employed in applications that include thermal insulation, high strength concrete, and hazardous waste management (Davidovits, 1991; Sun, 2005). Precast structures like railway sleepers, sewer pipes, box culverts and reinforced beams have been produced from geopolymer (Lloyd and Rangan, 2010; Tempest, 2010). Other reported areas of geopolymer application is in waste encapsulation, high strength concrete, thermal insulation and fire protection of structures (Davidovits, 1991; Provis and van Deventer, 2009). To demonstrate the environmental compatibility of geopolymer in the different areas of applications, leaching of environmentally relevant trace elements are usually studied but there are not too many studies. The following subsection summarizes relevant leachability studies found in the literature.

2.5   Background on Leaching and Mobility of Elements

Leaching tests are techniques used to investigate environmental properties or characteristics of any material, which can also be used for geopolymer. Leaching is a process where constituents present in a solid material dissolves into the pore water of the material when that material is in contact with an aqueous media. The liquid that contains the released constituent is called the leachate. Some factors such as amount of liquid that get in contact with the solid (L/S ratio), solubility of the elements, adsorption of the elements, pH of the pore water, state of the material, redox conditions and reaction

kinetics can potentially affect leaching from any material (Bin-Shafique, 2002; Schuwirth and Hofmann, 2006; Das, 2008).

There are a number of standard leaching test methods that have been developed to assess mobility of elements from solid materials. A good understanding of the material and their environment is necessary in order to choose the most appropriate leaching test. These test methods can be categorized into three types as shown in TABLE 2-4. In equilibrium oriented leaching test methods, equilibrium between the material and leaching solution is achieved by agitation of the mixture, while capacity oriented leaching test examines the maximum amount of each contaminants that can be released from the material under the worst case scenario (Schwantes and Batchelor, 2006). Dynamic oriented tests are used to investigate the mechanism responsible for release of contaminants from the solid material.

The most widely used leaching test methods in the United States are TCLP, WLT, SPLP, EP Tox, while the use of tests such as pH stat, NEN 7341, 7343 and 7345 are common in Europe. All the different tests are used to assess leachability of different material at different exposure scenarios. Results from the various leaching tests are expressed either as leachates concentration (mg/l) or as constituent released in mg/kg dry mass for granular material and mg/m^2 for the monolith materials.

2.5.1   Mobility of Elements from Geopolymer

Leaching test methods such as TCLP, NEN 7375, NEN 7341 have been used to assess mobility of elements from geopolymer (Bankowski et al., 2004; Izquierdo et al., 2010), NEN 7341 have been specifically used to assess the mobility of oxyanion forming elements.

TABLE 2-4: Summary of various leaching test methods

Type	Leaching test	Leaching medium	L/S	Particle size	Leaching duration	Reference
Equilibrium oriented	Toxicity Characteristics Leaching Procedure (TCLP)	Acetic acid	20	<9.5mm	18 hours	Schwantes and Batchelor (2006)
	Extraction Procedure Toxicity test (EP Tox)	0.04 M acetic acid (pH 5)	16	<9.5mm	24 hours	Schwantes and Batchelor (2006)
	Water Leach Tests (WLT)	Deionized water	20	<9.5mm	18 hours	ASTM (2006c)
	Equilibrium Leach Tests (ELT)	Deionized water	4	<150 μm	7 days	Schwantes and Batchelor (2006)
	Multiple Extraction Procedure (MEP)	0.04 M acetic acid (pH 3)	20	<9.5 mm	24 hours per stage (9 extraction stages)	USEPA (1986)

TABLE 2-4 (continued)

Type	Leaching test	Leaching medium	L/S	Particle size	Leaching duration	Reference
	Synthesis Precipitation Leach Procedure (SPLP)	Deionized water adjusted to pH 4-5	20	<9.5 mm	18 hours	USEPA (1994)
	pH Static leaching test	Deionized water adjusted to pH 4-13 by HNO_3 and NaOH	5	<4 mm	24 hours	Schwantes and Batchelor (2006)
	USEPA draft method 1313	Deionized water adjusted to pH 3-13 by HNO_3 and NaOH	10	<5 mm	24 hours	USEPA (2009b)
Capacity oriented	Availability test	Two steps: pH 4 and 7	100	<150 µm	3 hours each step	EA (2005a)

TABLE 2-4 (continued)

Type	Leaching test	Leaching medium	L/S	Particle size	Leaching duration	Reference
	Nordtest availability test	Two steps: pH 4 and 7	100	<125 μm	1st : 3 hours 2nd : 18 hours	Nordtest (1995)
Dynamic oriented	American Nuclear Society (ANS) leach test 16.1	Sequential extraction by deionized water	5 - 10	Monolith	Sample at 1, 2, 4, 8, 16, 32, 64 days	Schwantes and Batchelor (2006)
	Column test (NEN 7343)	Systematic L/S ratio increase	0.1 -10	<4 mm		Schwantes and Batchelor (2006)
	Tank test	Deionized water at pH 4		Monolith	Samples collected at 0.25, 1, 2.25, 4, 9, 16, 36, 64 days	EA (2005b)

TABLE 2-4 (continued)

Type	Leaching test	Leaching medium	L/S	Particle size	Leaching duration	Reference
	USEPA draft method 1315	Deionized water		Monolith	Samples collected at 0.08, 1, 2, 7, 14, 28, 42, 49 and 63 days	USEPA (2009c)

2.6   Oxyanion Forming Trace Elements

Oxyanions are negatively charged polyatomic species that contain oxygen ions (Cornelis et al., 2008). Common oxyanions are SO_4^{2-}, NO_3^-, AsO_4^{3-}, and PO_4^{3-}. Trace elements that form oxyanionic species include boron (B), arsenic (As), chromium (Cr), selenium (Se), vanadium (V), molybdenum (Mo), tungsten (W) and antimony (Sb). These elements can form different species of oxyanion depending on pH and redox potential. Among the elements, As, Cr and Se are considered elements of concern due to their toxicity and mobility at alkaline pH (Zhang, 2000; Wang, 2007; Izquierdo et al., 2010), and are listed by the USEPA as priority pollutants in drinking water (Min, 1997; USEPA, 2009a). Since most elements that form oxyanion exhibit similar behavior, understanding the behavior of As, Cr and Se would lead to understanding the behavior of the other elements.

2.6.1   Occurrence and Chemistry of Arsenic, Chromium and Selenium

Arsenic is a metalloid found in group 15 and period 4 of the periodic table, it occurs in association with sulfur containing minerals such as realgar (AsS), orpiment (As_2S_3) or arsenopyrite (FeAsS) (Magalhães, 2002). The element is released into the environment via weathering, volcanism, agricultural applications and waste stream of industrial process with high concentration in coal fly ash (Jackson, 1998; Moon et al., 2004). Its abundant in the earth crust is between 1.5 - 2.0 ppm (NAS, 1977).

Selenium is a non-metallic element found in group 16 and period 4 of the periodic table. This element is not abundant in the earth crust, comprising only 0.05 ppm of the earth crust (Zhang, 2000). Selenium is a micronutrient required by humans and animals to maintain good health, and considered a necessary constituent of human diets for many years (B'Hymer and Caruso, 2006). Deficiency of these micronutrient might inhibit growth and too much of it can also lead to death. Bond (2000) stated that due to the narrow range between the beneficial and harmful level of selenium, the USEPA listed the element among element of concern in drinking water and specified the maximum amount of the element allowed in drinking water (USEPA, 2009a).

Chromium is a transition element that occur in group 6 and period 4 of the periodic table, it is the 21st most abundant element in the earth crust with concentration of about 100 ppm (Barnhart, 1997). It occurs in nature as the mineral chromites ($FeCr_2O_4$) and crocoites ($PbCrO_4$) (Zhang, 2000). The chemical properties and maximum contaminant level (MCL) of these elements are summarized in TABLE 2-5.

TABLE 2-5: Chemical properties and MCL of As, Cr and Se.

Elements	Group	Atomic no	Atomic mass	Electron configuration	Oxidation states	MCL µg/l
As	15	33	74.92	$[Ar]4s^2 3d^{10} 4p^3$	-3, 0,+3,+5	10
Cr	6	24	52.00	$[Ar]3d^5 4s^1$	0,+3,+6	100
Se	16	34	78.96	$[Ar]4s^2 3d^{10} 4p^4$	-2,0, +4,+6	50

Sources: Zhang (2000); Paoletti (2002); Cornelis et al. (2008); USEPA (2009a)

In nature, Arsenic (As) occurs mainly in the As^{+3} (arsenite) and As^{+5} (arsenate) oxidation states (Alexandratos et al., 2007), with As^{+3} being more mobile and reported to be 25 - 60 times more toxic than As^{+5} (Moon et al., 2004). Cr^{+3} and Cr^{+6} oxidation state are the most abundant form of chromium (Cr) in nature, with Cr^{+6} being about 100 times more toxic and soluble than Cr^{+3} (Shtiza et al., 2009). Selenium (Se) exist in nature as Se^{+4} and Se^{+6} forming SeO_3^{2-}(selenite) and SeO_4^{2-} (selenate) oxyanionic species (Bond, 2000).

2.6.2   Environmental Aspect and Toxicity of As, Cr and Se

Oxyanions of As, Cr and Se are very mobile in high alkaline environment and have low mobility in the acidic environment due to bonding with metal oxyhydroxides (Zhang, 2000). TABLE 2-6 shows the redox states of As, Cr and Se oxyanionic species and their form of occurrence in alkaline environment. In this type of environment, As^{+3}, As^{+5}, Cr^{+3}, Cr^{+6}, Se^{+4} and Se^{+6} are the most predominant redox state because they are more soluble than those occurring in their elemental and reduced states (Cornelis et al., 2008).

TABLE 2-6: Redox states of the oxyanions in alkaline environment

Element	Oxidation states					
	-2	0	+3	+4	+5	+6
As		As^0	$H_2AsO_3^-$		AsO_4^{2-}	
Cr		Cr^0	$Cr(OH)_4^-$			CrO_4^{2-}
Se	HSe^-	Se^0		SeO_3^{2-}		SeO_4

Source: Cornelis et al. (2008)

Arsenic in the trivalent form is more toxic and a known carcinogen that causes cancer of the liver skin and kidney (Magalhães, 2002). Chromium on the other hand is most toxic in the hexavalent form and possess mutagenic properties that can damage circulatory system and cause carcinogenic changes in human (Soco and Kalembkiewicz, 2009).

2.7   Methods of Immobilizing the Leaching of Oxyanion Elements

According to Cornelis et al. (2008), calcium containing mineral phases and metalate precipitation exert control over the leaching of oxyanions. The authors stated that minerals such as CSH, ettringite, monosulfoaluminate and hydrocalumite can partially or fully replace their anions (OH^- or SO_4^{2-}) with oxyanions thereby causing reduction in mobility of these oxyanion forming elements (Cornelis et al., 2008). Several studies have demonstrated this by showing that mobility of As and other oxyanions in alkaline environment can be reduced by the addition of lime, which would result in the formation of either an insoluble calcium precipitate or oxyanion substituted calcium mineral phases (Moon et al., 2004; Zhu et al., 2006; Alexandratos et al., 2007; Wang et al., 2007).

2.7.1   Incorporation into Ettringite Structure

Ettringite is a hydrated calcium aluminum sulfate hydroxide mineral with chemical formula $(Ca_6Al_2(SO4)_3(OH)_{12} \cdot 26H_2O)$ and a needle like crystal structure depicted in FIGURE 2-4. It is an example of an AFt (alumina ferric oxide tri sulfate) phase present in cement system whose structure favors extensive ionic substitution potential that can make the immobilization of oxyanions possible. Substitution of SO_4^{2-} present in ettringite structure by oxyanions such as CrO_4^{2-}, AsO_4^{3-}, SeO_4^{2-}, CO_3^{2-}, and NO_3^- have been reported by Bone et al. (2004) and Cornelis et al. (2008). FIGURE 2-5 depicts an oxyanion substituted ettringite crystal structure.
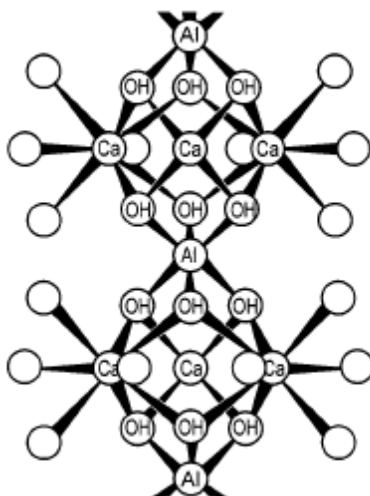
FIGURE 2-4: Schematics of ettringite crystal structure (Klemm, 1998)
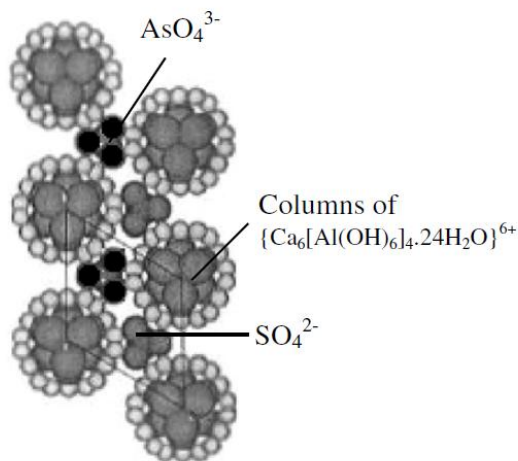
FIGURE 2-5: Oxyanion substituted ettringite structure (Cornelis et al., 2008)

2.7.2 Incorporation into Hydrocalumite Structure

Hydrocalumite is an anionic clay mineral composed of stacked portlandite-like octahedral layers where one third of the Ca^{2+} sites is occupied by Al^{3+} (Zhang and Reardon, 2003). The mineral has a chemical formula $Ca_4Al_2(OH)_2(OH)_{12} \cdot 6H_2O$ and structure shown in FIGURE 2-6 which have interlayer water molecule and anions.
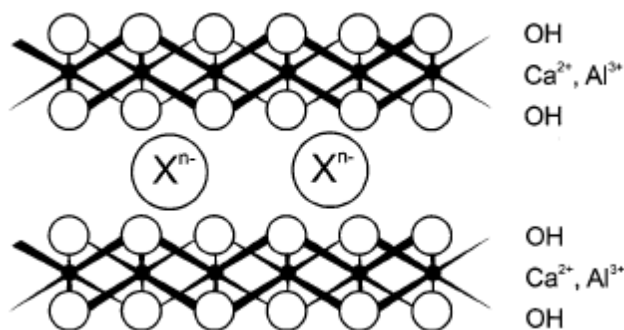
FIGURE 2-6: Schematics of hydrocalumite structure (Zhang and Reardon, 2003)

Zhang and Reardon (2003) reported that the substitution of Ca^{2+} with Al^{3+} result in net positive charges on the layers that enable incorporation of anion or oxyanion (X^{n-}) in order to balance the charges on the octahedral layers. Zhang and Reardon (2005)

demonstrated the incorporation of oxyanions such as Cr and Se which led to reduction in leaching of the elements.

2.7.3 Incorporation into Monosulfoaluminate Structure

Monosulfoaluminate is a mineral that can be found in products of cement hydration, it is an AFm (aluminiate ferric oxide monosulfate) phase that has chemical formula $Ca_4Al_2SO_4(OH)_{12} \cdot 6H_2O$ and a lamellar hexagonal platey structure shown in FIGURE 2-7.

main layer: $Ca_2Al(OH)_6^+$
interlayer: SO_4^{2-}, H_2O
main layer
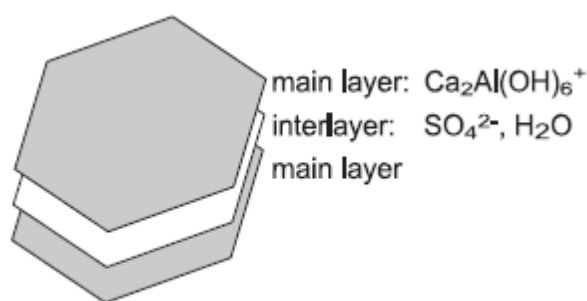
FIGURE 2-7: Schematics of monosulfoaluminate structure (Baur et al., 2004)

Monosulfoaluminate also exhibits similar anionic substitution as ettringite; in this case the SO_4^{2-} and OH^- in the structure are replaced by anions or oxyanions. Saikia et al. (2006) reported that oxyanions can also be incorporated between layers of monosulfoaluminate structure serving as interlayer anions.

2.7.4 Incorporation into Calcium Silicate Hydrate (CSH)

CSH is a principal hydration product formed during the hydration of alite and belite phases of Portland cement (Gougar et al., 1996). According to Yip and van Deventer (2003), CSH gel coexists with geopolymeric gel in geopolymer system if there is enough calcium present in the system. This CSH gel has positive charged surfaces which have the potential for adsorbing oxyanions such as, AsO_4^{3-}, AsO_3^{3-}, SeO_3^{2-} and

CrO_4^{2-} (Cornelis et al., 2008). The successful immobilization of Cr by CSH was reported by Gougar et al. (1996).

2.7.5   Formation of Precipitates

At pH of around 12.6, the formation of calcium metalate precipitates is reported to be effective at immobilizing oxyanion forming elements (Bone et al., 2004). According to Moon et al. (2004), formation of calcium metalate precipitate have been successful at immobilizing arsenic which occurs in the As^{+3} form as $HAsO_3^{2-}$ and As^{+5} as $HAsO_4^{2-}$. Magalhães (2002) stated that calcium arsenates such as weilite ($CaHAsO_4$), pharmacolite   ($CaHAsO_4 \cdot 2H_2O$),   haidingerite   ($CaHAsO_4 \cdot H_2O$),   phaunouxite ($Ca_3(AsO_4)_2 \cdot 11H_2O$) are particularly formed.

2.8   Mineralogical and Microstructural Characterization of Geopolymer

X-Ray diffractometer (XRD) analysis is used to analyze mineral phases present in solid materials. XRD analysis of geopolymer made from fly ash shows the presence of quartz (SiO_2), mullite ($Al_6Si_2O_{13}$) zeolites such as hydroxysodalite ($Na_4Al_3Si_3O_{12}OH$) and herchelite ($NaAlSi_2O_6 \cdot 3H_2O$), and a diffuse halo peaks at 2θ angle of between 20° – 40° (Fernández-Jiménez and Palomo, 2005; Fernández-Jiménez et al., 2007; Zhang et al., 2009; Guo et al., 2010). This suggests that geopolymer contains both crystalline and amorphous (non crystalline) phases.

Microstructure of geopolymers have been observed by a lot of researchers using the scanning electron microscope (SEM) which is an instrument used to produce high resolution image of sample surfaces (Das, 2008). The structure of fly ash based geopolymer reveals that the material consists of crust of shapeless reaction product and presence of unreacted spherical fly ash particles depending on the degree of reaction

(Fernández-Jiménez and Palomo, 2009). Some of these unreacted fly ash particles are sometimes covered with the reaction products.

2.9   Geochemical Modeling

Geochemical modeling tools have been increasingly used to assess environmental impact and speciation of elements from materials (Halim et al., 2005) in order to answer environmental questions such as: (1) How fast contaminants move and when it will reach a certain point? (2) Whether the concentration of the contaminant exceeds regulatory limits? (3) What processes will hinder or immobilize the contaminants? (4) What is the state of the particular site under investigation? Geochemical modeling have been used in the assessment of high level nuclear waste repositories, exploratory and feasibility studies of mining sites, and speciation of elements from the interaction between landfill leachates and liners (Zhu and Anderson, 2002).

According to Zhu and Anderson (2002), geochemical models are divided into speciation-solubility model, reaction-path model and reactive transport model based on their level of complexity. Speciation-solubility models perform batch calculations and provide no spatial or temporal information about the contaminant, reaction path models on the other hand are used to simulate successive reaction steps in response to mass or energy flux thereby providing some temporal information about the progress of the reaction. Reactive transport models are very complex models that provide both temporal and spatial information of the chemical reactions. The most basic and least expensive models belong to the speciation-solubility model group, they are suitable for answering questions about concentration of constituents species present in an aqueous solution, and their saturation states with respect to various minerals in the aqueous system. Common

speciation-solubility models are MINTEQA2, MINEQL+, geochemist's workbench, EQ3/EQ6, SOLMINEQ.88,WATEQ4F and PHREEQC (Zhu and Anderson, 2002; Zhu, 2009). All these models involve batch calculations and serves as the basis for the reaction path and reactive transport models (Zhu and Anderson, 2002).

PHREEQC (Parkhurst and Appelo, 1999) is the most widely used speciation-solubility modeling tools with capability that includes performing speciation and saturation index calculations, batch and one dimensional (1D) reaction transport calculation, and inverse mass balance modeling (Parkhurst and Appelo, 1999; Zhu and Anderson, 2002; Bone et al., 2004). According to Parkhurst and Appelo (1999), the acronym PHREEQC stands for pH values (PH), redox (RE), equilibrium (EQ), and C programming language (C) which are the most important parameters in the model. The model utilizes solubility products (K_{sp}) of aqueous solution, minerals and solid solutions to calculate the equilibrium state of the system under specific conditions using databases included in the program which contains information on equilibrium constants and properties of the different species of minerals, elements and solid solution.

Equilibrium state between the aqueous solution and mineral phases present is evaluated based on value of the calculated saturation indexes (SI) of the system which is obtained by relating the ion activity product (IAP) observed in solution and the theoretical solubility product (K_{sp}) using Equation 2.2 (Appelo and Postma, 2005; Andrews, 2007).

$$SI = \log (IAP/K_{sp}) \tag{2.2}$$

Andrews (2007) defined SI as the concentration at which dissolved concentration of mineral components is saturated with respect to the solution. A negative SI value (SI <

0) indicates that the solution is undersaturated with respect to the mineral thereby making the mineral dissolve, positive SI value (SI > 0) means that the solution is supersaturated with respect to the mineral and the mineral will precipitate, and when SI equals zero, the solution is in equilibrium with respect to a mineral (Andrews, 2007; Zhu, 2009). For SI close to zero, the phase is in near equilibrium state with the solution and can be considered as the controlling phase (Schiopu et al., 2009).

2.10   Summary

Despite the growing interest in geopolymer technology, there have been few studies on the environmental characterization of the material. These studies have revealed that geopolymer could leach out elements that include As, Cr and Se which are considered priority pollutants in drinking water by the USEPA.

According to Cornelis et al. (2008), mobility of oxyanion forming elements can be reduced using calcium containing mineral phases and metalate precipitation. Ettringite was found to favor ionic substitution in which the SO_4^{2-} present in its structure is replaced by the oxyanions (Bone et al., 2004). It was also reported by Zhang and Reardon (2003) that the net positive charge on hydrocalumite structure can enable incorporation of oxyanions to balance the charge on the mineral. Monosulfoaluminate was also found to exhibit similar ionic substitution as ettringite (Saikia et al., 2006). In this case, the SO_4^{2-} and OH^- in the structure are replaced by the oxyanions. Formation of calcium metalate can also reduce the mobility of the oxyanion forming elements (Bone et al., 2004; Moon et al., 2004). CSH which coexists with geopolymer gel also have potential for absorbing oxyanions thereby reducing the elements mobility. It is evident from the literature that calcium containing mineral phases can successfully lead to a reduction in mobility of

oxyanion forming elements which exist in different oxidation states, and whose mobility and toxicity depends on the specie of the element present in any solution. Geochemical modeling has been identified as a tool that can be used to assess the speciation of these elements. PHREEQC, a widely used speciation-solubility modeling tool was considered an ideal tool for determining the speciation of elements such as As, Cr and Se.

This dissertation would in addition to investigating the mobility leaching mechanisms of oxyanions (As, Cr, Se) focus on using calcium containing mineral phases in reducing the mobility of the elements from fly ash based geopolymer concrete, and the use of PHREEQC/PHREEPLOT to predict the species of each element that would be released from the material.

CHAPTER 3: EXPERIMENTAL PROTOCOL

3.1   Research Approach

The research approach employed is a quantitative approach which entails the use of experimental methods to test the stated hypotheses. This approach involves making geopolymer concretes with varying amount of hydrated lime added during synthesis, subjecting the material to established experimental techniques at the service life and end of life of the material life cycle. Cementitious materials like geopolymer concrete exist in monolith form during its service life and in granular / crushed form at end of life. Appropriate test methods are chosen for the different stage of the material life cycle.

3.2   Materials

3.2.1   Coal Fly Ash (CFA)

The CFA used in this study was obtained from a coal fired power plant in Southeastern United States and classified as a Class F ash (as per TABLES 2-1 and 2-2) based on its chemical composition. The material consists of high amount of oxides of silicon and aluminum and a low amount of calcium oxide making it a suitable source material for geopolymer synthesis.

3.2.2   Silica Fume (SF)

The SF used in this study was purchased from Ohio valley alloy services and contains 98% amorphous silica and meets standard specification for silica fume used in cement (ASTM, 2010b). Since higher amount of silica (SiO_2) is required for geopolymer

synthesis, silica fume (SF) was added to increase the silica to alumina ratio (Si/Al) in order to aid the formation of higher order poly(sialate-siloxo) and poly(sialate-disiloxo) geopolymer structure.

3.2.3   Sodium Hydroxide (NaOH)

Sodium hydroxide (NaOH) is one of the components in the activating solution responsible for dissolution of the starting fly ash during geopolymer synthesis. The NaOH used is a commercial grade NaOH pearls with 98% purity.

3.2.4   Hydrated Lime (Ca(OH)$_2$)

High calcium hydrated lime (Ca(OH)$_2$) supplied by UNIVAR was used in the study. The hydrated lime has about 95% Ca(OH)$_2$ content with no Mg(OH)$_2$ which conforms to the specification of type N hydrated lime used in mortar and Portland cement concrete (ASTM, 2006b).

3.2.5   Aggregates

The coarse (CA) and fine (FA) aggregates used in the study are the same type used in making Portland cement concrete. The CA and FA are respectively a ⅜ inches granite stone and silica sand. The aggregates were used in the saturated surface dry (SSD) condition.

3.3   Experimental Method

The experimental method is divided into five different phases that are summarized in TABLE 3-1. It consists of the various tasks that are completed to achieve the research objectives and test the stated hypotheses. Detailed information of the different experimental phases is presented in subsequent chapters of this dissertation. Since the material exist in the monolith form during its service life and in crushed or

granular form at end of life, some of the geopolymer concretes were tested in the monolith form and others in the granular/powder form.

TABLE 3-1: Experimental phases for the dissertation

Phase	Task description
I	Characterization of the materials / geopolymer products
	a. XRF analysis
	b. ANC/BNC test
	a. Stabilized pH and moisture content
	b. Bulk density and PSD
II	Synthesis of fly ash geopolymer concretes and sample preparation
	a. Geopolymer concrete without lime
	b. Geopolymer concrete with lime
	c. Crushing and sub sampling
	d. Grinding and sieving
III	Laboratory leaching test methods
	a. Availability test
	b. Tank leaching test
	c. pH stat test
	d. Water leach test
IV	Mineralogical and microstructural characterization
	a. XRD analysis
	b. SEM/EDX analysis

TABLE 3-1 (continued)

Phase	Task description
V	Geochemical modeling using PHREEQC/PHREEPLOT
	a. Speciation modeling
	b. Model simulation results and interpretation

3.4   Quality Assurance and Quality Control

Proper sampling technique is used to obtain representative samples of the geopolymer concrete. Dry granular samples were placed in ziplock bags and stored in a dry storage container. All samples were immediately labeled to avoid confusion with other samples. To ensure accuracy and precision in all measurements, all the analysis except the XRD and SEM are performed in duplicate or triplicate. Blank analyses are also included in some analytical methods using the same reagents and equipments but without the samples, this will confirm the presence of any contamination during the analytical methods.

All glasswares and labwares were acid washed and rinsed three times with deionized water (DI) before each use. Only recently calibrated scales are utilized in all weight measurements. All equipments are properly cleaned before testing another sample to avoid cross contamination of samples. All samples are stored according to standard storage requirements for each type of sample; liquid for cation analysis are acidified to pH < 2 to minimize metal cations from precipitating and adsorption onto the storage container wall (USGS, 1998) while liquid samples for anion analysis are not acidified. All the liquid samples are then stored in a refrigerator maintained at 4^oC or less.

3.5   Statistical Analysis of Data

All raw data obtained from the analysis are transformed into easily understandable data form. The mean and standard deviation of all duplicate and triplicate measurements are determined. Non parametric statistical analysis such as Kruskal-Wallis test was used to statistically compare the results obtained from the four geopolymer concrete samples. Tukey's HSD pairwise comparison was used to determine which geopolymer concrete sample is significantly different from the other. JMP statistical software version 9.0 by SAS was utilized in all statistical analysis at a 95% confidence interval.

3.6   Pilot study

This section describes preliminary research studies that was completed on fly ash based geopolymer concrete and paste in order to become familiarize with the synthesis of the geopolymer and conducting the experimental methods. Majority of the work have been on geopolymer paste. Geopolymer concrete samples were later produced with recycled concrete aggregate (RCA) replacing some of the coarse aggregate. RCA was incorporated into geopolymer concrete to create an outlet for using demolished concrete waste and study how excess calcium in the RCA affect mobility of elements from the produced geopolymer. Most of the results from the preliminary investigation have been presented in conferences (Sanusi and Ogunro, 2009; Ogunro and Sanusi, 2010; Sanusi et al., 2011).

3.6.1   Element Mobility from Fly Ash Based Geopolymer Paste

Mobility of 29 elements from geopolymer paste was studied using short term (6 hours) pH leaching test (Ogunro and Sanusi, 2010). In this investigation, geopolymer

paste whose components by weight include 67% Class F coal fly ash, 10% NaOH and 8% SF was produced by mixing activating solution (dissolving SF in hot concentrated NaOH) with CFA. The mixture was cast in cylindrical mold and cured in the oven at $75^{o}C$ for 24 hours. Compressive strength of the cylinders was determined at 28 days, the mortar crushed and pulverized to fine particles required for the pH leaching test. The pH dependence leaching test used was performed at a liquid to solid (L/S) ratio of 10 with continuous pH control based on a slight modification of the European standard pH test CEN/TS 14997 (CEN, 2006). In the test method, the leaching solution pH was continuously controlled to pH 3, 5, 7, 9, 11 and 13 using HNO_3 or NaOH for 6 hours, and the leachates filtered using 0.45µm membrane filter.

The results obtained reveals that mobility of elements varies across the pH range. Elements such as barium (Ba), beryllium (Be), cobalt (Co), copper (Cu), manganese (Mn), zinc (Zn), iron (Fe), magnesium (Mg), boron (B), strontium (Sr), lithium (Li) and nickel (Ni) display high mobility at low pH which decreases as the pH increases from acidic to the alkaline pH (FIGURE 3-1 and 3-2). Elements with very high mobility from the geopolymer paste include aluminum (Al), sodium (Na), silicon (Si), calcium (Ca) and potassium (K) (FIGURE 3-3) due to their high solubility during the geopolymerization process. The mobility of these elements is almost constant at the acidic pH range and increases gradually in the alkaline pH. Mobility of silver (Ag), cadmium (Cd), lead (Pb), antimony (Sb), tin (Sn) and thallium (Tl) is very low across the pH range. The oxyanion forming elements such as arsenic (As), selenium (Se), vanadium (V), molybdenum (Mo) and chromium (Cr) on the other hand display lower mobility in the acidic pH, their highest mobility occurs at pH between 9 and 11(FIGURE 3-4).
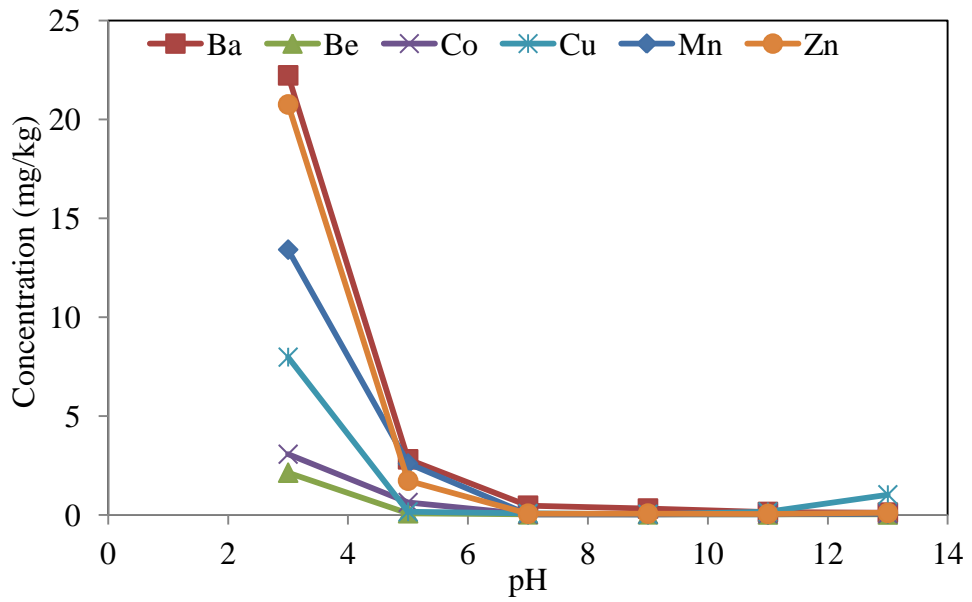
FIGURE 3-1: Mobility of elements from the geopolymer paste (category 1)
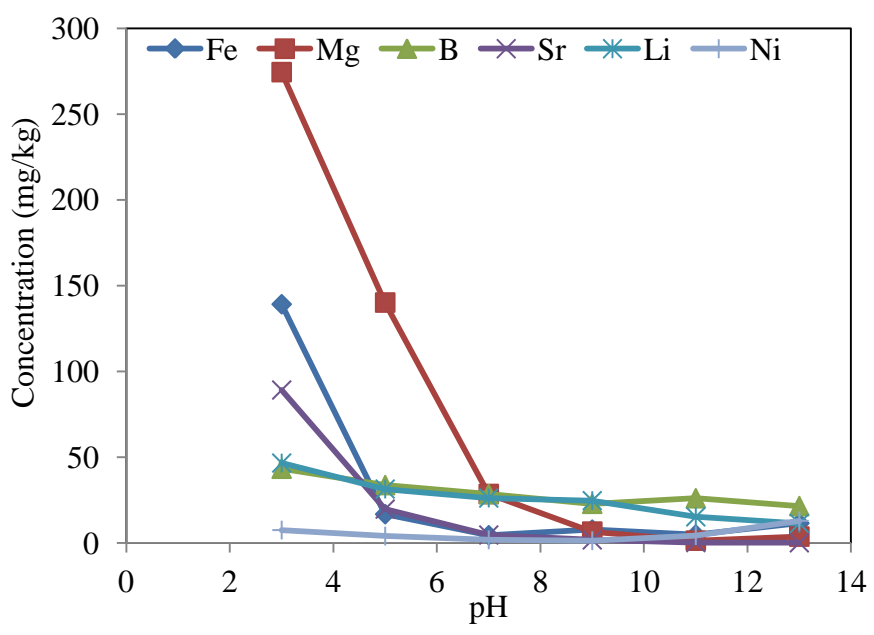
FIGURE 3-2: Mobility of elements from the geopolymer paste (category 2)
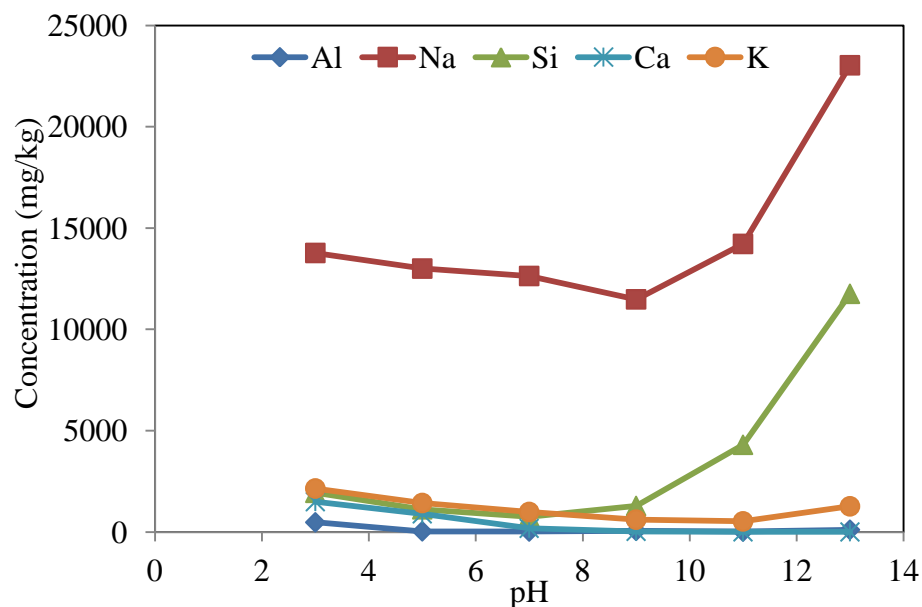
FIGURE 3-3: Mobility of elements from the geopolymer paste (category 3)
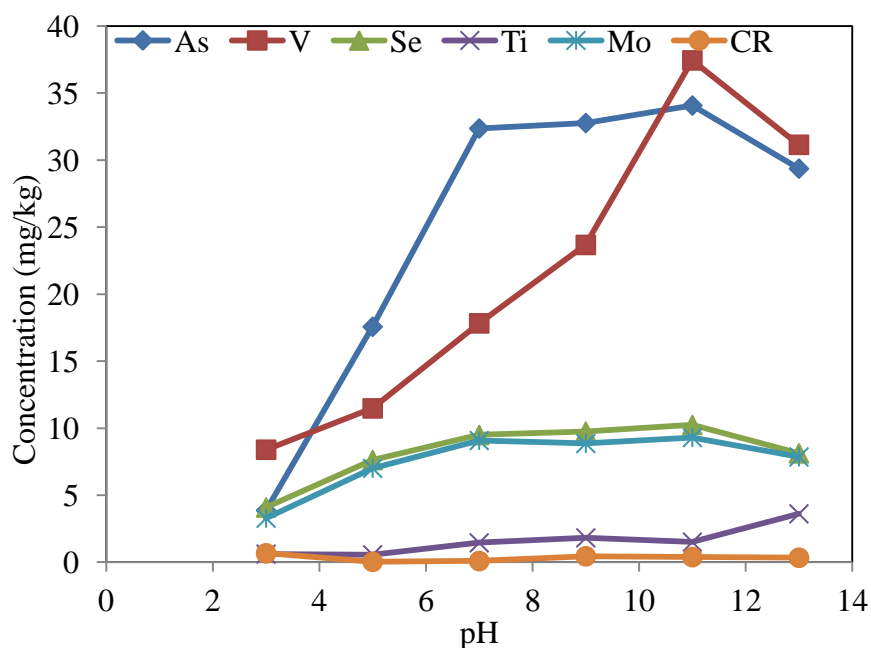
FIGURE 3-4: Mobility of elements from the geopolymer paste (category 4)

The preliminary study reveals that depending on the pH of the environment where geopolymer is been utilized, different elements can potentially leach out. In an acidic environment, Ba, Be, Co, Cu, Mn, Fe, Mg, B, Sr, Li and Ni are elements that would leach

out more while As, V, Se, Tl, Mo and Cr would leach out more in an alkaline environment similar to the pH of the pore solution within the geopolymer (pH > 9). Consequently, the focus of this research is to investigate the leachability of some target oxyanions (As, Se and Cr).

3.6.2   Leaching of Oxyanion Forming Elements from Fly Ash Based Geopolymer Paste

Based on the results obtained from the pH leaching test (Section 3.6.1) which showed that oxyanion forming elements leach more at the alkaline pH, there is thus a need to find the most appropriate leaching test that can effectively predict the maximum leaching of these elements. The Dutch availability test happens to be the most widely used test for this type of environmental assessment. The test is a two step extraction procedure conducted at pH 7 and pH 4, with the extraction step conducted at pH 7 designed to determine the leaching of oxyanion forming elements. But with the higher mobility of the oxyanion forming elements at alkaline pH, the conventional availability test conducted at pH 7 would underestimate their leaching, thereby creating an opportunity for modification of the test to reflect the alkaline pH of the geopolymer (Sanusi and Ogunro, 2009).

The aim of the study is to determine which availability test method is better for oxyanion element leaching. Geopolymer paste was produced from CFA, NaOH and SF using the mix design presented in section 3.6.1, and oven cured for 24 hours before curing at ambient temperature until the 28 days test date. The geopolymer specimens were crushed, pulverized and size reduced to particles <150µm required for the availability test. The availability test (NEN 7341) and a modification of the test (MNEN) was used to determine the leaching of As, Se and Cr from the geopolymer paste. TABLE

3-2 shows the experimental conditions for the two tests. In situations where pH needs to be controlled, HNO_3 was used to control the pH for the duration of the extraction step or procedure.

TABLE 3-2: Experimental conditions for the availability tests

Test		pH conditions	Test duration
MNEN	1st step	No pH control	18 hours
	2nd step	4 ± 0.5	3 hours
NEN	1st step	7 ± 0.5	3 hours
	2nd step	4 ± 0.5	3 hours

Results obtained from the investigation were statistically compared using the Wilcoxon signed rank test at 95% confidence interval ($\alpha=0.05$). The hypotheses tested in this preliminary study is that standard leaching test method conducted at neutral pH is adequate for predicting the leaching of oxyanion forming elements (As, Cr, Se). The null (Ho) and alternative (Ha) hypothesis utilized in the statistical comparison are listed below:

Ho: The concentrations of As, Cr and Se measured in the NEN 7341 and MNEN are not different (NEN 7341 = MNEN). The test methods are the same.

Ha: The concentrations of As, Cr and Se measured in the NEN 7341 are generally less than the concentration measured in MNEN (NEN 7341 < MNEN). The MNEN test method gave results with higher measured concentrations.

The statistical comparison showed that there is no significant difference between the results from the two test methods for As (p-value=0.6250), Se (p-value=0.6250), and Cr (p-value=0.1250). In conclusion, it was observed that although the NEN 7341 was

conducted at pH 7, it is still effective at predicting the leaching of the oxyanion elements such as As, Cr and Se and there is no need to consider a modification of the test to reflect the alkaline nature of the geopolymer (Sanusi and Ogunro, 2011b).

3.6.3 Mitigating Leachability from Geopolymer Concrete using RCA

Based on extensive literature on the immobilizing oxyanions (presented in Section 2.7), this study focused on the use of additional calcium in geopolymer which would lead to the formation of calcium containing mineral phases needed for the reduction in mobility of oxyanion forming elements (Sanusi et al., 2011). Three mix of geopolymer concretes were made using CFA, SF, natural coarse and fine aggregate, with recycled concrete aggregate (RCA) used as partial replacement for the coarse aggregate. The mixes made are: GC - geopolymer concrete with 0% RCA, RC10 – geopolymer concrete with 10% RCA, and RC50- geopolymer concrete with 50% RCA. The RCA was used to respectively replace 10% and 50% of the coarse aggregate content in the RC10 and RC50 concrete samples.

The CA, FA, CFA and RCA were mixed in a rotary mixer for 3 minutes before adding the activating solution and the mixture was further mixed for an additional 3 minutes. The concrete was cast in cylindrical mold, aged for 24 hours before oven curing at 75°C for another 24 hours. Compressive strength of the concretes were determined at 28 days, and the concretes crushed and size reduced to particle $<$ 150μm. Dutch availability test was used to assess the mobility of As, Cr and Se from the different geopolymer concrete mix.

The compressive strength result (FIGURE 3-5) showed that replacing coarse aggregate with RCA lead to increase in strength of the geopolymer concrete. The

leaching result presented in FIGURE 3-6 reveals that there is a reduction in mobility of As and Se as the replacement of coarse aggregate with RCA increases. The study showed that the use of RCA which contains soluble calcium would lead to an increase in strength of geopolymer concrete and a reduction in mobility of the oxyanion elements analyzed.
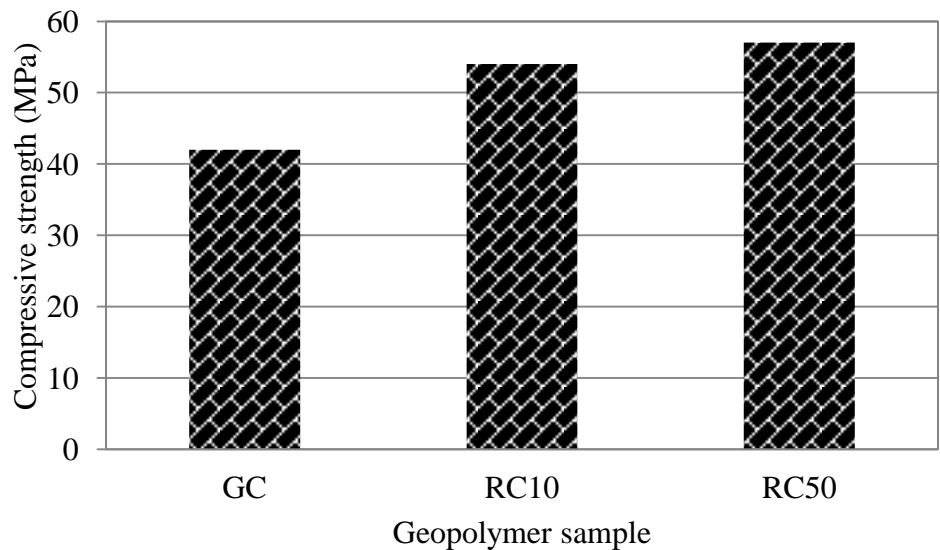
FIGURE 3-5: Compressive strength of the fly ash based geopolymer concretes
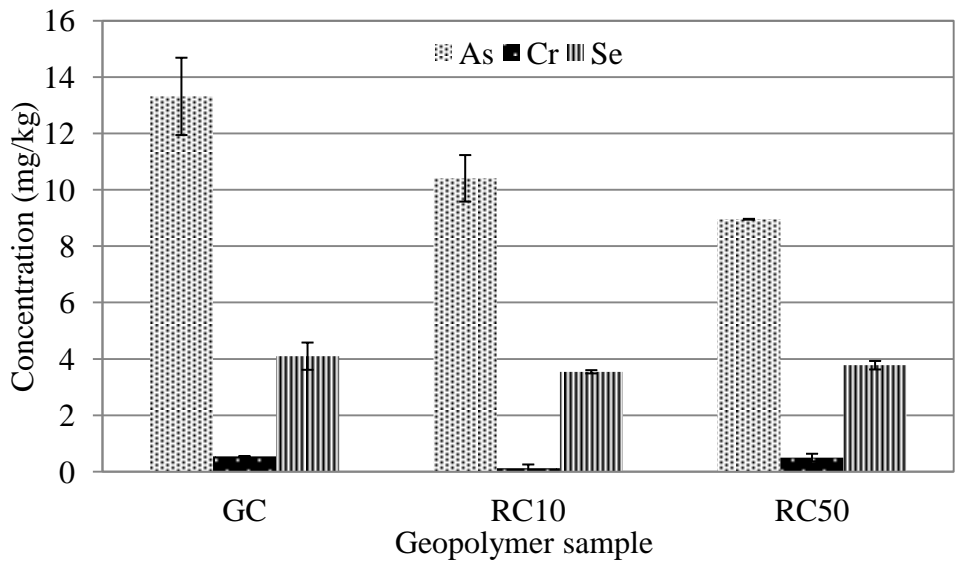
FIGURE 3-6: Concentration of the leached oxyanion forming elements

3.6.4   Influence of Lime on Strength and Mobility of Elements from Geopolymer Paste

Motivation for studying the influence of lime on strength and mobility of elements from geopolymer paste came from findings in the literature that Calcium containing mineral phases can be used to reduce mobility of oxyanion elements and from the result obtained from using RCA as partial replacement in geopolymer concrete presented in section 3.6.3. In this particular study, two geopolymer mix (GPC and GP3) were made using CFA, SF, NaOH and $Ca(OH)_2$, with the GP3 mix having 3% additional calcium in the form of $Ca(OH)_2$ (Sanusi and Ogunro, 2011a). The CFA was mixed with the activating solution which contains SF dissolved in hot concentrated NaOH. The resulting geopolymer paste was cast in cylindrical mold and cured in the oven for 24 hours at $75^{\circ}C$.

Compressive strength of the geopolymers were determined after 28 days of curing, and the tank leaching test based on the USEPA draft method 1315 (USEPA, 2009c) was used to investigate the mobility of elements from the monolithic geopolymer samples. In this leaching test, the monolithic samples were submerged in deionized water for 64 days in a tightly sealed container. The water was removed and replenished at nine successive leaching intervals as specified by the leaching standard.

The result showed that there is an observed reduction in compressive strength of the geopolymer mix made with extra $Ca(OH)_2$ (FIGURE 3-7). The compressive strength of the geopolymer paste dropped from 52 MPa in the GPC to 45 MPa for GP3, a 13% reduction in the strength. It is suspected that the extra calcium result in formation of calcium silicate hydrate (CSH) that hindered the geopolymerization process. Inductively coupled plasma mass spectrometer (ICP-MS) was used to determine the concentration of

16 elements in the leachates collected from the leaching test. It was observed that there was a slight reduction in the mobility of As, B, Ba, Cr, Fe, Mg, Mo, Se, S, and Zn from GP3 mix when compared with GPC (FIGURE 3-8) suggesting that the added calcium resulted in slight leachability reduction. On the basis of these preliminary findings, a more rigorous and targeted study was developed to test all the hypotheses stipulated in chapter one.
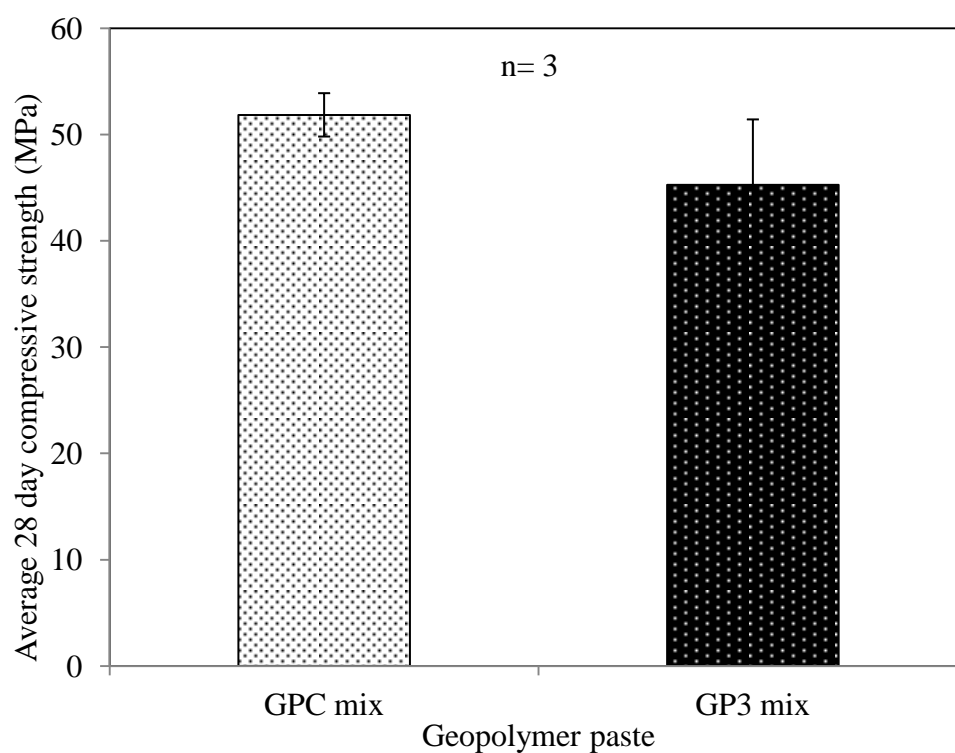
FIGURE 3-7: Compressive strength comparison for two geopolymer paste mixes
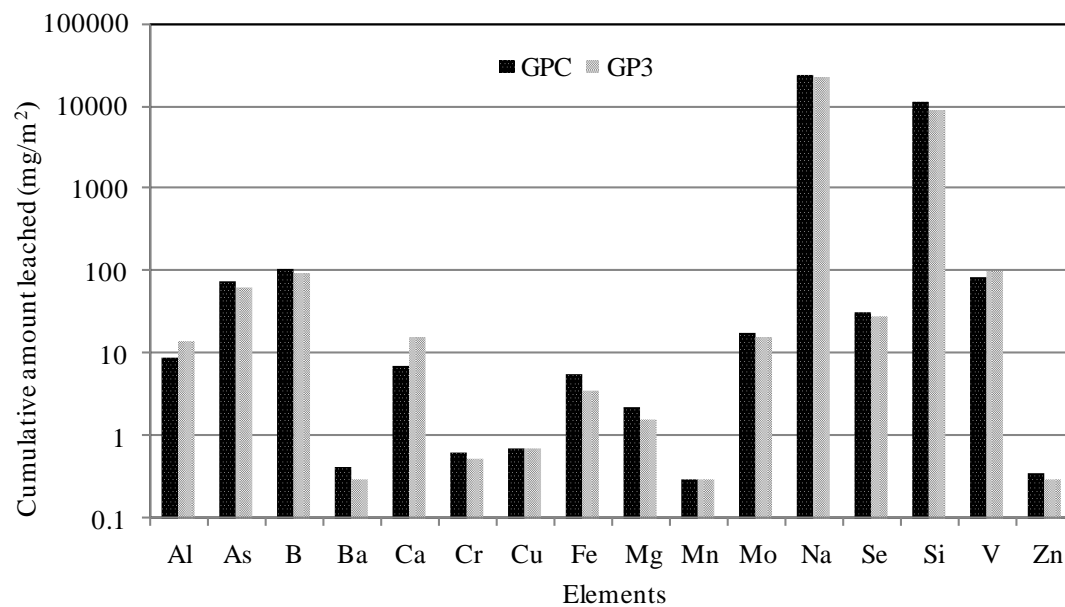
FIGURE 3-8: Cumulative amount of elements leached from the two geopolymer paste

CHAPTER 4: SYNTHESIS OF GEOPOLYMER CONCRETE AND SAMPLE
PREPARATION

4.1   Synthesis and Preparation of the Geopolymer Concretes

Geopolymer concrete samples were made using the same mix design developed
by Tempest (2010). The mix design used in this study is presented in TABLE 4-1. This
mix was modified by incorporating varying amount of hydrated lime (0%, 0.5%, 1.0%,
and 2.0%) which slightly increased the mass of the total components without changing
the proportion of NaOH (10% NaOH/CFA) and SF (7.5% SF/CFA) in the mix. Due to
the added lime, the water to cementitious material (w/c) ratio varies from 0.364 to 0.358.
According to the mix design, the aggregates (CA and FA) make up 68% of the total
geopolymer concrete mix, while the SF content is 1.6%, NaOH is 2.1%, water and CFA
content are respectively 8.9% and 21%.

The activating solution required for the geopolymer synthesis was prepared the
previous day by dissolving SF in hot concentrated NaOH solution and allowing the
mixture to equilibrate in the oven for 24 hours. The geopolymer concretes were made in a
conventional concrete batch mixer, the FA, CA, $Ca(OH)_2$ and CFA was thoroughly
mixed in a rotary mixer for 3 minutes, and the liquid component (activating solution)
later added and mixed together for additional 2 minutes. The resulting geopolymer
concrete was cast into 76.2mm (3 inches) by 152.4mm (6 inches) plastic cylindrical
molds in three layers, and consolidated by rodding each layer 25 times. Eighteen (18)

cylinders were made for each geopolymer concrete mix. After aging for 24 hours at ambient temperature, nine cylinders were cured in the oven at 75°C for 24 hours while the remaining nine samples cured without heat at room temperature. The concrete samples were removed from the molds after 48 hours of casting and allowed to aged for 7 and 28 days at room temperature (25°C).

TABLE 4-1: Mix design for the geopolymer concrete (kg/m^3)

Mix	Ca(OH)$_2$ (%)	CFA	FA	CA	SF	NaOH	H$_2$O	w/c
GPC	0 (0)	483	773	774	36	48	207	0.364
GP1	3 (0.5)	483	773	774	36	48	207	0.363
GP2	5(1.0)	483	773	774	36	48	207	0.361
GP3	10(2.0)	483	773	774	36	48	207	0.358

FIGURE 4-1 shows the schematic for the synthesis of geopolymer concrete cured in the oven at 75°C. Compressive strength of three specimen from each batch were determined at 7 and 28 days using the Universal Testing Machine (UTM) in accordance to the standard method for determining compressive strength of cylindrical samples (ASTM, 2010a).

4.2   Sampling and Sample Preparation

Sample preparation is considered one important part of the analytical process for which the samples are prepared to simulate and meet the requirements of specific test scenario. Material in the monolith form would be used for service life analysis while materials in crushed or granular form would be used for end of life analysis. Samples for end of life investigation are crushed into smaller fragments in a steel mortar shown in

FIGURE 4-2. The fragments are then combined and thoroughly homogenized to form a composite sample.
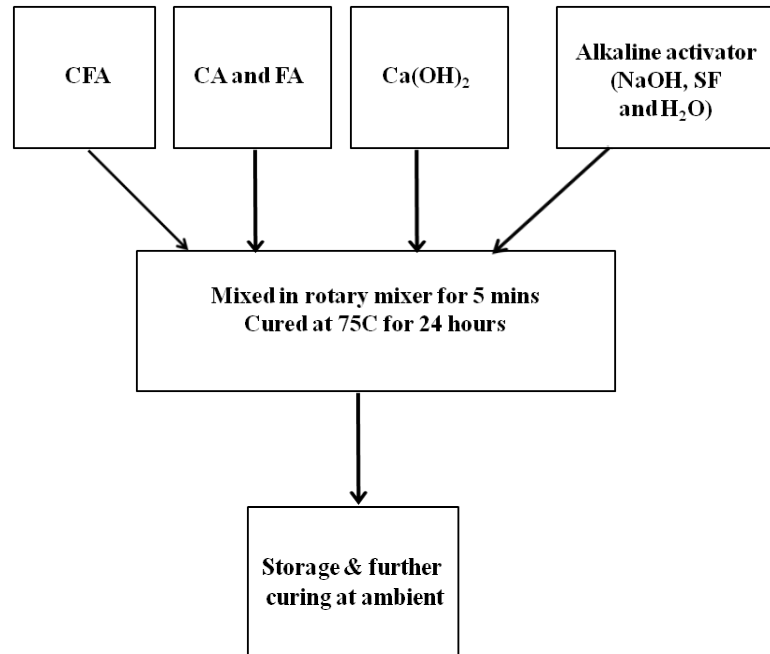
FIGURE 4-1: Schematics of the geopolymer concrete production

FIGURE 4-2: Steel pestle and mortar used in crushing the geopolymer concrete

Representative samples of each geopolymer concrete are obtained using cone and quartering method (FIGURE 4-3) in accordance with the procedures outlined in ASTM C702 (ASTM, 2003). In the cone and quartering process, the sample is poured into a heap to form a radial symmetry which is flattened and divided into four quadrants, opposite quadrants are combined to form reduced sample and the other quadrant discarded. This sub sampling process is continued as needed to obtain the needed amount of representative sample.
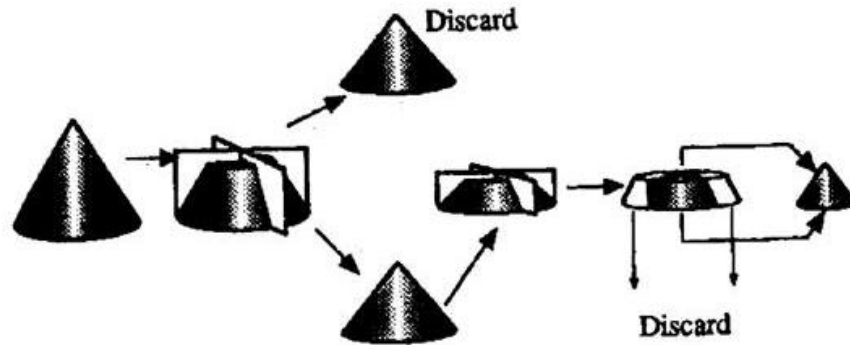
FIGURE 4-3: Cone and quartering process (After (Allen, 2003))

FIGURE 4-4: Crushed and size reduced geopolymer concrete sample

The representative sample (right image in FIGURE 4-4) is ground into fine powder using the ring grinder shown in FIGURE 4-5. Test samples required for the analytical tests are obtained by sieving the representative samples to particle size less than 150 μm (sieve #100).

FIGURE 4-5: Rocklab ring grinder used in grinding the geopolymer concrete samples

4.3   Summary

This chapter presents the synthesis of different geopolymer concrete mixes and the preparation of the concrete samples for analysis. The geopolymer concrete created has consistent workability and w/c ratio of about 0.36. The w/c is the ratio of the water used in the synthesis to the cementitious solids which include the amount of CFA, SF, NaOH and $Ca(OH)_2$ in the mix design. As the amount of $Ca(OH)_2$ increases, the workability of the geopolymer concrete reduces because the material harden faster. At above 2% $Ca(OH)_2$, the geopolymer concrete harden before placement in the mold which makes the addition of 2% $Ca(OH)_2$ the optimum amount that can be used in the geopolymer concrete synthesis in accordance with the procedure used for this study.

The use of two curing regime (heat curing at 75°C and curing without heat) aims to identify the effect heat curing has on the leachability and strength of geopolymer concrete. The main observation from the synthesis of geopolymer concrete using the two curing regime is the presence of excessive efflorescence on the surface of the geopolymer concrete cured without heat (FIGURE 4-6). The heat cured geopolymer concrete samples does not exhibit any efflorescence. Efflorescence is a white powdery deposit of soluble salts such as sodium carbonate hydrate, sodium carbonate or sodium phosphate hydrate on the surface of concrete when the soluble salt migrate to the surface of the concrete and moisture evaporates leaving behind the salt deposit on the surface which then crystallize (PCA, 2012). Temuujin et al. (2009) reported that efflorescence is an indication of insufficient geopolymerization which implies that the heat cured geopolymer concrete forms greater level of geopolymerization.

FIGURE 4-6: Cured geopolymer concrete a) cured without heat, b) heat cured

CHAPTER 5: CHARACTERIZATION OF THE MATERIALS

Characterization of the starting materials and the produced geopolymer concretes are discussed in this chapter. All the characterization is completed according to standard protocols. The properties covered are chemical composition and particle size distribution of the starting materials, compressive strength of the geopolymer concretes, acid/base neutralization capacity, moisture content and bulk density of all the materials.

5.1   Chemical Composition by X-Ray Fluorescence (XRF) Analysis

The chemical composition of the CFA and SF presented in TABLE 5-1 was determined using XRF analysis. The analysis was completed by sending the samples to the geological sciences department at the Michigan State University, East Lansing, Michigan.

TABLE 5-1: Chemical composition of the CFA and SF (mass %)

	SiO_2	Al_2O_3	CaO	Fe_2O_3	MgO	Na_2O	K_2O	MnO	P_2O_5	TiO_2	LOI*
CFA	54.83	28.24	2.45	4.99	0.90	0.22	2.42	0.90	0.23	1.59	3.81
SF	98.48	0.18	0.17	0.18	0.08	0.00	0.12	0.08	0.01	0.00	0.74

*LOI = Loss on ignition

The CFA contains 88% $SiO_2+Al_2O_3+Fe_2O_3$ and 2.5% CaO (low calcium) making the material to be classified as a class F ash according to the ASTM C618 standard. This type of ash is widely used in the synthesis of geopolymer although Class C (high calcium) ash can also be used. The only problem with the use of Class C ash is that it

makes the geopolymer set very fast (Tempest, 2010). The SF on the other hand contains 98% SiO_2, a high content of reactive silica required for the synthesis of higher order geopolymer with higher strength. The use of SF as a source of reactive silica is a deviation from the norm of using sodium silicate (Na_2SiO_3), this is because we want to increase the use of waste material in the synthesis of our geopolymer.

5.2   Particle Size Distribution (PSD)

Sieve analysis based on ASTM C136 (ASTM, 2006a) standards was performed on the CA and FA to determine the particle size distribution (PSD), the result obtained from this analysis is presented in FIGURE 5-1. The PSD of CA and FA meet the requirements for the aggregates that would produce concrete that are very easy to place. For the fine particle sizes, Beckman coulter LS 13 320 laser diffraction particle size analyzer (FIGURE 5-2) was used to determine the PSD of CFA and SF (FIGURE 5-3 and 5-4). The instrument uses the principle of light scattering to determine the particle size distribution of sample in powder form.
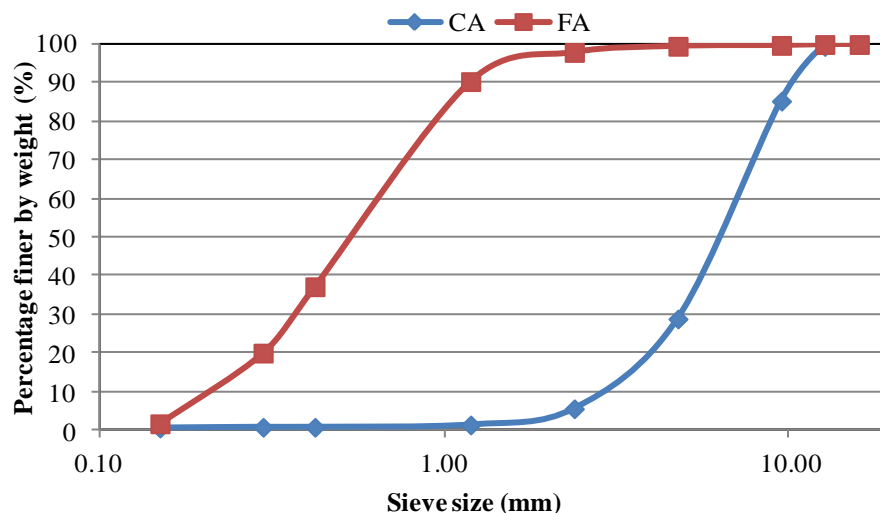
FIGURE 5-1: Particle size distribution of the aggregates

The principle of light scattering involves analyzing light scattering pattern (diffraction) produced when particles of different sizes are exposed to a beam of light (Beckman Coulter, 2011). In the laser instrument, particles of the sample are suspended in water, diluted to decrease interference, and pass through a cell where laser beam is directed towards the particles (OEWRI, 2008). The PSD of the CFA and SF was determined by measuring the pattern of light scattered by the particles in the sample since each particle has different scattering pattern which is correlated to the particle size distribution of the sample.

As shown in FIGURES 5-3 and 5-4, the CFA has particle that range in size from 0.04 μm to 309 μm while the SF has particle size in the range of 0.04 μm to 1800 μm. The two materials have relatively well graded particle size distribution and mean particle size of 47 μm and 277 μm respectively.

FIGURE 5-2: Laser diffraction particle size analyzer
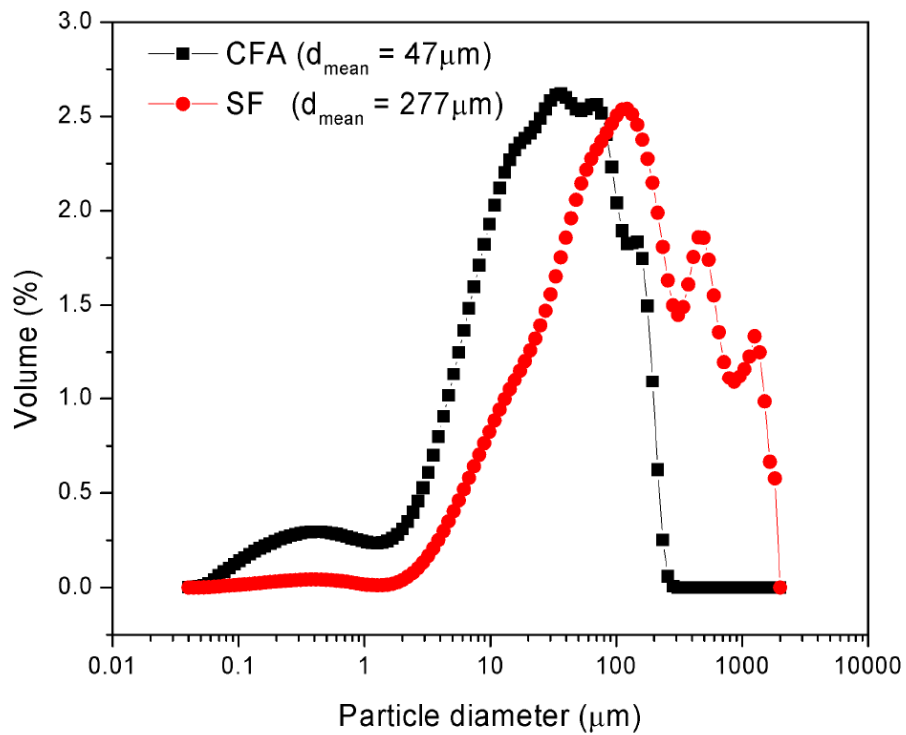
FIGURE 5-3: Particle size distribution of CFA and SF (volume %)
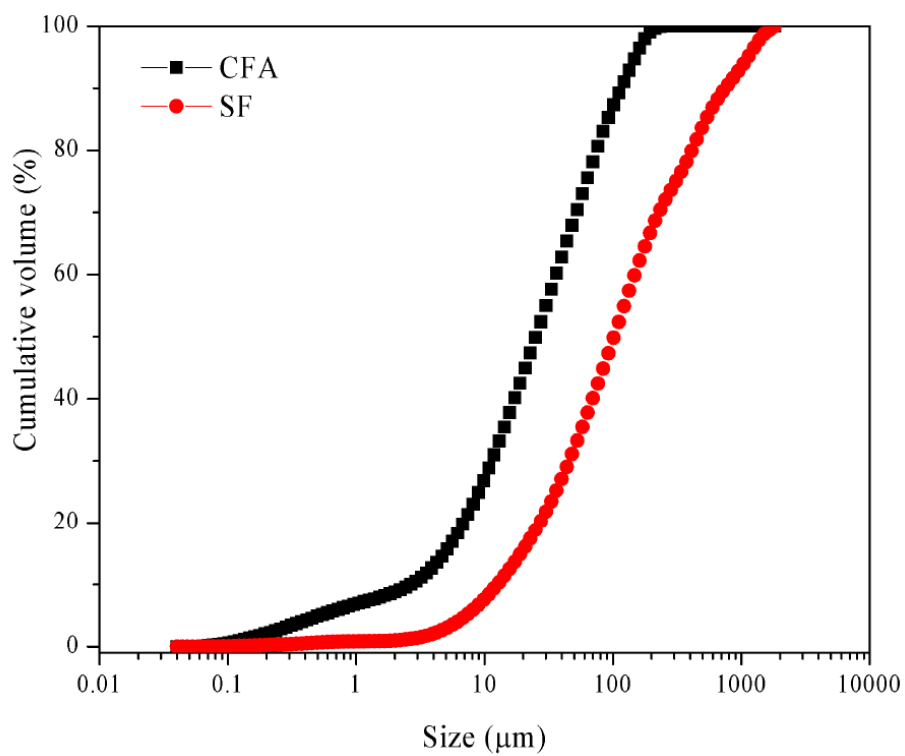
FIGURE 5-4: Particle size distribution of CFA and SF (cumulative volume %)

5.3   Compressive Strength of the Geopolymer Concrete

Compressive strength of the geopolymer concretes was determined at 7 and 28 days in accordance to the standard test method for compressive strength of cylindrical samples. FIGURES 5-5 and 5-6 present the average compressive strength from three specimens of the geopolymer samples cured at 75°C and ones cured without heat.

For the heat cured geopolymer concrete (FIGURE 5-5), the GPC sample exhibit the highest strength, with 7 day strength of 47 MPa and 28 days strength of 56 MPa. The lowest compressive strength was measured in the GP1 sample with 0.5% hydrated lime content. The 7 days strength is 37 MPa and the 28 days strength is 42 MPa which are lower than the strengths measured in the GPC specimens that do not contain additional hydrated lime. When 1.0% hydrated lime was added (GP1), the strength of the concrete increased slightly to 44 MPa for 7 days and 51 MPa for 28 days. Further addition of lime up to 2.0% resulted in reduction in the strength of the GP3 geopolymer concrete to 42 MPa at 7 days and 43 MPa at 28 days.
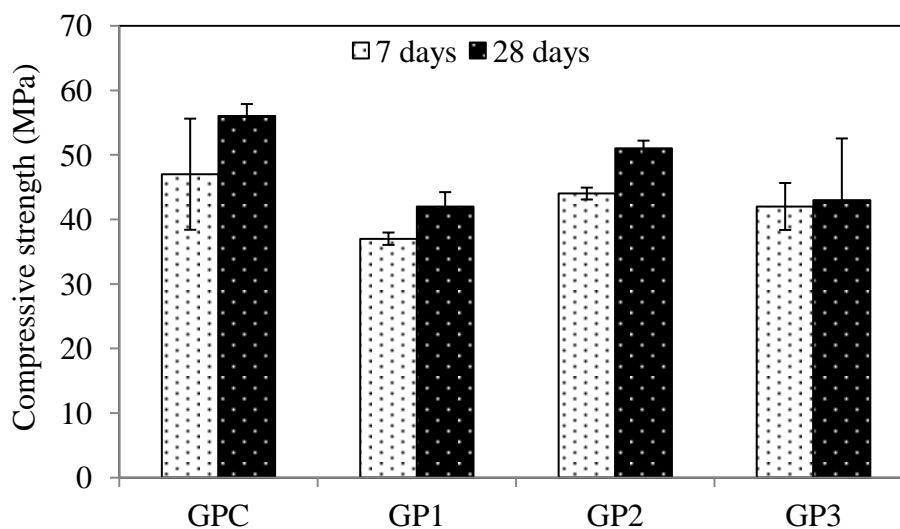
FIGURE 5-5: Compressive strength of the geopolymer concrete cured with heat

The highest compressive strength of the geopolymer concrete cured without heat (FIGURE 5-6) is less than 20 MPa for all the geopolymer concrete samples. The 7 days compressive strength of the GPC and GP1 sample are the lowest strength (7 MPa) which increase gradually by 1 MPa as the hydrated lime content increases from 1.0% and 2.0% in the GP2 and GP3 samples respectively. At 28 days on the other hand, the GPC produces the highest compressive strength of 18 MPa which reduces as the amount of hydrated lime in the geopolymer concrete increases from 0.5% to 1.0% and finally 2.0% in the GP1, GP2 and GP3 samples. According to Yip et al. (2005), previous studies found that the addition of calcium should positively impart the compressive strength of geopolymers, but that same conclusion cannot be made for the geopolymer concretes produced in this study.

All the geopolymer concretes produced except the 7 days sample cured without heat shows reduction in the overall compressive strength as the content of hydrated lime increases from 0% to 2%. In all these samples, there was an observed increased in compressive strength at 1.0% hydrated lime content when compared with the previous sample with 0.5% hydrated lime. The most important observation from the result is that the heat cured geopolymer concrete produced the highest compressive strength and the average 28 days compressive strength of samples exceeds the design strength of 41 MPa (6,000 psi).

Kruskal-Wallis test and Tukey-Kramer HSD pairwise comparison test conducted at 95% confidence level ($\alpha = 0.05$) are the statistical analysis tools used in this section. The results from the statistical analysis are presented in appendix C. According to the Kruskal-Wallis test result shown in appendix C1, the 7 days compressive strength of the

geopolymer concrete cured without heat are not significantly different (p-value = 0.0216). The Tukey-Kramer pairwise comparison of the compressive strength showed that the following pairs have significantly different compressive strength: GP3vs GPC (p-value = 0.0009), GP3 vs GP1 (p-value = 0.0042) and GP2 vs GPC (p-value = 0.0158). On the other hand, the 28 day compressive strength of the geopolymer concrete cured without heat (appendix C2) is not significantly different (p-value = 0.4415), so there is no need for pairwise comparison.

As shown in appendix C3 and C4, the 7 day compressive strength of the geopolymer cured with heat did not show any significant difference (p-value = 0.2479) but the statistical analysis of 28 days strength reveals that there is significant difference (p-value = 0.0237) between the compressive strength of the geopolymer concrete samples. The pairwise comparison showed the some pair of the geopolymer concrete samples: GP2 vs GP1 (p-value = 0.0312) and GPC vs GP3 (p-value= 0.0488) have compressive strength that are significantly different.
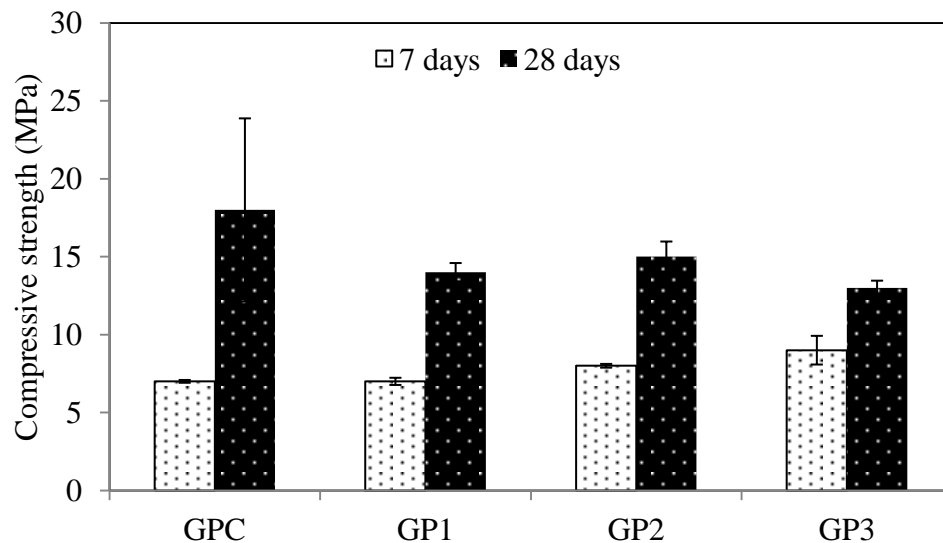
FIGURE 5-6: Compressive strength of geopolymer concrete cured without heat

5.4   Acid and Base Neutralization Capacity (ANC/BNC)

The quantity of acid or base added to each material to maintain a constant pre-defined pH value is termed the acid and base neutralization capacity (ANC/BNC) of the material. The amount of acid and base required to bring the starting materials and produced geopolymer concretes to pre-defined pH values were determined by completing the pretest titration outlined in the draft USEPA method 1313 (USEPA, 2009b) and used to plot the acid/base titration curve of the samples.

The ANC/BNC procedure involves adding samples of the material into eight containers containing deionized water and acid or base at liquid to solid ratio (L/S) of 10. pH of the resulting suspension was measured after 24 hours and used to plot the ANC/BNC curve of the material. FIGURES 5-7 to 5-12 show the ANC/BNC curves of CFA, SF, GPC, GP1, GP2, and GP3. Information from these figures shows the natural pH of the materials when acid addition is zero milliequivalent (meq) per gram of the material. Other information shown is the acid or base addition that will get the material to the target pH values of 1, 3, 5, 7, 9, 11 and 13 required for the pH dependence extraction.
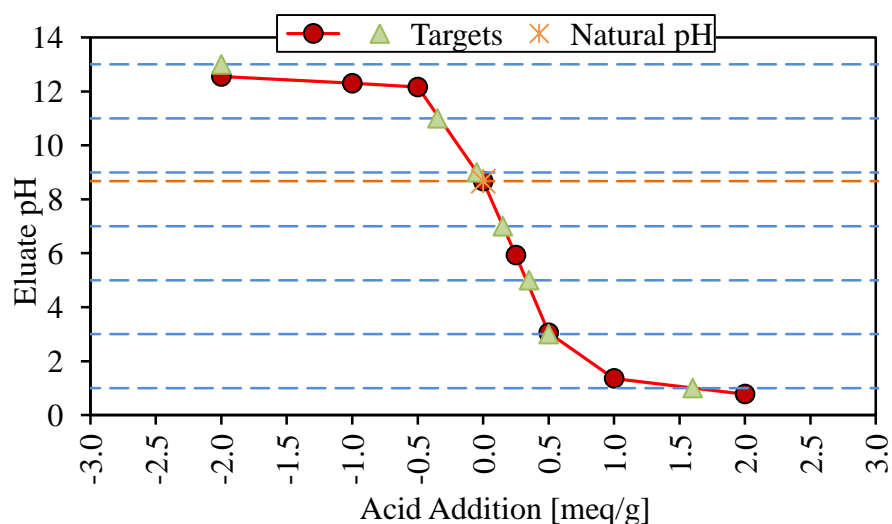
FIGURE 5-7: ANC/BNC curve of CFA
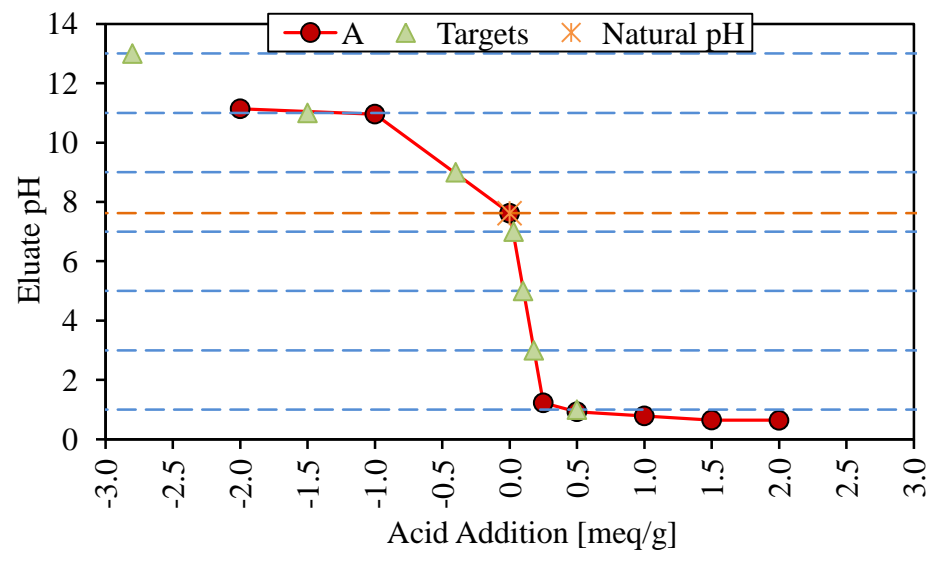
FIGURE 5-8: ANC/BNC curve of SF
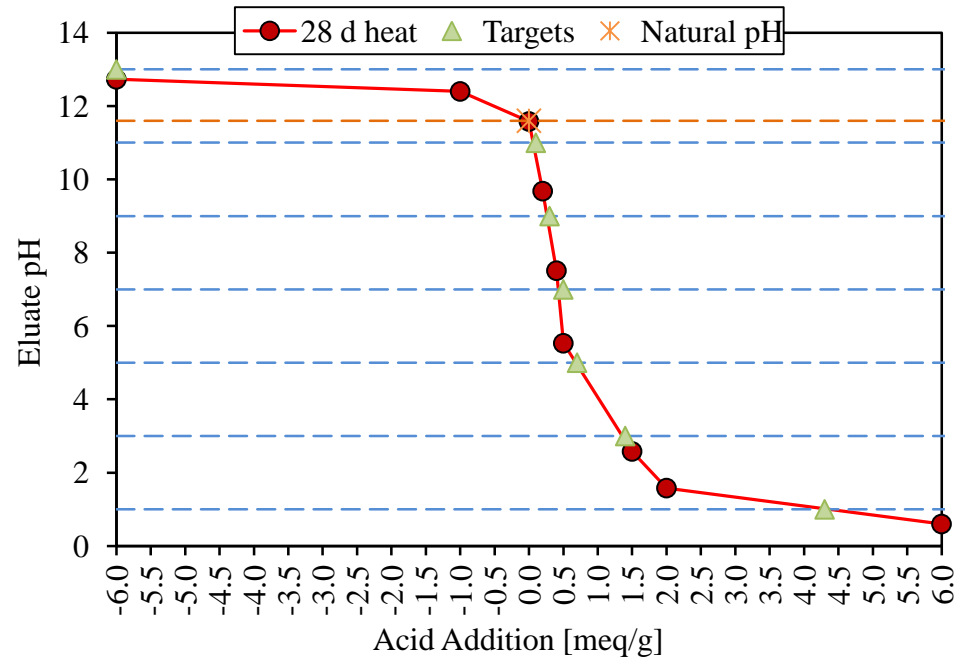
FIGURE 5-9: ANC/BNC curve of GPC
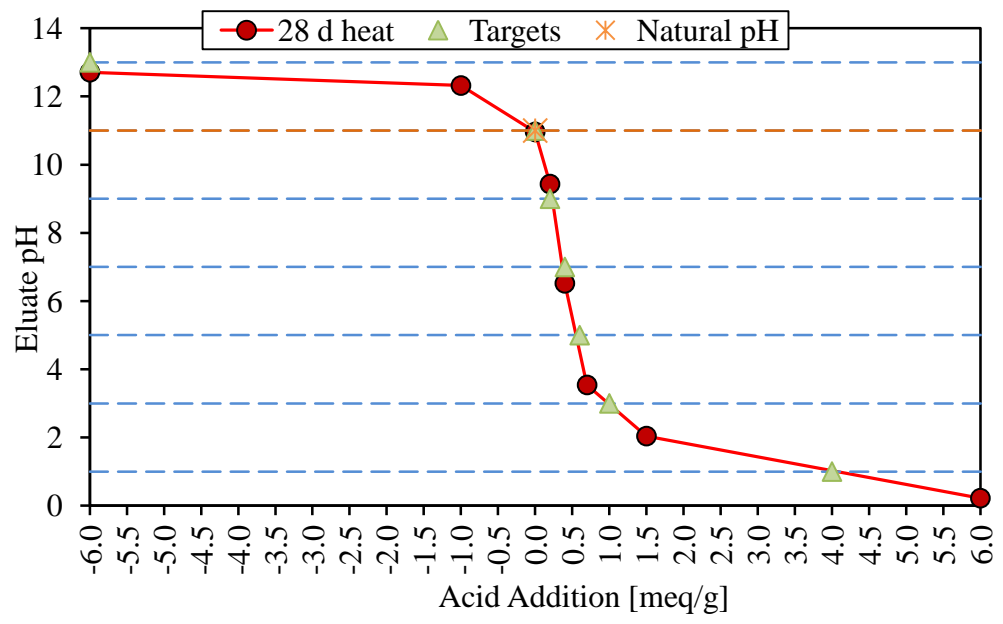
FIGURE 5-10: ANC/BNC curve of GP1
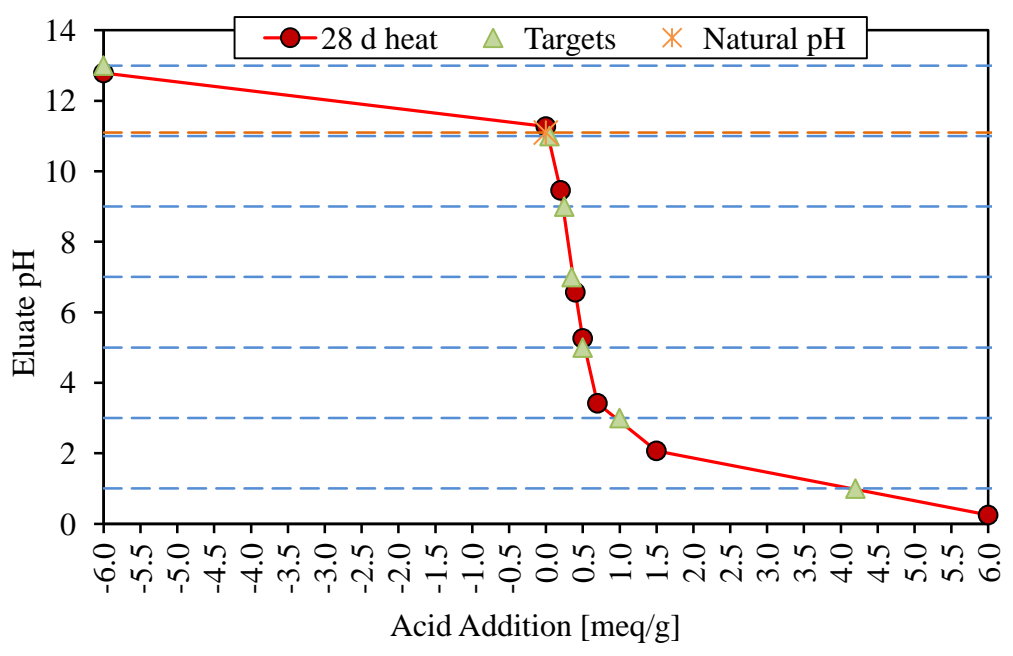
FIGURE 5-11: ANC/BNC curve of GP2
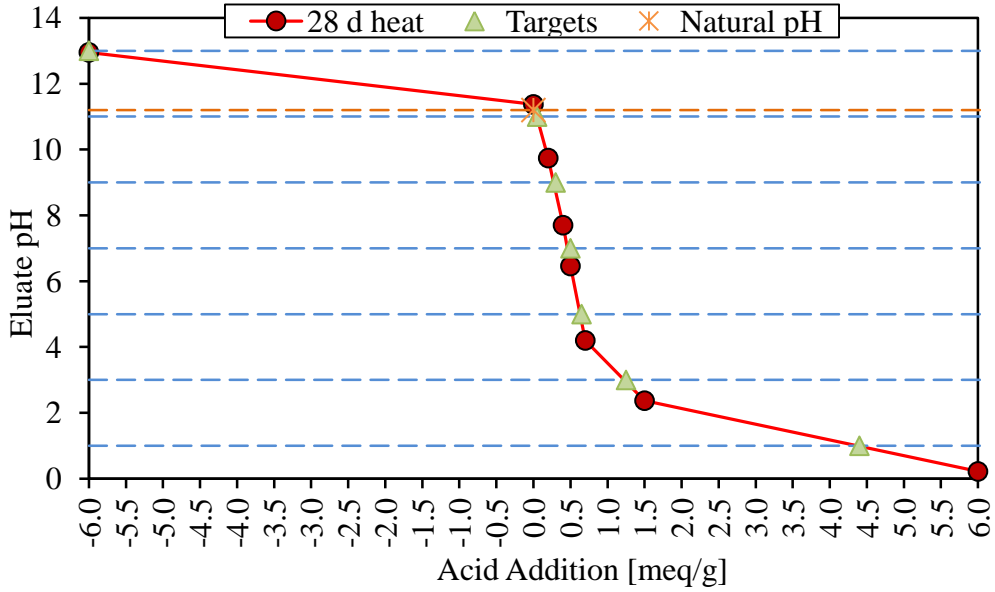
FIGURE 5-12: ANC/BNC curve of GP3

5.5   Material Natural pH

Natural pH of the materials was determined from the pre titration test conducted to determine the ANC/BNC as shown in FIGURES 5-7 to 5-12. TABLE 5-2 summarizes the natural pH of all the materials. According to TABLE 5-2, the CFA and the geopolymer concrete samples (GPC, GP1, GP2, and GP3) are all alkaline materials while the SF has a pH that makes it a material with neutral pH.

TABLE 5-2: Natural pH of the materials

Material	Natural pH
CFA	8.67
SF	7.62
GPC	11.60
GP1	11.00
GP2	11.10
GP3	11.20

5.6   Moisture Content and Bulk Density

As-received moisture content of the materials was determined by drying the samples at 105°C for 24 hours. As shown in TABLE 5-3, most of the materials have moisture content greater than 1%, only the SF has moisture content of less than 1%. Bulk density of loose dry fly ash is reported to be about 1,000 kg/m^3(Sear, 2001) but the CFA has a bulk density of about 900 kg/m^3. The bulk density of the monolithic geopolymer concretes were determined to be 2300 kg/m^3.

TABLE 5-3: Moisture content and bulk density of the materials

Material	Moisture content (%)	Bulk density (kg/m^3)
CFA	1.8	897.8
SF	0.5	378.4
GPC	1.4	2300.0
GP1	1.7	2300.0
GP2	1.9	2300.0
GP3	1.9	2300.0

5.7   Summary

The geopolymer concretes are alkaline material with pH > 11 and bulk density of 2300 kg/m^3. This bulk density is equivalent to the density of normal weight concrete. The average 28 days compressive strength of the heat cured geopolymer range from 42 MPa (6013 psi) to 56 MPa (8117 psi) while the average 7 days compressive strength is 37 MPa (5367 psi) to 47 MPa (6817 psi). In terms of 28 days compressive strength, the heat cured geopolymer concrete is similar in strength to high strength concrete with compressive strength of about 40 MPa (6,000psi) (Mehta and Monteiro, 2006). On the other hand,

geopolymer concretes cured without heat have average 28 days compressive strength that ranges from 13 MPa (1937 psi) to 18 MPa (2647 psi) and an average 7 days compressive strength that ranges from 7 MPa (1015 psi) to 9 MPa (1305 psi). It is obvious from the results that heat curing is a requirement for the production of geopolymer concrete with acceptable compressive strength for structural uses. Hydrated lime did not positively impact the compressive strength of the geopolymer concretes, it result in the reduction in strength of geopolymer concrete as the lime content increases but exhibit high strength at the optimal lime addition of 1%.

Due to the presence of efflorescence on the surface of the geopolymer concretes cured without heat and their low compressive strength, the material was not considered for further investigation since it would only be suitable for low strength structural applications like walkway, curbs and road divider. The heat cured geopolymer concretes on the other hand are considered for further investigation because they meet the basic strength requirement (40 MPa or 6000 psi) for concrete used in high strength structural applications.

CHAPTER 6: LABORATORY LEACHING TEST METHODS

6.1   Introduction

The leaching test methods designed to evaluate leaching of elements from cementitious material such as geopolymer concrete samples during their service life (in monolith form) and at the end of service life (in granular form) are presented in TABLE 6-1. Batch leaching test such as the pH dependence test, water leach test and Dutch availability test are considered for granular state of the samples while the tank test is used for monolithic state of the samples. After completion of the leaching test, the samples were filtered and the filtrate (leachate) for cation analysis was acidified to pH < 2 using 50% HNO_3 in order to minimize metal precipitation and adsorption onto the sample containers prior to using the inductively coupled plasma atomic emission spectroscopy (ICP-AES). Ion chromatography (IC) was used for anion analysis of water leached samples and the leachates were not acidified.

According to the preliminary investigation presented in Section 3.6.1, elements such as As, Cr, Se, V and Mo that form oxyanion leach out more in the high pH condition similar to the alkaline state that would exist in the pore solution of geopolymer concretes. Although the concentration of other elements in the leachates is measured, this chapter would focus mainly on the leaching of As, Cr and Se since they are considered elements with more environmental concerns due to their mobility and toxicity at the different oxidation states.

TABLE 6-1: Relevant leaching test during life cycle of cementitious materials

Material	Life cycle period	condition	Area of use	Relevant leaching test
Cementitious materials	Service life	Monolith	Foundation, Façade, containers, sewer pipes	Tank test
	End of service life (after demolition)	Granular and reduced fragments	Disposal, aggregates in concrete and road construction	pH dependence test Availability test & Column test

Source: Van der Sloot and Kosson (2003)

6.2   pH Dependence Leaching Test

The pH dependence test is conducted to determine mobility of elements from the geopolymer concrete samples when they are exposed to different pH condition. The test was based on the USEPA draft method 1313 (USEPA, 2009b). In this test, deionized water was added to granular/powdered geopolymer concrete samples in nine plastic bottles at L/S ratio of 10. HNO_3 or NaOH was used to maintain the pH to pre-selected pH values of 3, 5, 7, 9, 11 and 13. The amount of HNO_3 or NaOH required to make the material reach the selected pH values was obtained from the pre titration curve presented in FIGURES 5-7 to 5-12. FIGURE 6-1 shows the experimental setup for the pH dependence test. Three method blanks without the samples are added to the pH extraction in order to identify any contaminations that might be introduced by the deionized water, HNO_3 or NaOH. The analyses were carried out in duplicates, stopped after 24 hours and the leachates filtered, then acidified before storing at 4^oC.

FIGURE 6-1: pH dependence test experimental setup

The concentrations (mg/l) of elements measured in the leachates using the ICP-AES were used to calculate the amount of the element leached (mg/kg) from each material. In cases where the measured concentration is less than the detection limit (DL) of the instrument, the concentration value DL/2 was used in the calculation of the amount leached. The average (n=2) result of the pH dependence mobility of As, Cr and Se from the CFA, SF, GPC, GP1, GP2 and GP3 expressed in mg/kg are presented in FIGURES 6-2 to 6-7 while FIGURES D-1 to D-6 in appendix D show the pH dependence mobility of the other elements. As shown in FIGURES 6-2 to 6-4, the mobility of the three elements (As, Cr and Se) is highest at pH 1 but reduces as the pH increases. As mobility from CFA reached 32 mg/kg at pH 1 and reduces to 1 mg/kg at pH 4 and pH 11. The amount leached increases slightly at pH 7 to 4 mg/kg. The highest mobility in the alkaline pH is 7 mg/kg while 32 mg/kg is the highest at the acidic pH range. Mobility of As from the SF

is constant at 8 mg/kg irrespective of the pH although it was difficult filtering the leachates obtained from the extractions between pH 4 and 11.
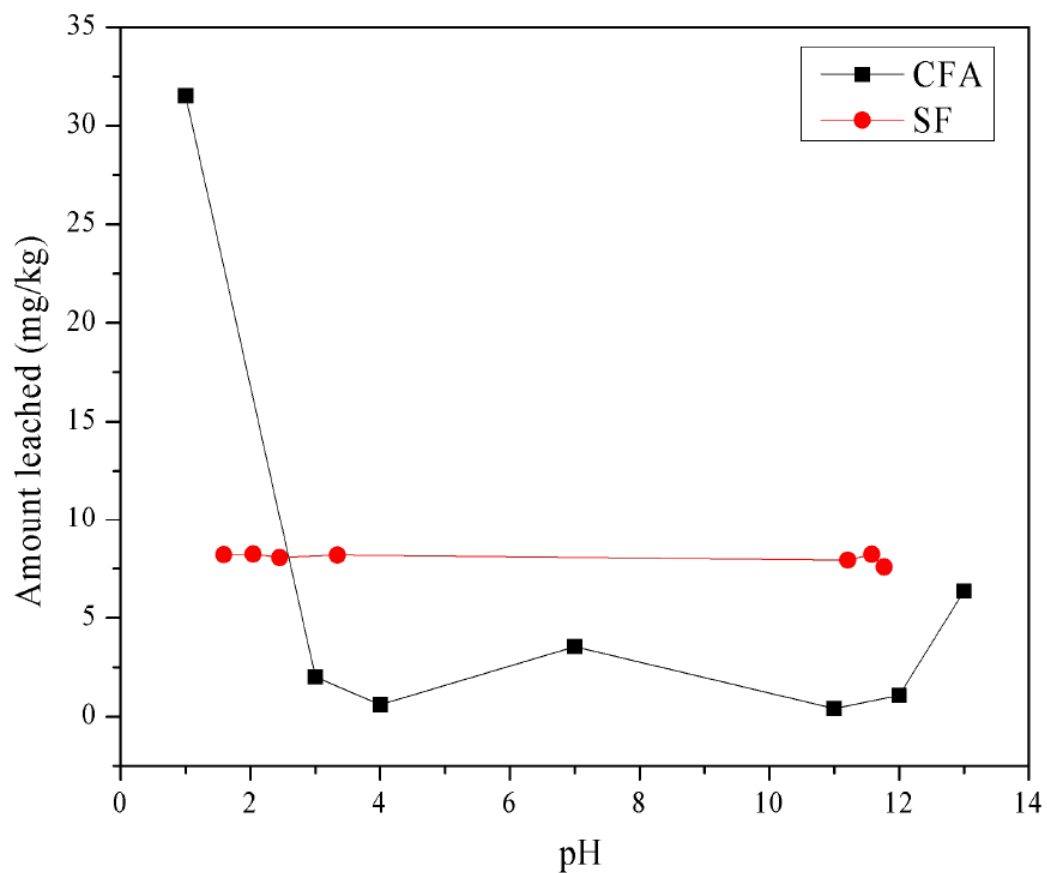
FIGURE 6-2: pH dependence mobility of As from the CFA and SF

The amount of Cr leached from both the CFA and SF is lower than the amount of As leached (FIGURE 6-3). The highest amount of Cr released (18 mg/kg) from CFA occurs at pH 1 while the highest amount released (4 mg/kg) in the alkaline pH occurs at pH 13. On the other hand, the amount of Cr released from the SF is less than 1 mg/kg as shown in FIGURE 6-3.
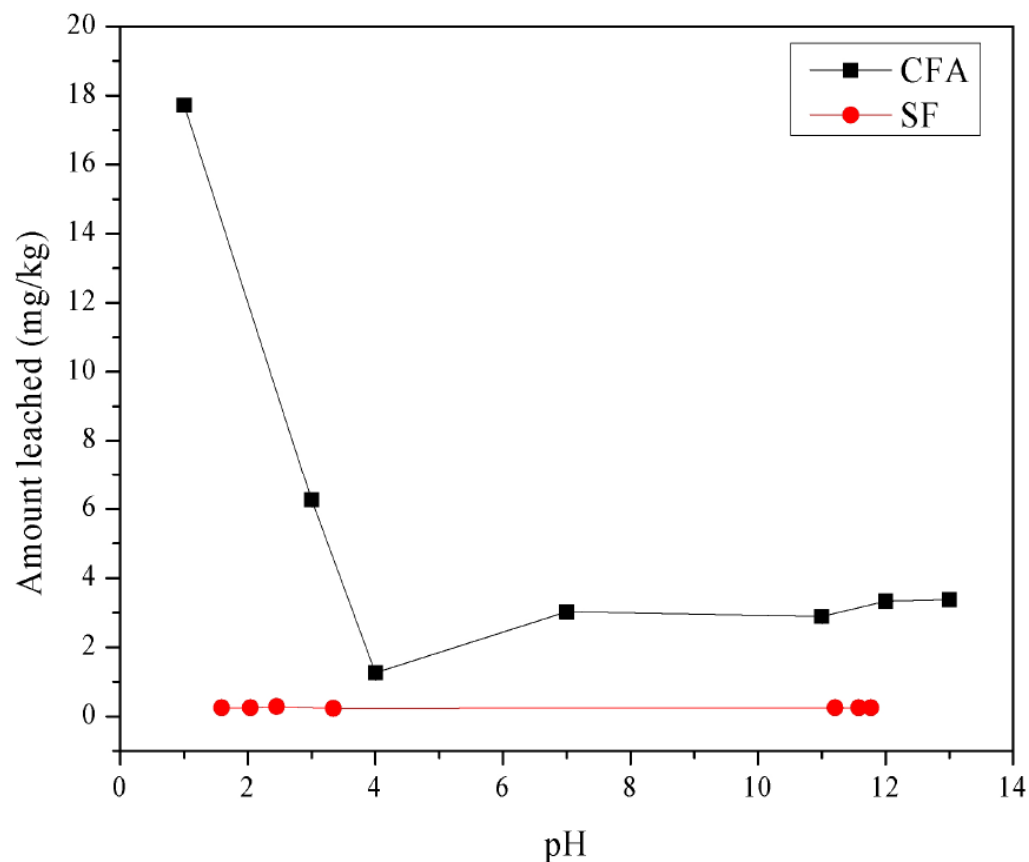
FIGURE 6-3: pH dependence mobility of Cr leached from the CFA and SF

Highest mobility of Se (11.8 mg/kg) occurs in the acidic pH which reduces to the lowest mobility of 1.5 mg/kg at pH 4. At the neutral pH, the amount of the element released increases slightly to 8 mg/kg and then starts to drop to another low mobility of 3 mg/kg at pH 11. After this point, the mobility of Se increases to another high value of 8.5 mg/kg at pH 13. The mobility of Se from the SF is constant at 6 mg/kg from pH 1 to 11, but drops to the lowest amount of 5 mg/kg at pH 13. Presented in FIGURES D-1, D-2, and D-3 in appendix D, the mobility of Al, Ca, Fe, Mg, B, Ba, Cu, Mn, V and Zn from CFA is highest in the acidic pH. Na, Mo and Si have the highest mobility from the CFA occurring in the alkaline pH.
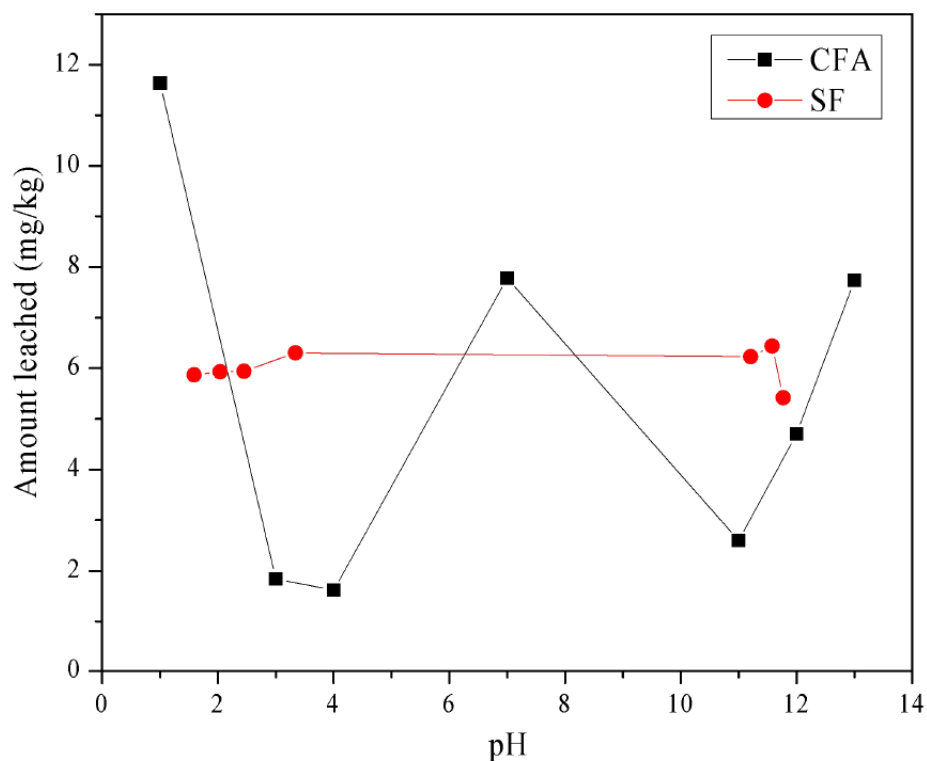
FIGURE 6-4: pH dependence mobility of Se from the CFA and SF

Elements that include Al, Si, Ca, V, Mo and Fe have constant mobility across the pH range (FIGURES D-1, D-2, and D-3 in appendix D). Others like Na and B exhibit higher mobility in the alkaline pH while the remaining elements (Mg, Ba, Cu, Mn, and Zn) displays higher mobility in the acidic pH.

Different pattern of element release were observed from the geopolymer concrete samples as shown in FIGURES 6-5 to 6-7 and FIGURES D-4 to D-6 (in appendix D). In all the geopolymer concrete samples, the leaching of As starting with high value at low pH reduces with increasing pH and reached the lowest value in the pH range of 3 - 7 (FIGURE 6-5). The highest amount leached occurs in the alkaline pH of 13. In the alkaline pH, among all the geopolymer samples, GP2 exhibits the lowest mobility of As while GP3 displays the lowest at pH 1.
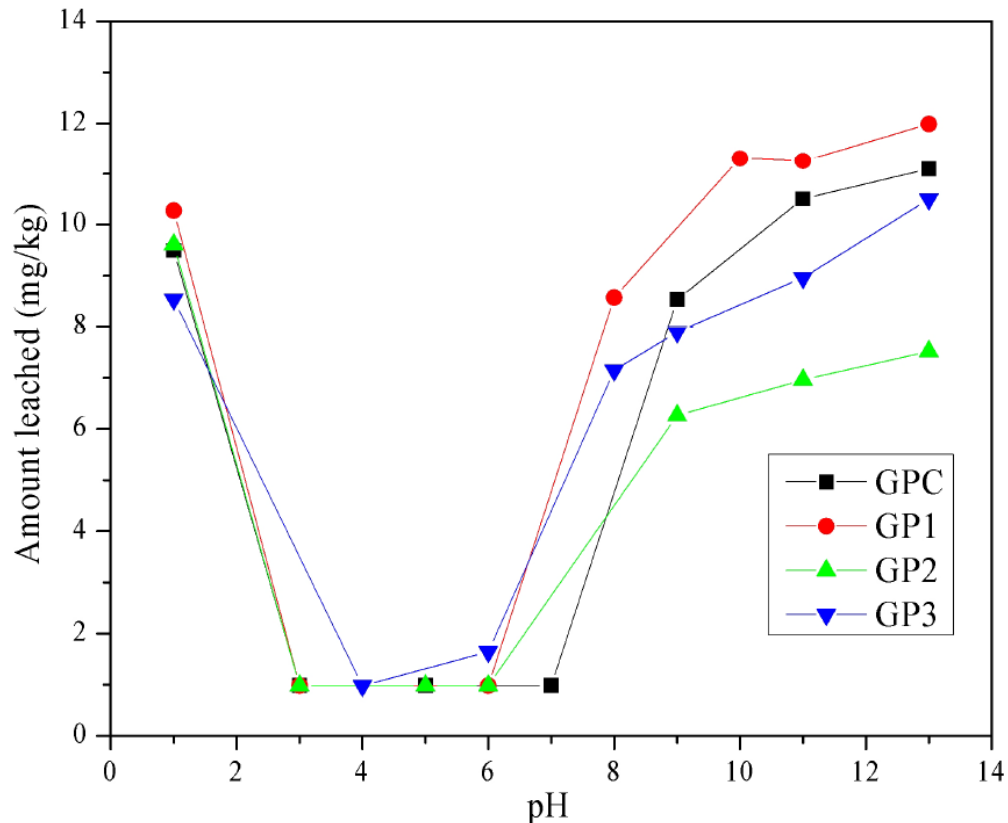
FIGURE 6-5: pH dependence mobility of As from the geopolymer concretes

The mobility of Cr from the geopolymer concrete samples shown in FIGURE 6-6 reveals that the element leach out more at pH 1 but drops rapidly at pH between 3 and 4 depending on the geopolymer concrete sample. The lowest mobility of this element occurs in the alkaline pH range. GP2 samples has the minimum amount of the Cr leached in the acidic pH but the mobility from the other materials becomes the same from pH 5 (FIGURE 6-6).   The concentration of the Cr measured in the leachates from the geopolymer concretes at pH 5 to pH 13 is less than the detection limit (DL) of the instrument.
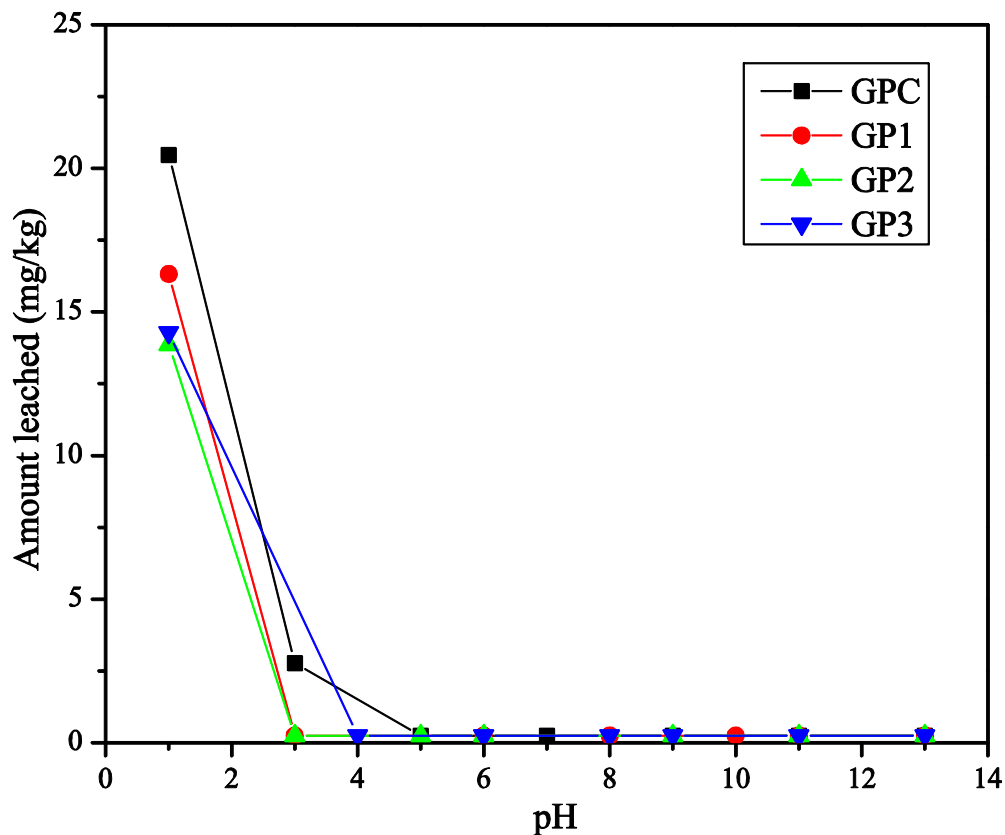
FIGURE 6-6: pH dependence mobility of Cr from the geopolymer concretes

Mobility of Se from the geopolymer concretes presented in FIGURE 6-7 reveals that in most of the samples, the element leach out more in the alkaline pH. The lowest amount of Se was leached at pH between 3 and 6 with an amount 1.5 mg/kg after that its starts to increase as the pH increases until it reached the highest mobility at pH 13. GP2 samples display constant mobility throughout the pH range mainly because the concentration measured in the leachates is less than the DL and the value DL/2 was used to calculate the amount leached from the material. It can be seen from the results presented in FIGURES 6-5 to 6-7 that the mobility of the elements is reduced in the GP2 geopolymer concretes which has 1.0% hydrated lime added during the synthesis. Mobility of two other oxyanion forming elements (Mo and V) presented in FIGURE D-4

in appendix D shows that these elements have the lowest mobility from the GP2 concrete

samples.
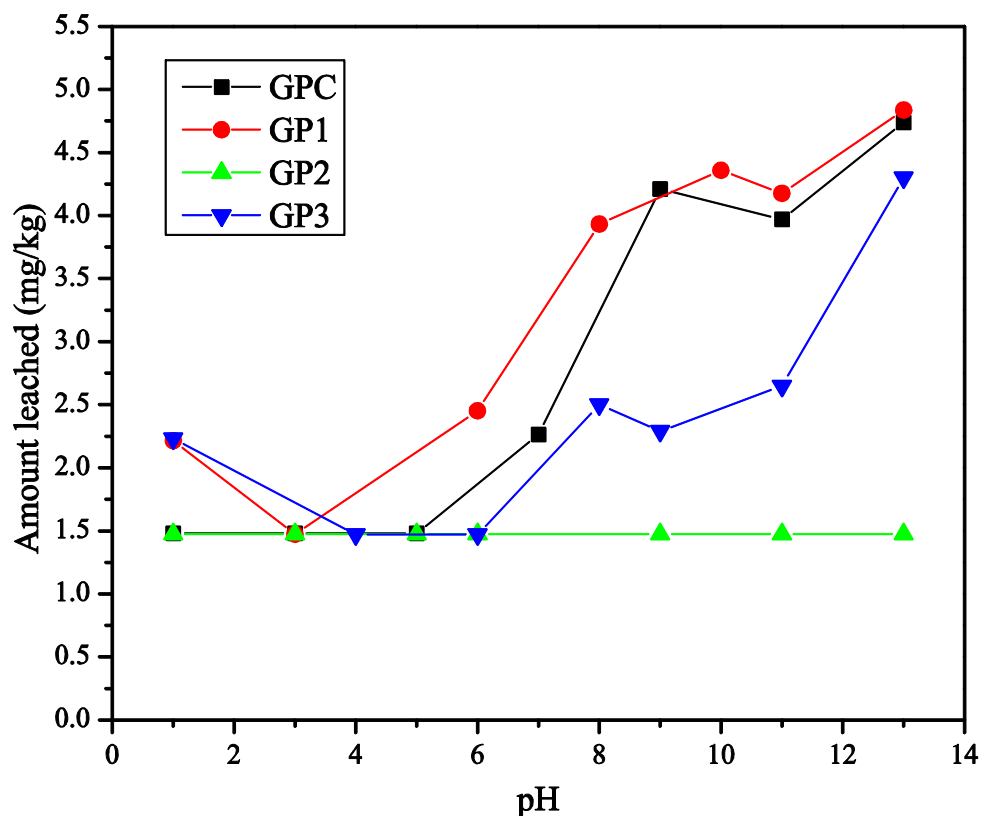
FIGURE 6-7: pH dependence mobility of Se from the geopolymer concretes

Different leaching pattern was observed for the other elements as shown in

appendix D (FIGURES D-5 and D-6). All the elements except Si and Na display higher

mobility in the acidic pH. The mobility of Na and Si is highest in the alkaline pH.

Elements such as Al, Si, Na, Fe, Mg and Ca have very high mobility from the

geopolymer concretes while the mobility of elements like B, Ba, Cu, Mn and Zn are

moderate. In all, mobility from the GP2 sample is still the lowest. This suggests that GP2

geopolymer concrete was able to help reduce the mobility of majority of the elements that

are released from the geopolymer concrete, and may provide an indication of the range of the optimum Ca content required to immobilize majority of the element.

6.3   Dutch Availability Test

The samples was subjected to the Dutch availability test to determine the maximum amount of each element leachable from the starting material and geopolymer samples under the worst-case environmental condition (EA, 2005a). The test is performed at room temperature on size reduced sample (<150 µm) in order to ensure complete dissolution of the constituents (Cappuyns and Swennen, 2008). The test method consists of two extraction steps in which the pH was maintained at 7 and 4 using HNO_3. The extraction at pH 7 is conducted to simulate the leaching of oxyanion forming elements and at pH 4 as the most extreme natural pH condition for cationic elements' mobility (Fällman, 1997).

This test method for which schematic is presented in FIGURE 6-8, 8 g of dry sample was weighed into an acid washed beaker, and deionized water added at a liquid to solid (L/S) ratio of 50. The suspension was agitated using magnetic stirrer while the pH continuously controlled to pH 7 ± 0.5 using 2M HNO_3 for 3 hours after which the mixture was filtered through a 0.45µm membrane filter. The residue from the filtration process was used for the second extraction step and the pH controlled to pH 4 ± 0.5 for additional 3 hours. The liquid obtained after the filtration was combined with the liquid from the first extraction step and acidified to pH < 2 using 50% V/V HNO_3. Concentrations of As, Cr and Se in the leachates are measured using the ICP-AES and were used to calculate the average (n=3) availability of each element from the materials expressed in mg/kg of the tested material.
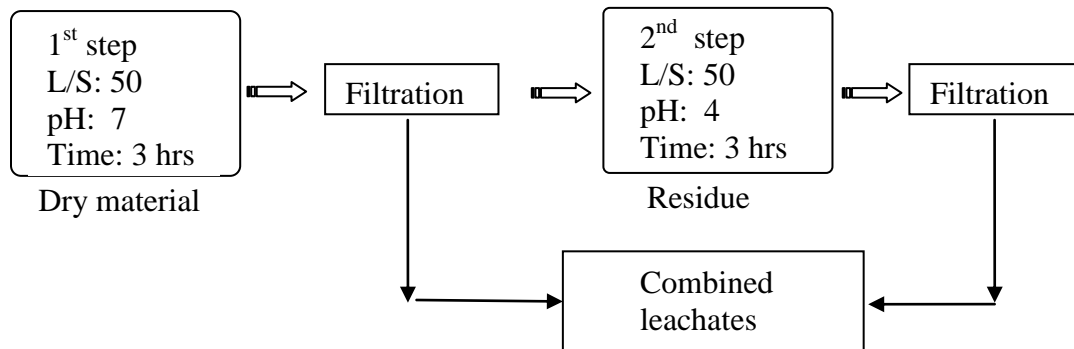
FIGURE 6-8: Schematics of the Dutch availability test

FIGURE 6-9 shows the amount of the elements leached from the CFA and SF while FIGURE 6-10 contains result for the geopolymer concrete samples. It can be seen from these results that As and Se are the two elements that leach considerably from all the materials. The amount of Cr leached is however very small in all the materials tested.
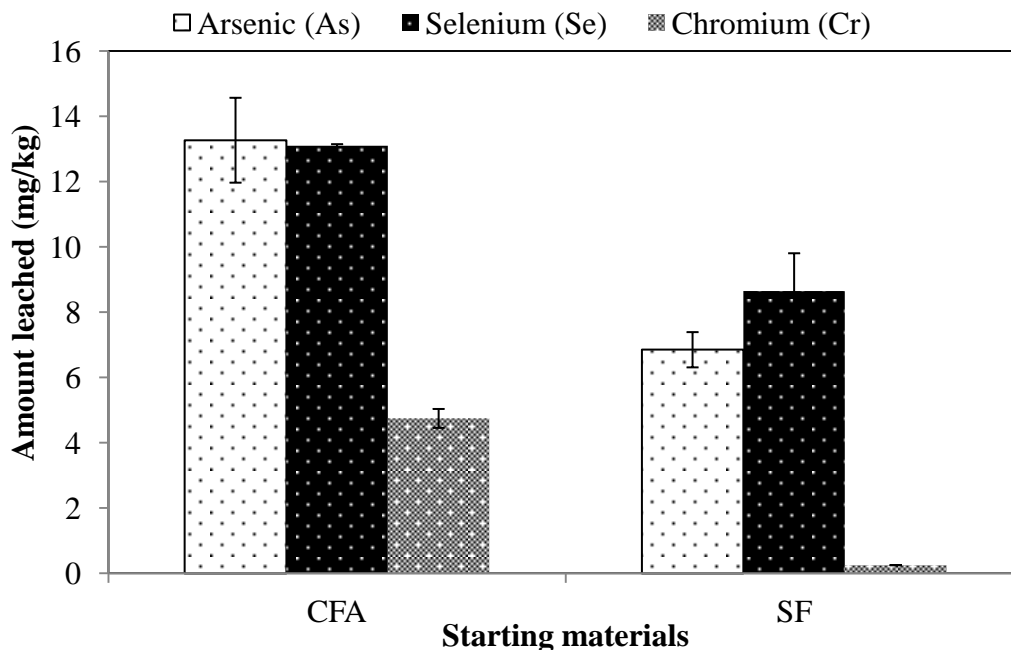
FIGURE 6-9: Availability of As, Se and Cr from the starting materials

According to the availability test result presented in FIGURE 6-9, the mobility of As from CFA reached 13 mg/kg whereas the mobility of Se is about 12.9 mg/kg and Cr is around 4 mg/kg. The SF on the hand indicates more leaching of Se than As and Cr. The amount of Se leached in the SF is 8 mg/kg while the amount of As and Cr released from the material are respectively 7 mg/kg and 0.5 mg/kg. It can be seen from the result that As and Se are readily available for leaching in the starting materials.
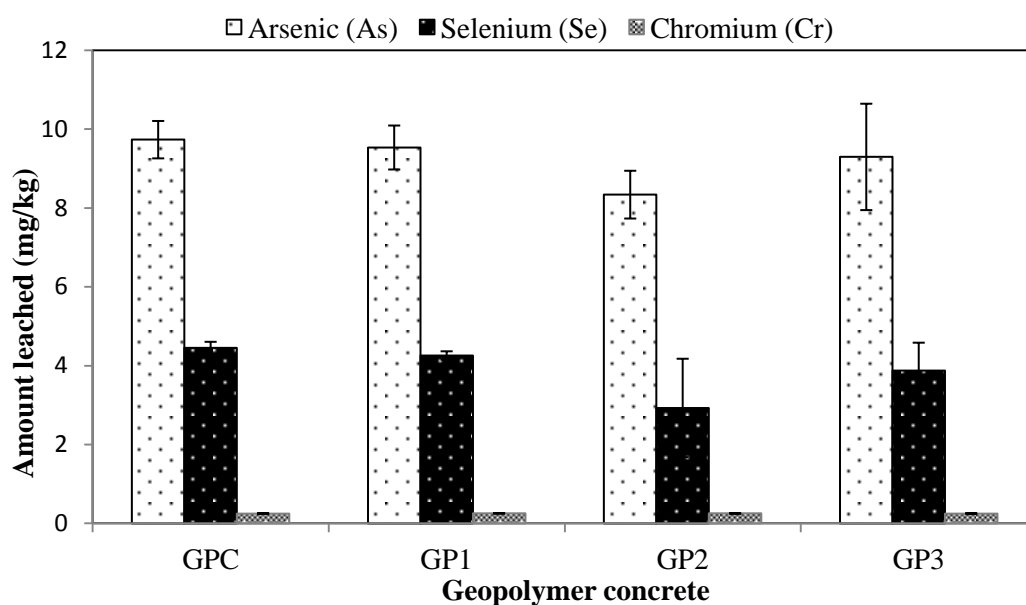
FIGURE 6-10: Availability of As, Cr and Se from geopolymer concrete samples

Mobility of As is highest in all the geopolymer concrete samples (see FIGURE 6-10) with the maximum amount leached close to 10 mg/kg. In the case of Cr, its mobility from the geopolymer concrete is very small which signifies that the material is not readily leachable. One very important observation from the results shown in FIGURE 6-10 is that the GP2 geopolymer concrete have lower amount of leached elements. There was a 10.5% reduction in the amount of As leached from the GP1 to GP2 sample and from GP2

to GP3 sample the mobility of As later increased by 11.7%. The reduction of Se from the GP1 to GP2 sample was 25% and from GP2 to GP3, there was a 10% increase in the mobility. Cr on the other hand, shows almost constant mobility from the geopolymer concrete samples. The result suggests that the GP2 geopolymer concrete with 1.0% additional hydrated lime lead to considerable reduction in the amount of As and Se released from the geopolymer concrete.

6.4   Tank Test

Tank test based on the USEPA draft method 1315 (USEPA, 2009c) was used to determine element mobility from the monolithic fly ash based geopolymer concrete. The test is designed to provide the release rates of the constituent elements in the monolithic geopolymer concrete. In this test, monolithic cylinder sample of the geopolymer concretes was completely submerged or immersed in a given volume of deionized water (FIGURE 6-11 and 6-12) and kept in static condition at ambient temperature. Amount of deionized water added during the test was based on a liquid to solid exposed surface area (L/Sa) ratio of 7 ± 1. The deionized water was replenished with fresh deionized water at nine intervals: 0.08 day, 1 day, 2 days, 7 days, 14 days, 28 days, 42 days, 49 days and 64 days and the weight of the monolith geopolymer determined after each leaching interval in order to measure the amount of water absorbed into the solid matrix at the end of each interval (USEPA, 2009c). The collected leachates were filtered through a 0.45µm membrane filter and later acidified to pH < 2 using HNO_3. Concentration of As, Cr and Se measured in the leachates were used to determined the average (n=2) amount of the elements released from the monolithic geopolymer concrete samples.
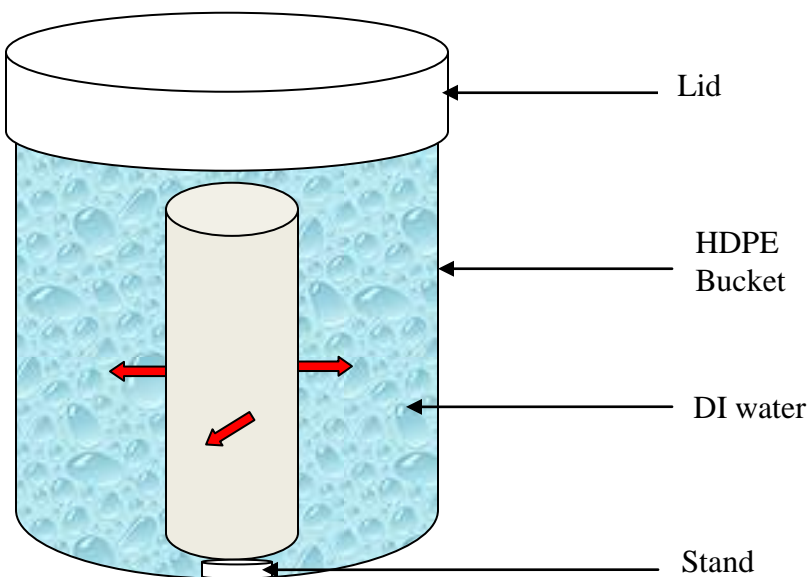
FIGURE 6-11: Schematic of the tank leaching test

FIGURE 6-12: the tank leaching test setup

The release of As, Cr and Se over the leaching duration from the geopolymer concrete is presented in FIGURES 6-13 to 6-15. Each figure shows the cumulative

amount of each element released (mg/m^2) and the release flux (mg/m^2.s) across the exposed surface of the geopolymer concrete. The cumulative release plot and flux plot were used to determine the mechanism responsible for the leaching.
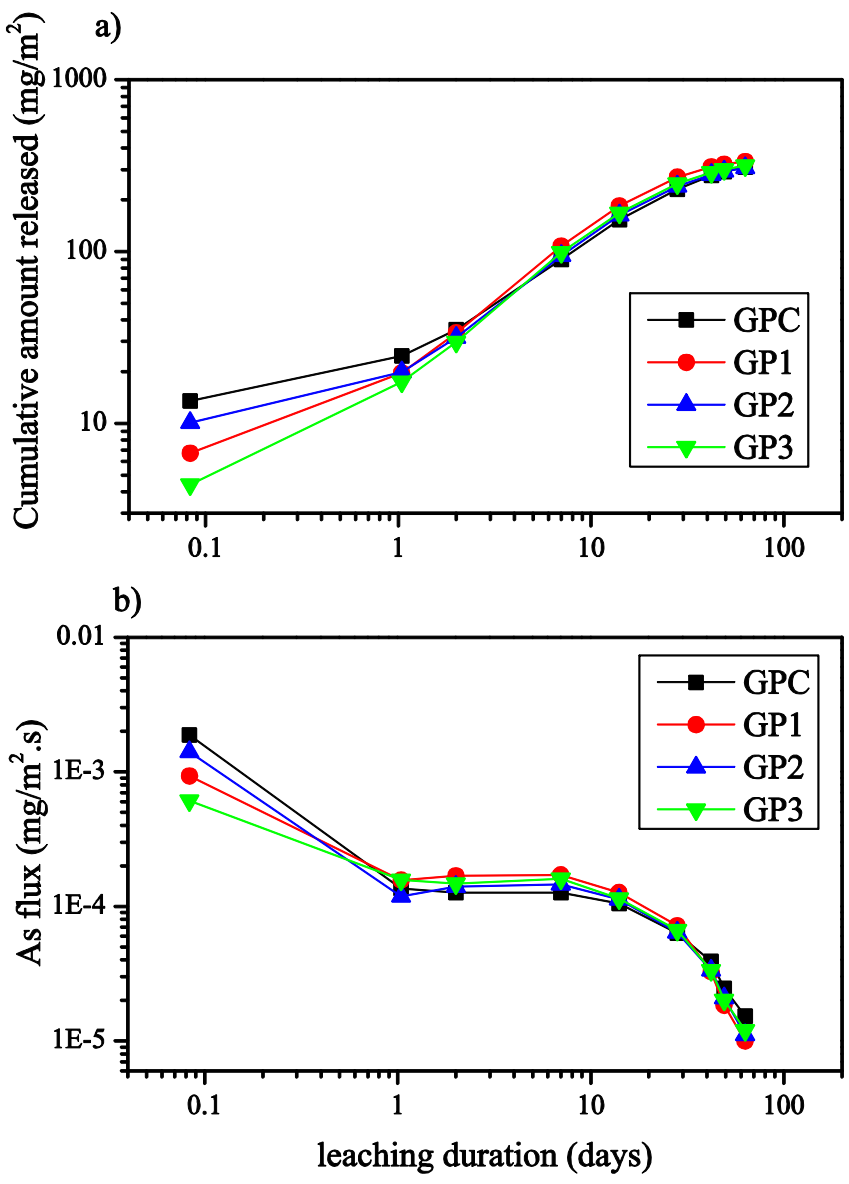
FIGURE 6-13: Release of As from the geopolymer concrete samples

As shown in FIGURE 6-13, the cumulative amount of As released from the geopolymer concretes reached 300 mg/m^2 and the plot can be divided into three regions

which depict the leaching mechanism of the element. From the beginning of the test to 1 day, surface wash-off is the controlling mechanism. This mechanism is due to initial wash-off of soluble material on the outside of the monolith concrete. EA (2005b) reported that the slope of the region is less than or equal to 0.35. Between 1 day and 9 days of leaching, diffusion controlled mobility is the dominant leaching mechanism. This is the normal mechanism responsible for leaching from monolithic materials and the slope of the cumulative release plot is 0.5 ± 0.15 (EA, 2005b). After 9 days of leaching, the dominant mechanism changes to depletion which is associated with reduction in amount of the element released. In the surface wash-off region of the plot, As mobility from the GPC sample is the highest while the lowest mobility occurs in the GP3 sample (FIGURE 6-13) but at the region where depletion dominates, the GP2 sample has the lowest mobility of As (FIGURE E-1 in appendix E).

The cumulative release plot of Se shown in FIGURE 6-14 reveals that the element exhibits the same leaching behavior as As. The leaching mechanism is also divided into surface wash-off, diffusion and depletion. The maximum amount of Se leached in this case reaches 130 mg/m^2. During the initial stage of the leaching, the GP1 and GP3 samples exhibits the lowest release of Se but in the depletion region of the plot, mobility of Se from the GP2 sample is the lowest (FIGURE E-2 in appendix E).
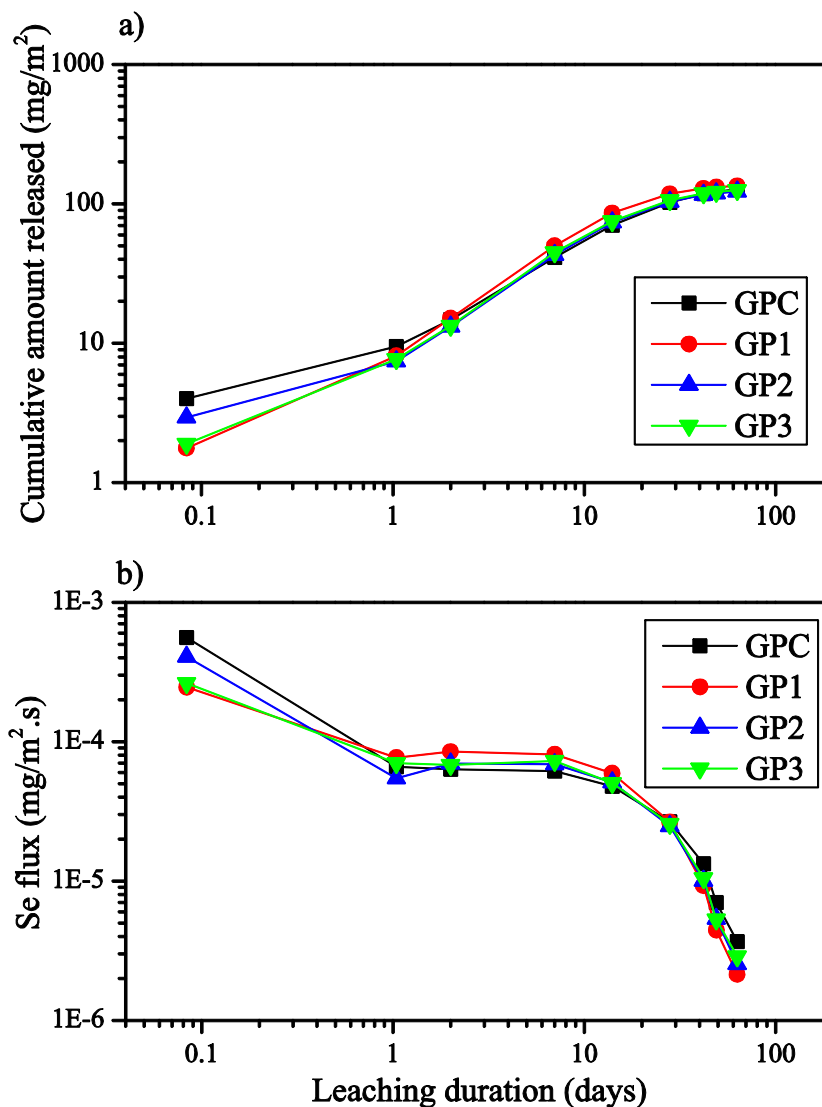
FIGURE 6-14: Release of Se from the geopolymer concrete samples

From FIGURES 6-13 and 6-14, it is obvious that the cumulative release of As and Se tend to a flat plateau towards the end of the leaching duration and the flux tend to zero with the value dropping rapidly towards the end of the leaching. This leads to depletion of the element as the leaching progresses. Cr on the other hand, exhibits an ever increasing cumulative release as shown in FIGURE 6-15. The element does not display similar leaching behavior to the previous two elements; there is still more of the element

available for leaching at the end of the leaching duration. The entire geopolymer concrete sample display the same pattern of Cr release that reached a maximum value of 3 mg/m^2. The release mechanism in this case is a combination of surface wash-off, diffusion and dissolution.
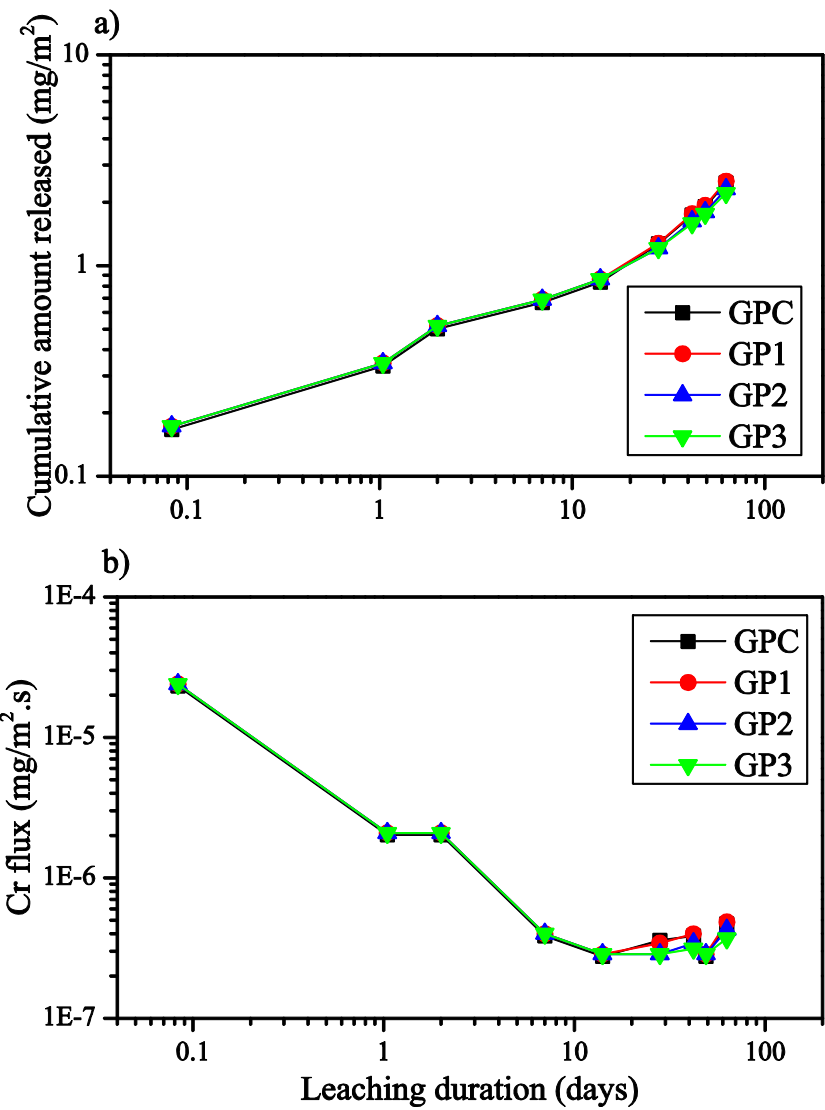
FIGURE 6-15: Release of Cr from the geopolymer concrete samples

The cumulative release plots showed that As has the highest mobility from the geopolymer concretes and that the mobility of As and Se attains a plateau which indicates reduction in elements availability (depletion of the elements). Cr mobility on the other hand continues to increase over the leaching duration.

6.4.1 Leachability Index (LX) of the Elements

To further understand the mobility of these elements from the geopolymer concretes, the fickian diffusion model based on fick's second law of diffusion was employed to determine the leachability index (LX) of the elements (Kosson et al., 2002; Dermatas et al., 2004), which would give the relative mobility of the elements. An analytical solution (Equation 6.1) of the fickian diffusion model which assume zero concentration at the solid-liquid interface (Kosson et al., 2002) was used to calculate the effective diffusion coefficient (D_e) for each leaching interval using the relationship in Equation 6.2.

$$\overline{\qquad} \tag{6.1}$$

$$\underline{\qquad} = \equiv \tag{6.2}$$

Where   is the effective diffusion coefficient for each element (m^2/s), M is the cumulative amount of element leached (mg/m^2), ρ is the bulk density of the monolithic geopolymer concrete (kg/m^3),   is the maximum leachable amount of each element determined from the availability test (mg/kg),   is the cumulative time at the end of the current leaching interval i (s) and   is the cumulative time at the end of the previous leaching interval i-1 (s).

The LX defined mathematically using Equation 6.3 (Pariatamby et al., 2006) was determined from the negative logarithms of the mean effective diffusion coefficient calculated from Equation 6.2. The LX values are presented in TABLE 6-2.

$$\qquad \qquad - \qquad \qquad - \qquad \qquad \qquad \qquad (6.3)$$

Where n is the number of particular leaching period, m is the total number of individual leaching periods, β is a constant (1.0 m^2/s) and D_i is the effective diffusion coefficient of constituent i (m^2/s).

TABLE 6-2: Leachability index (LX) of As, Se and Cr from geopolymer concrete

	LX value		
	As	Se	Cr
GPC	10.6	10.7	11.4
GP1	10.5	10.5	11.4
GP2	10.4	10.3	11.4
GP3	10.5	10.5	11.5

According to Dermatas et al. (2004) and EA (2005b), the relative mobility of the elements or any other contaminants is evaluated using the LX value which varies from 5 (very mobile) to 15 (immobile). TABLE 6-3 contains information used to interpret the LX value. The lower the LX value the higher mobility of the element. The LX value shown in TABLE 6-2 reveals that As and Se have high mobility from the geopolymer concrete samples while Cr has average mobility from the same geopolymer concrete

samples. The LX value can therefore be used in making decision on utilization of the geopolymer concrete. Dermatas et al. (2004) reported that any material that has elements or contaminant LX value less than 8 is not suitable for disposal or utilization in applications such walkways.

TABLE 6-3 :The LX range for different rate of mobility

Low mobility	$LX > 12.5$
Average mobility	$11.0 < LX < 12.5$
High mobility	$LX < 11.0$

Source: EA (2005b)

6.4.2   Depletion of the Elements in Relation to Availability

The amount of each element leached per unit mass in the tank test over the 64 days leaching duration was estimated in order to determine the depletion of the element in relation to the availability as obtained from the Dutch availability test. The amount leached per unit mass in the tank test (U tank) is calculated using equation 6.4.

$$\overline{\qquad}$$
(6.4)

Where U tank is the amount of each component leached in the tank test (mg/kg), C_{64} is the cumulative amount of the element leached after 64 days (mg/m^2), A is the surface area of the sample (m^2), and m is the mass of the sample (kg).

FIGURES 6-16 to 6-18 shows the comparison of the amount of As, Se and Cr leached from the monolith geopolymer concrete in relation to the amount leached using the availability test. As shown in FIGURE 6-16, for the GP1 and GP2 samples, the estimated amount of As leached in the tank test exceeds the amount leached in the availability test.
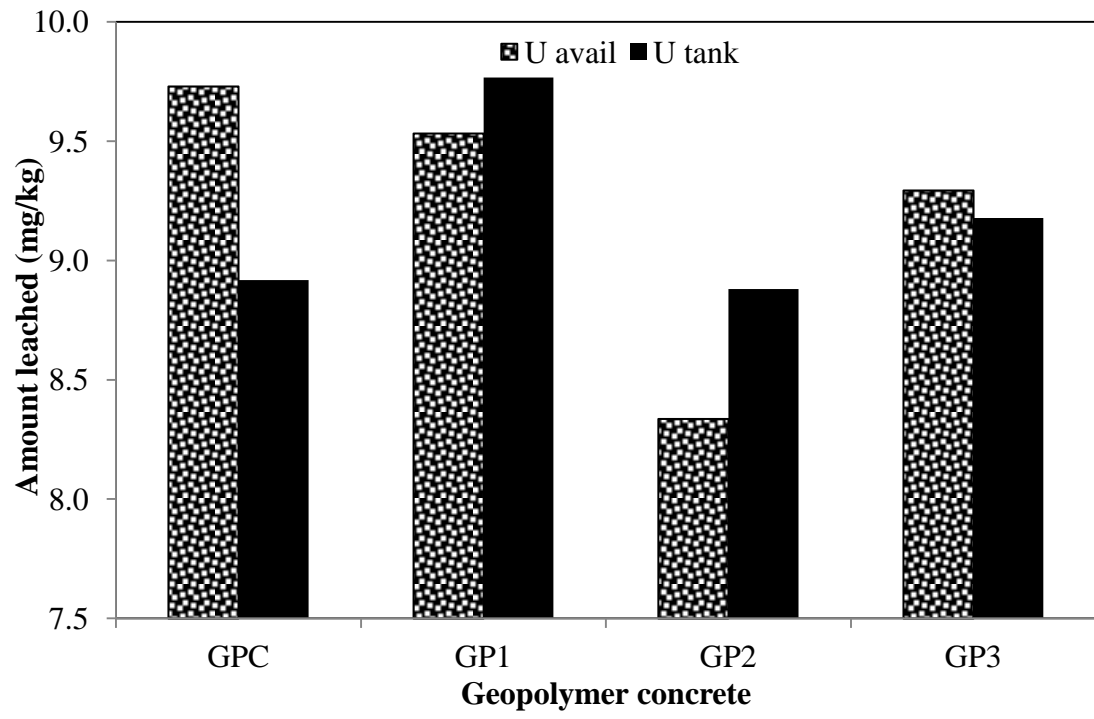
FIGURE 6-16: As availability in tank test in relation to total availability
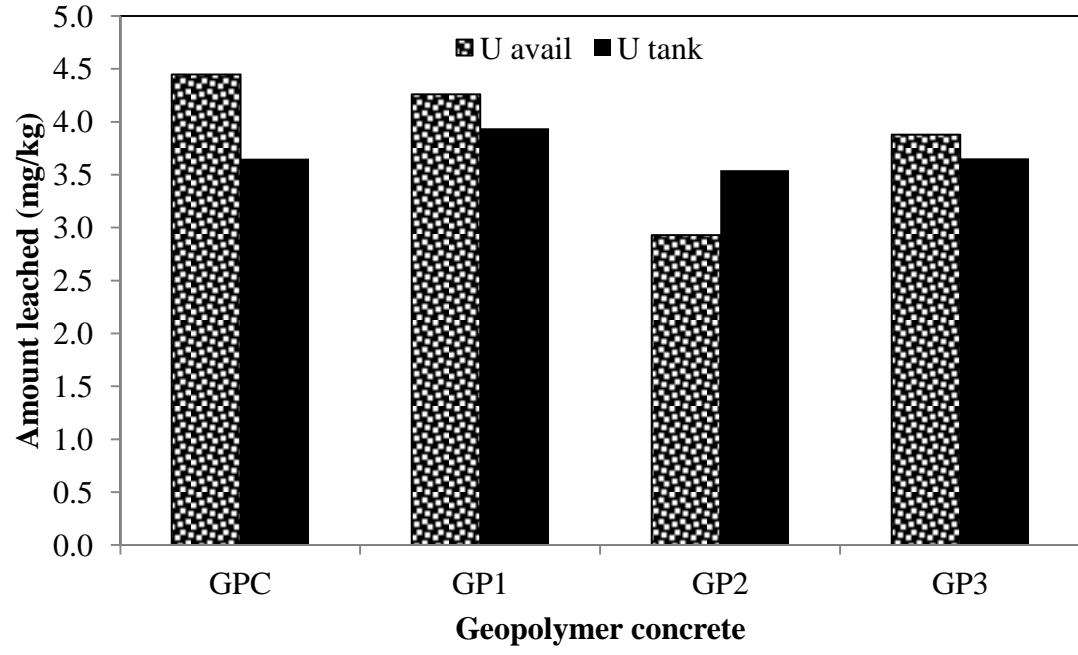
FIGURE 6-17: Se availability in tank test in relation to total availability

The amount of Se estimated in the tank test for GP2 exceeds the amount leached in the availability test (FIGURE 6-17). In the case of Cr, the estimated amount is much lower than the amount leached in the availability test (FIGURE 6-18). These results were used to determine the extent of depletion of the each element. As presented in TABLE 6-4, the extent of depletion is presented as the percentage depletion of each element in relation to the availability. The percentage depletion of As and Se is very high, while Cr have low depletion. The greater than 100 % result suggests that at the end of the 64 days leaching duration, all of the As in GP1 and GP2 and all the Se in GP2 that are available for leaching have been released. On the other hand, result with value less than 100% suggests that there is still some amount of the element that can be leached from the sample.
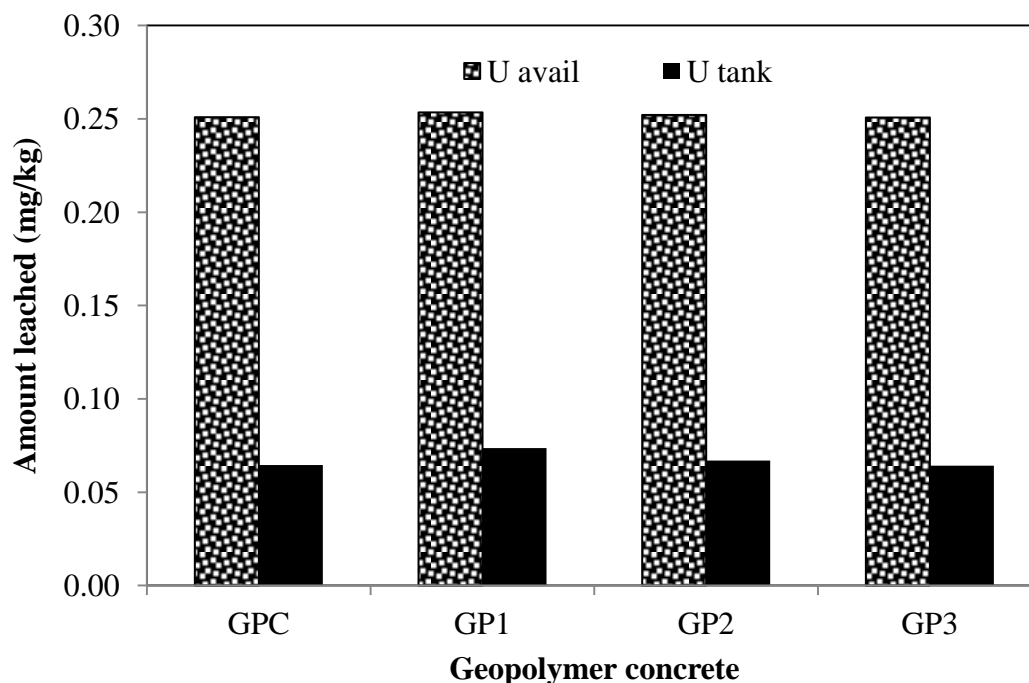
FIGURE 6-18: Cr availability in tank test in relation to total availability

TABLE 6-4: Percentage depletion in relation to total available fraction
Percentage after 64 days (%)

	As	Se	Cr
GPC	92	82	26
GP1	102	92	29
GP2	107	121	27
GP3	99	94	26

6.5   Water Leach Test

The water leach test (WLT) was used to obtain aqueous solution of the concentration of dissolved elements used for the geochemical speciation modeling. Standard procedure described in ASTM D3987(ASTM, 2006c) was used. In this test method, 200 ml of deionized water was added to 10 g of the granular geopolymer concrete sample at L/S ratio of 20. The mixture was agitated for 18 hours and allowed to settle for 15 minutes before filtering through a 0.45μm membrane filter. The ICP-AES and IC were used to respectively measure the concentration of cations and anions in the leachates. TABLE 6-5 shows the measured average (n=2) pH and temperature of the leachates, while TABLES 6-6 and 6-7 contains average (n=2) concentration of cations and anions measured in the leachates. This information is used as inputs into the geochemical modeling program.

TABLE 6-5: Temp and pH of the water leach test leachates

	GPC	GP1	GP2	GP3
pH	11.23	11.26	11.51	11.14
Temperature [C]	25	25	25	25

TABLE 6-6: concentration of cations in the water leach test leachates

Concentration (mg/l)

Elements	GPC	GP1	GP2	GP3
Al	0.45	1.26	0.75	0.69
As	1.02	1.02	1.02	0.93
Ba	0.03	0.03	0.03	0.03
B	1.78	1.79	1.78	1.65
Ca	0.64	1.05	0.78	1.13
Cr	0.03	0.03	0.03	0.03
Cu	0.03	0.03	0.03	0.03
Fe	0.33	0.63	0.47	0.42
Mg	0.16	0.26	0.22	0.19
Mn	0.03	0.03	0.03	0.03
Mo	0.27	0.26	0.26	0.24
Se	0.41	0.42	0.42	0.37
Si	160.00	169.50	183.00	153.00
Na	564.50	556.00	550.00	555.00
V	1.69	1.93	2.11	2.08
Zn	0.03	0.03	0.03	0.03

TABLE 6-7: Concentration of anions in the water leach test leachate

Elements	Concentration (mg/l)			
	GPC	GP1	GP2	GP3
Br^-	0.05	0.05	0.05	0.05
Cl^-	1.20	1.30	1.95	9.70
F^-	0.40	0.40	0.37	0.35
$NO3^-$	0.20	0.11	0.11	0.20
$PO4^{3-}$	31.50	32.50	33.00	16.00
$SO4^{2-}$	155.00	150.00	150.00	145.00

As shown in TABLE 6-5, the pH of the material is greater than 11 which is a confirmation of the material pH result presented in section 5.5. As shown in FIGURE 6-5, concentrations of As, Se, B and Mo are lowest in the GP3 concrete. Higher concentration of Al, Ca, V and Mg were measured in the leachates as the amount of hydrated lime in the geopolymer concretes increases. The high amount of NaOH added during the geopolymer synthesis results in the very high concentration of Na and Si measured in the leachates. Elements such as Ba, Cr, Mn, Zn and Cu have constant concentration in all the geopolymer concrete samples mainly because their measured concentrations in less than the DL of the ICP-AES.

The anion concentrations measured in the leachates (TABLE 6-7) reveal that the concentrations of SO_4^{2-} and PO_4^{3-} are high in all geopolymer concrete products with GP3 exhibiting slightly lower values. Concentration of F^- measured in the leachates are equivalent in all geopolymer with GP2 and GP3 samples containing slightly lower values while Cl^- exhibits an increasing concentration as the amount of added hydrated lime

increases in the geopolymer concrete samples. Br⁻ concentration measured in the leachates is less than the DL of the instrument.

6.6   Risk Associated with Release of the Oxyanion Elements

To assess the potential risk associated with the release of elements from geopolymer concrete especially the oxyanion forming elements (As, Cr, Se), TCLP regulatory limit (TABLE 6-8) was used to estimate the maximum allowable amount of each element that could be released from geopolymer concrete which was then compared with the actual amount of the elements released from the geopolymer concrete as shown in TABLE 6-9. The amount of the oxyanion elements (As, Cr, Se) released from the geopolymer concrete was calculated using results obtained from the WLT conducted using leaching solution at neutral pH (Section 6.5). Although the TCLP test is usually performed using acidic leaching solution, it was still used to estimate the leaching of the oxyanion forming elements from the alkaline geopolymer concrete because TCLP has maximum allowable concentration that can be used to classify material and waste as a characteristics hazardous waste. One limitation of estimating the release of oxyanion elements (As, Cr, Se) using the TCLP regulatory limits is that the actual amount released might be higher than the reported values.

TABLE 6-8: TCLP Regulatory limits of As, Cr and Se

Elements	Concentration (mg/l)
As	5.0
Cr	5.0
Se	1.0

TABLE 6-9: Comparison of amount leached from geopolymer (mg/kg)

	TCLP			Geopolymer		
	As	Cr	Se	As	Cr	Se
GPC	50.68	50.68	10.14	10.37	0.25	4.11
GP1	50.68	50.68	10.14	10.33	0.25	4.24
GP2	50.68	50.68	10.14	10.29	0.25	4.28
GP3	50.68	50.68	10.14	9.37	0.25	3.79

From the result, the amount of As released from the geopolymer concretes is about 20% of the released amount based on the maximum allowable concentration for the TCLP. The amount of Cr and Se released from the geopolymer concrete is also less than the regulatory amount based on the TCLP test.

The risk associated with the oxyanion forming elements (As, Cr, Se) was assessed using the USEPA risk based screening levels which considered only human health risks (USEPA, 2012). Health risks considered are inhalation of particles, incidental ingestion and dermal contact. The assessment was based on residential risk screening level and performed using the risk-based screening level calculator which utilized the combination of exposure assumptions with chemical toxicity values to determine the risk associated levels. TABLE 6-10 shows the calculated residential risk based screening levels for the human health risk considered.

TABLE 6-10: Residential risk based screening levels

Elements	Concentration (mg/kg)		
	Ingestion	Dermal	Inhalation
As	2.35E+01	2.79E+02	2.13E+04
Cr	NA	NA	NA
Se	3.91E+02	NA	2.84E+07

NA – None available

Based on the information in TABLE 6-10, all the amount of oxyanion elements released from the geopolymer concretes are lower than the human risk based screening levels. This suggests that the human health risk associated with the use of geopolymer concrete is minimal.

6.7   Summary

The pH dependence test is a powerful laboratory tool for the environmental assessment of any material. The test on geopolymer concrete reveals that the oxyanion forming elements As and Se are released more in the alkaline pH. In general, the leaching trend for the elements is similar in all the geopolymer concrete samples. Most of the geopolymer concrete displays similar leaching pattern for As and Se and the GP2 sample exhibit the lowest mobility of As and Se in the alkaline pH. Mobility of Cr from the geopolymer concretes is however different, with highest mobility at pH 1 that reduces to negligible amount after pH 4 or 5.

As and Se are elements that are available for leaching from the materials according to the Dutch availability test. The mobility of these two elements from the GP2 sample is the lowest. The tank test showed that As and Se have high mobility from the

geopolymer concretes and that the amount of these element leached from the material approaches a constant value as the leaching duration increases which means that the element are being depleted from the geopolymer concretes. Cr on the other hand has moderate mobility from the geopolymer concretes. The total amount of Cr released from the geopolymer is relatively small but the cumulative amount released from the geopolymer concretes is increasing as the leaching process progresses. After 64 days of leaching As and Se depletion from GP2 exceeds 100% which means that all the element have leached out. Cr on the other hand has low depletion suggesting that there is still some amount of the element available for leaching.

The release of the oxyanion forming elements (As, Cr, Se) from the geopolymer concrete is lower than the estimated release of the elements based on maximum allowable values from the TCLP regulatory limits. Limited risk based assessment performed on the geopolymer concretes indicate that the human health risk (incidental ingestion, dermal contact and inhalation of particles) associated with the material is minimal.

CHAPTER 7: MINERALOGICAL AND MICROSTRUCTURAL CHARACTERIZATION

7.1   Mineralogical and Microstructural Analysis

The mineralogy and microstructure of the crushed, pulverized geopolymer samples and the starting materials was determined using X-ray diffraction (XRD) and scanning electron microscope (SEM).

7.2   X-Ray Diffraction (XRD) Analysis

XRD analysis on the samples aims to confirm the formation of mineral phases that might be responsible for adsorbing the oxyanion forming trace elements. PANalytical X'pert PRO model PW 3040 equipped with θ-θ goniometer and Cu X-ray tube operated at 45 KV and 40 mA that generates Kα radiation with a wavelength of 1.54Å was used. In this analysis, the sample is front loaded into a zero background sample holder and mounted on the instrument's stage. X-rays beams from the x-ray source were irradiated on the sample and the interaction of the x-ray with the sample creates diffracted x-ray beams whose intensity is recorded by the detector (FIGURE 7-1). Diffractogram are produced by collecting data in the 2θ angle range of 4° to 80° with a step size of 0.05^o. The measured peak positions and relative intensity of the diffraction beams are used to determine the crystalline mineral phases present in the samples by comparing the peak positions (2θ) and intensities from the diffractogram to reference data

found in the American Mineralogist Crystal Structure Database (AMSCD). XPowder[1], a

free phase identification software was used for the phase identification.
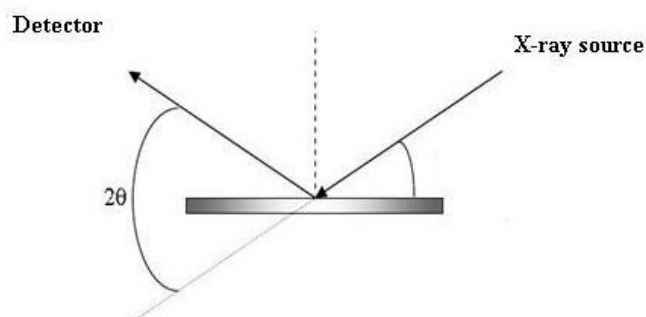
FIGURE 7-1: Schematic of the XRD setup

FIGURES 7-2 to 7-6 show the XRD diffractogram of the starting materials (CFA

and SF) and the geopolymer concretes (GPC, GP1, GP2, and GP3). The diffractogram of

CFA shown in FIGURE 7-2 did not indicate the presence of many crystalline phases,

most likely because there are no sufficient peaks to identify the presence of the phases.

There is a diffuse halo peak at 2θ from 15° to about 35° which suggest the presence of

amorphous content. The two crystalline phases identified in the fly ash sample are quartz

(SiO_2) and mullite ($2Al_2O_3 \ SiO_2$). These two mineral phases are among the principal

minerals found in coal fly ash (Rattanasak and Chindaprasirt, 2009). Mineral phases such

as hematite (Fe_2O_3), and magnetite (Fe_3O_4) are other mineral phases present in coal fly

ash. There was no observed crystalline phases in the silica fume (FIGURE 7-2), there

was however a halo peak located between 2θ angle of between 15° and 30° which

indicate the presence of glassy or amorphous content.

---

[1] XPowder is a software for powder X-ray diffraction analysis
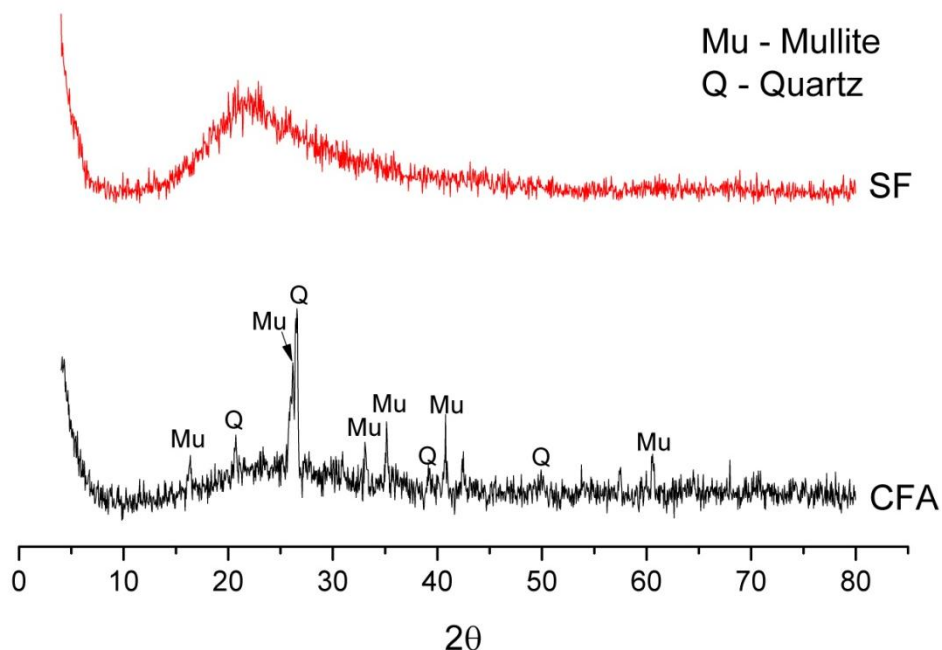
FIGURE 7-2: XRD diffractogram for the CFA and SF used

FIGURE 7-3 shows the diffractogram of the geopolymer concrete with 0% hydrated lime (GPC), some of the crystalline phases present in the material cannot be fully characterized due to peaks with unmatched mineral phases. Minerals that were successfully identified are quartz, riebeckite, and gypsum as shown in the figure. The sample also exhibits a not too noticeable hump at 2θ angle of between 25°-30° that is associated with the amorphous content of geopolymer. Quartz (SiO_2) is the major crystalline phase in the GPC sample which is attributed to the fact that the material contains silica sand used in the production of the geopolymer concrete. The other minerals found in the geopolymer concrete sample are riebeckite ($Na_2(Fe,Mg)_3Fe_2Si_8O_{22}(OH)_2$ - Sodium Iron Magnesium Silicate) and gypsum ($CaSO_4$). Riebeckite is a sodium rich silicate mineral formed in a highly alkali environment, whose

presence in geopolymer mineralogy has not been reported in any literature on the mineralogy of geopolymer. According to Miyano and Klein (1983), riebeckite is formed by reaction of iron oxides and quartz in the presence of water. The presence of a lot of sodium ion, quartz and iron oxides might have actually resulted in the production of riebeckite instead of calcium containing mineral phases. Occurrence of gypsum in the sample might be as a result of the absence of ettringite since gypsum is required for the formation of ettringite or monosulfoaluminate hydrate (Zheng et al., 2011).

FIGURE 7-4 shows the diffractogram of the GP1 sample which contains 0.5% hydrated lime. According to the information in the figure, the addition of 0.5% hydrated lime to the geopolymer system led to the formation of new mineral phases. In addition to quartz, minerals identified in GP1 include bearsite $(Be_2(AsO_4)(OH).4H_2O)$, beraunite $(Fe^{2+} Fe^{3+}_5(OH)_5(PO_4)_4 \cdot 4H_2O)$ and lime (CaO).
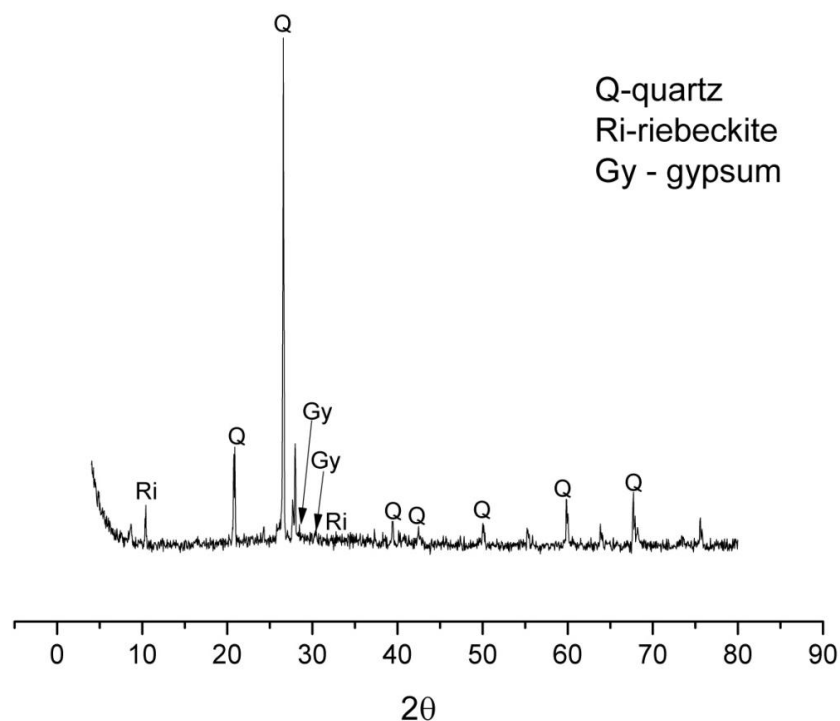
FIGURE 7-3: XRD diffractogram for the GPC geopolymer concrete
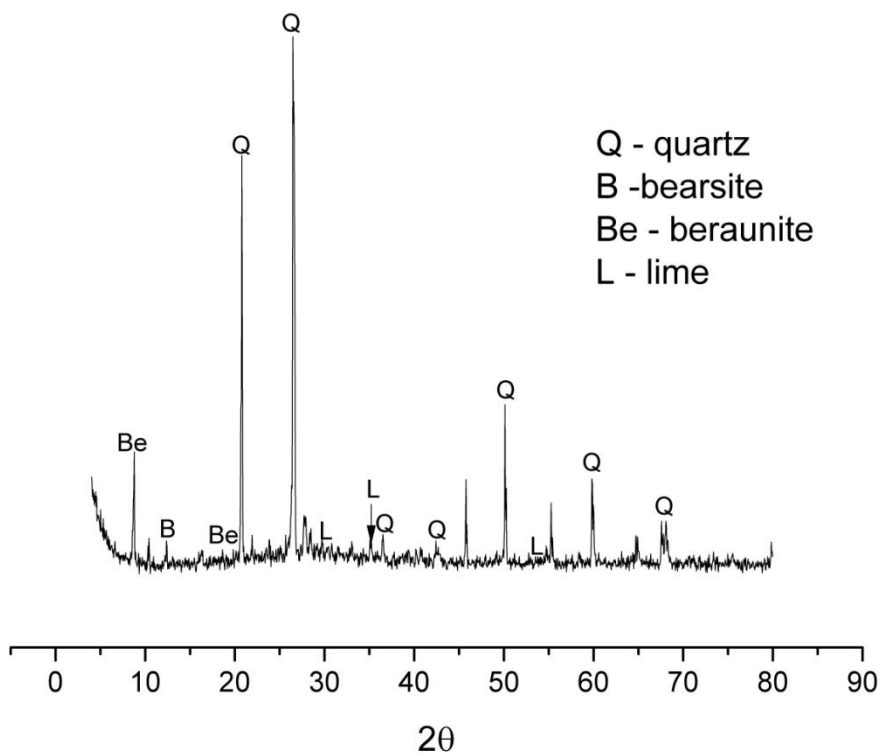
FIGURE 7-4: XRD diffractogram for the GP1 geopolymer concrete

The riebeckite that was found in the GPC has disappeared or is converted to another mineral, most likely beraunite which is a hydrated iron phosphate hydroxide. Other obvious difference between the GPC and GP1 is the presence of lime and bearsite, an arsenic containing mineral phase. The XRD pattern in FIGURE 7-5 shows the mineral phases present in the GP2 sample that contains 1.0% hydrated lime. These diffractogram reveals the presence of quartz (SiO_2), heinrichite ($Ba(UO_2)_2(AsO_4)_2 \cdot 11H_2O$), magnetite ($Fe_3O_4$), downeyite ($SeO_2$), guyanaite ($CrO(OH)$ and cadmoselite ($CdSe$). There seems to be stronger quartz peak and some unmatch peaks. In GP2, there is disappearance of the riebeckite formed in GPC and formation of the bearsite that occurs in GP1. Heinrichite, an asernic containing mineral phase was also found in this sample.
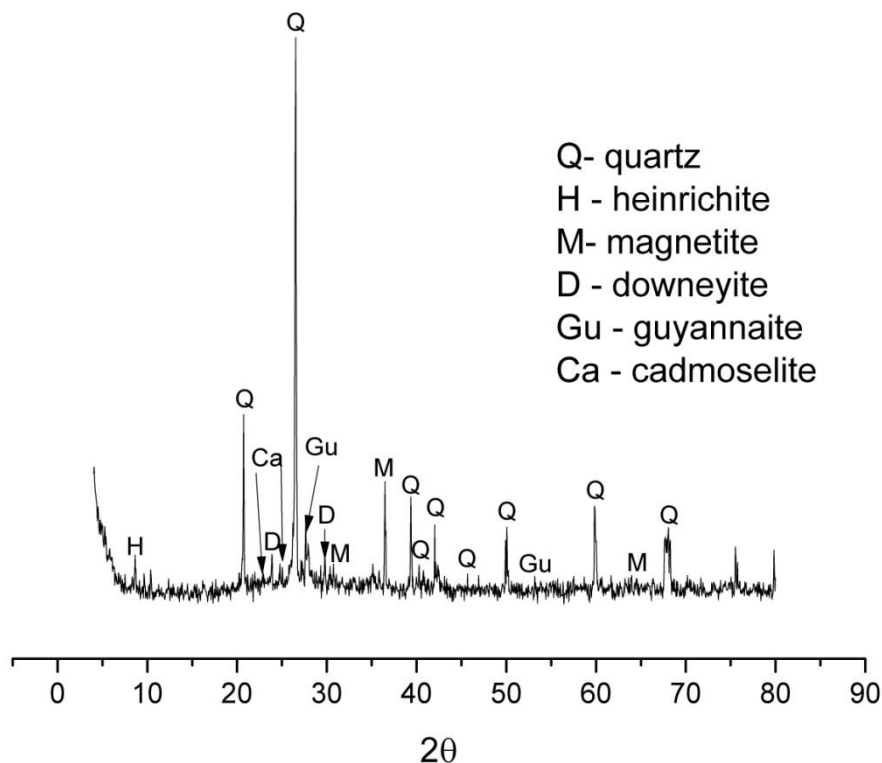
FIGURE 7-5: XRD diffractogram for the GP2 geopolymer concrete

Although the mineral downeyite was identified in this geopolymer sample, the presence of the mineral is doubted because this mineral is reported to be hygroscopic and unstable under normal atmospheric conditions (Finkelman and Mrose, 1977). Only two mineral phases can be successfully identified in GP3 as shown in FIGURE 7-6. These two minerals are quartz and beraunite which are the minerals that can be found in the other geopolymer concrete samples. TABLE 7-1 summarizes the mineral phases identified in all the geopolymer concretes. Only quartz is common to all the geopolymer concrete and beraunite was identified in only the GP1 and GP3 samples. The other mineral phases were only identified once.
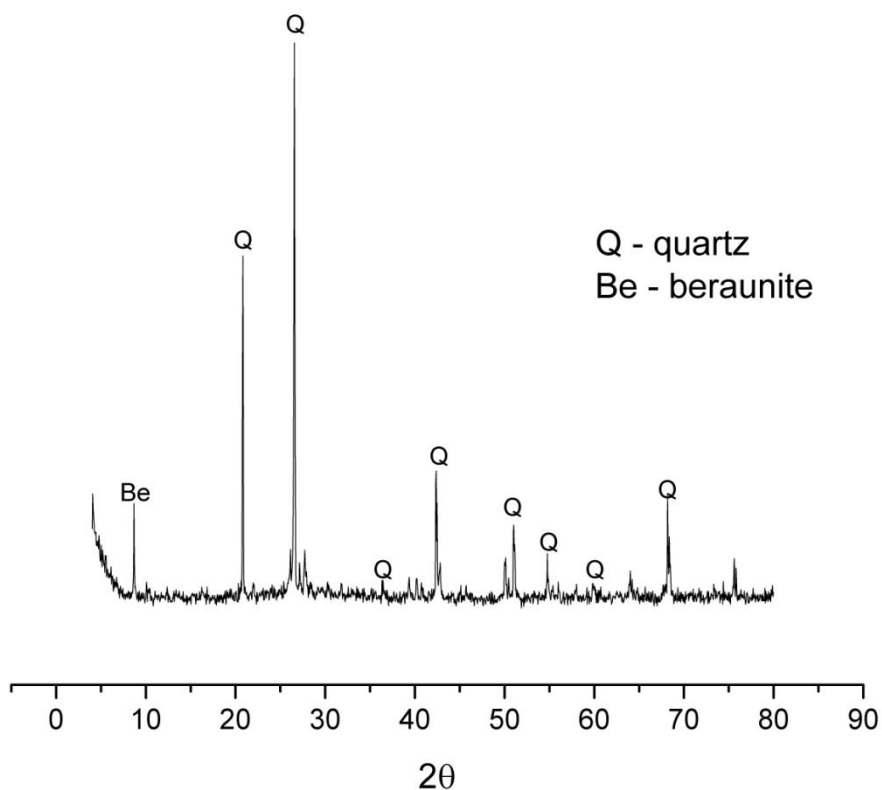
FIGURE 7-6: XRD diffractogram for the GP3 geopolymer concrete

TABLE 7-1: Mineral phases detected in the geopolymer concretes

Mineral phases	Chemical formula	GPC	GP1	GP2	GP3
Quartz	SiO_2	✓	✓	✓	✓
Riebeckite	$Na_2(Fe,Mg)_3Fe_2Si_8O_{22}(OH)_2$	✓			
Gypsum	$CaSO_4$	✓			
Bearsite	$Be_2(AsO_4)(OH).4H_2O$		✓		
Beraunite	$Fe^{2+}Fe^{3+}_5(OH)_5(PO_4)_4\cdot 4H_2O)$		✓		✓
Lime	CaO		✓		
Heinrichite	$Ba(UO_2)_2(AsO_4)_2\bullet 11H_2O$			✓	
Magnetite	Fe_3O_4			✓	
Downeyite	SeO_2			✓	
Guyanaite	$CrO(OH)$			✓	
Cadmoselite	$CdSe$			✓	

7.3   Scanning Electron Microscope (SEM) Analysis

JOEL scanning electron microscope (SEM) model JSM-6480 (FIGURE 7-7) equipped with energy dispersive x-ray spectroscopy (EDX) was used to characterize the samples. Imaging of the sample to determine the microstructure was achieved by irradiating it with focused electron beams from a cathode, detector in the SEM converts signal emitted by the sample to intensity that produces images of the sample surface (Chancey, 2008). To avoid distorted images, the sample was coated with Gold (Au), a conductive material using a sputtering device. Coating is necessary to allow the discharge of electron build up thereby eliminating charging effect that occurs when the sample is irradiated with electron beams with high accelerating voltage.

After coating, the sample is placed in the sample chamber which is evacuated to create a vacuum inside. The sample is then irradiated with electron beam at 7 KV accelerating voltage and the interaction of sample surface with the electron beams produces images on the display which was adjusted to X 1,300 magnification to acquire the SEM images of the sample.

FIGURE 7-7: JOEL SEM equipped with energy dispersive spectrometry (EDX)

FIGURES 7-8 to 7-12 show the SEM micrographs of the starting materials and the produced geopolymer concretes. As shown in FIGURE 7-8, the CFA comprises of spherical particles with smooth surfaces while the SF is made up of smaller particles that clump together easily. The CFA has a mean particle size of 47 μm while the SF has mean particle size of 277 μm.
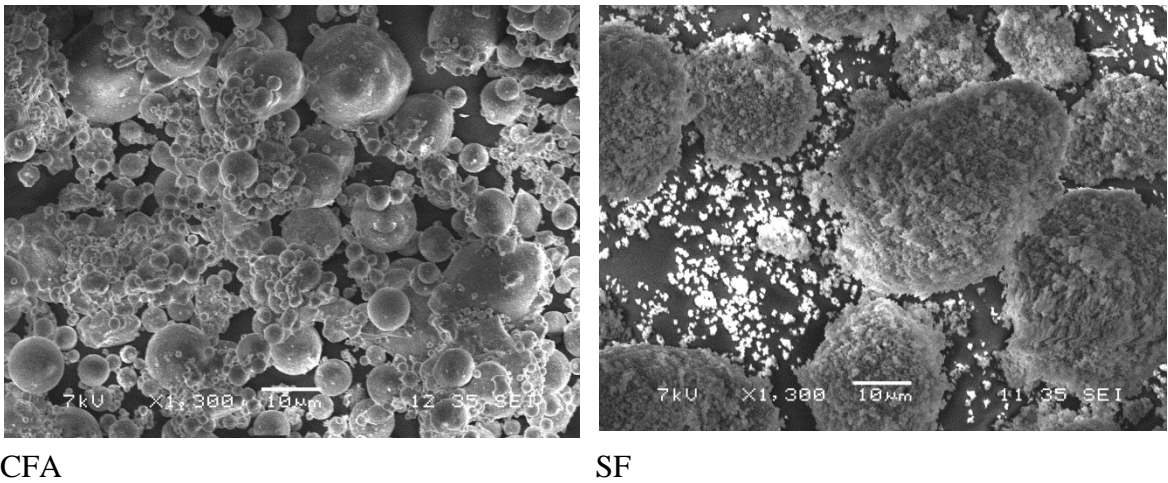
CFA   SF
FIGURE 7-8: SEM micrograph of CFA and SF

Micrograph of the geopolymer concretes (FIGURES 7-9 to 7-12) showed that the material is very similar in microstructure. It shows a homogenous featureless hydration product that result from the dissolution of the CFA and SF by the strong alkaline liquid.
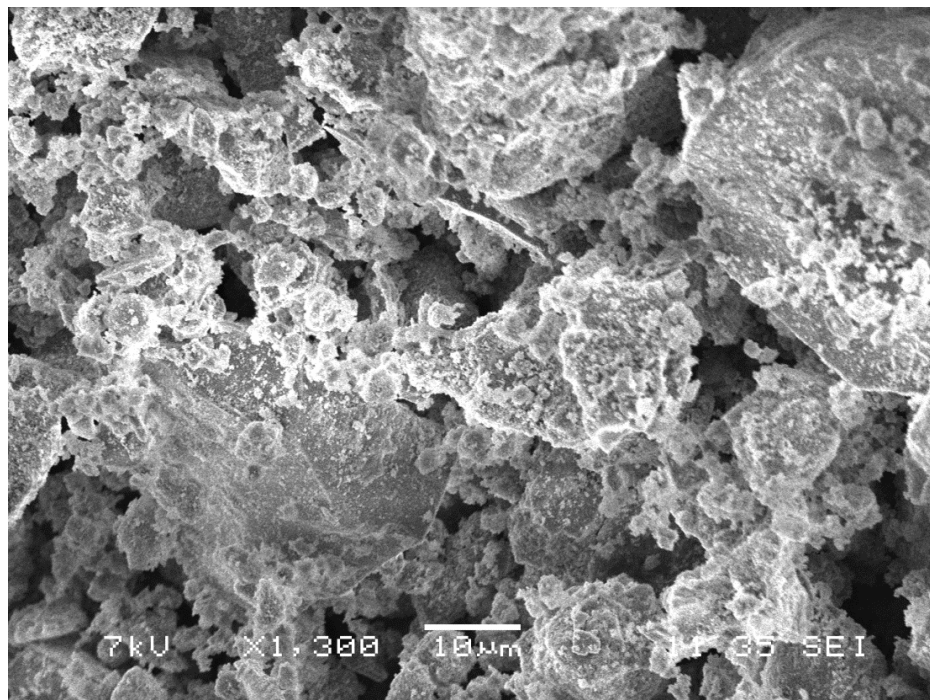
FIGURE 7-9: SEM micrograph of the GPC geopolymer concrete
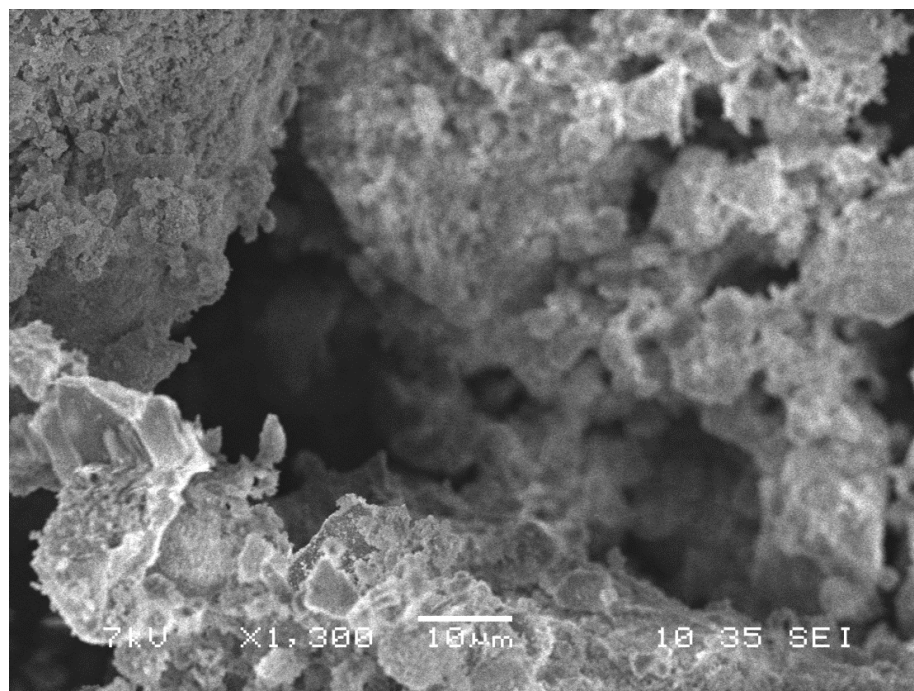
FIGURE 7-10: SEM micrograph of the GP1 geopolymer concrete
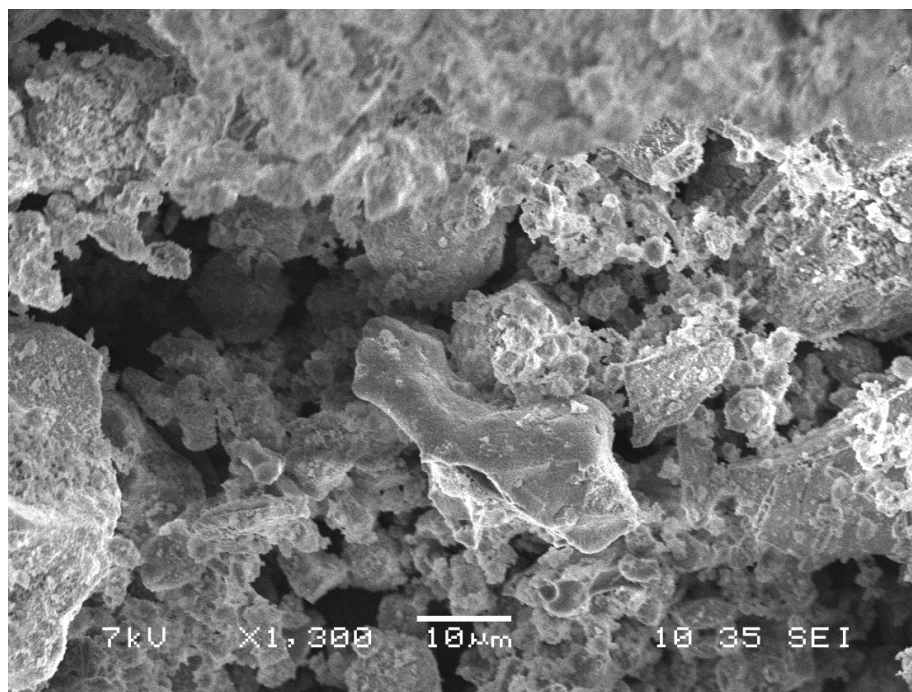
FIGURE 7-11: SEM micrograph of the GP2 geopolymer concrete
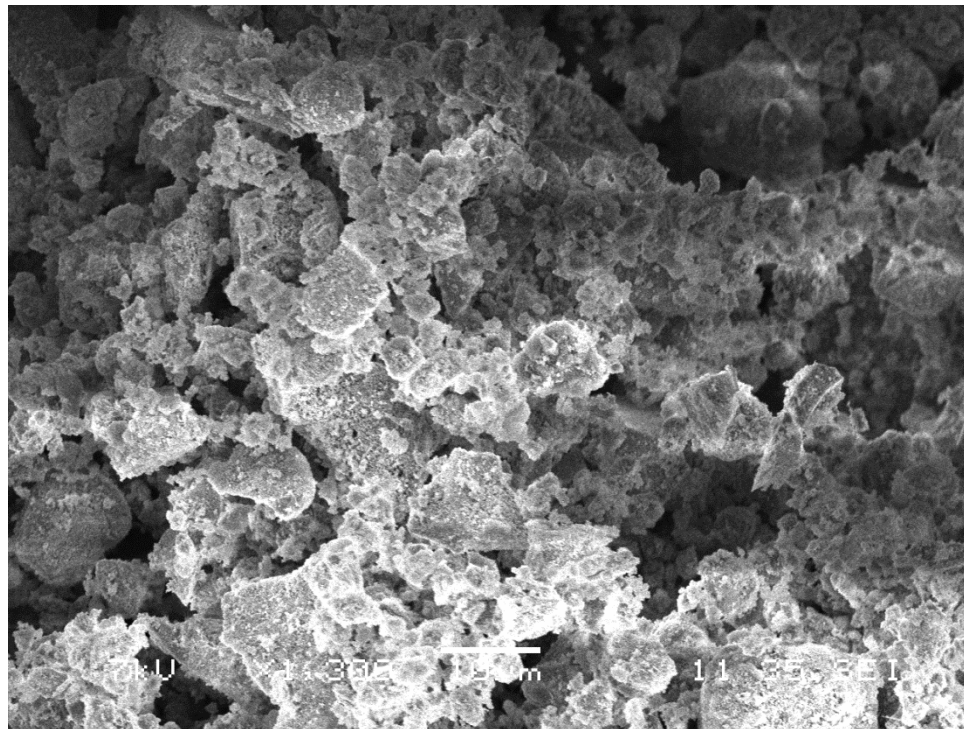
FIGURE 7-12: SEM micrograph of the GP3 geopolymer concrete

From these micrographs, the addition of hydrated lime during the geopolymer synthesis did not significantly alter the surface morphology of the geopolymer. In all the geopolymer concrete samples, the dense featureless product is the aluminosilicate matrix of geopolymer. Unfortunately, there was no observed presence of unreacted or partially reacted CFA particles which is normally seen in the microstructure of geopolymer.

7.4   Energy Dispersive X-Ray Spectroscopy (EDX) Analysis

Elemental composition of the geopolymer concrete was determined through the use of the EDX attached to the SEM. According to Chancey (2008), electron beams at accelerating voltage between 15 KV to 25 KV are normally used to irradiate the sample. Interaction of these electron beams with the sample generates characteristics X-ray photons with energies specific to the elements contained in the sample. Detectors in the EDX detect photons and correlate their respective energies with the elements that emit them. The EDX spectrums obtained from the EDX analysis are presented in FIGURES 7-13 to 7-18. As expected, majority of elements identified in all the materials (CFA, SF and geopolymer samples) are Si, Al, C and O which is due to the aluminosilicate nature of both the starting materials and produced geopolymer concretes. Unfortunately, the EDX analysis did not identify the presence of minor elements such as As, Cr and Se (TABLE 7-2).
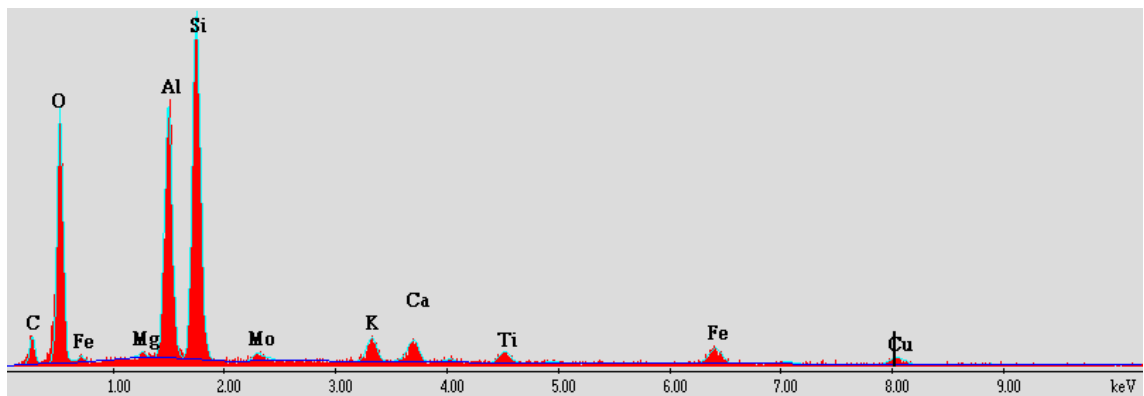
FIGURE 7-13: EDX spectrum of CFA
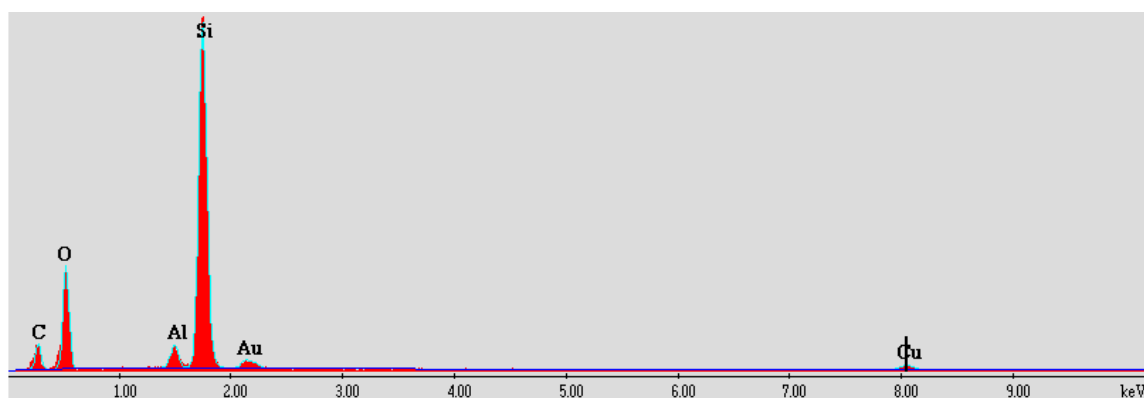
FIGURE 7-14: EDX spectrum of SF
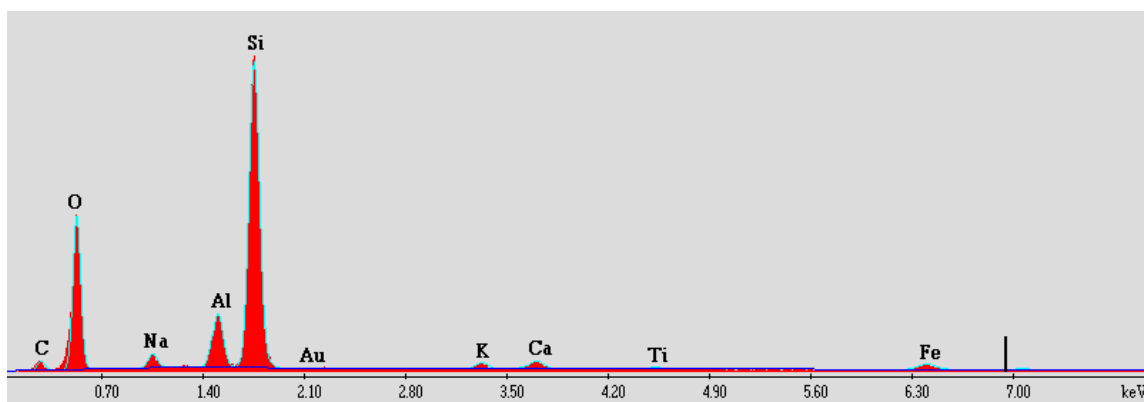
FIGURE 7-15: EDX spectrum of GPC
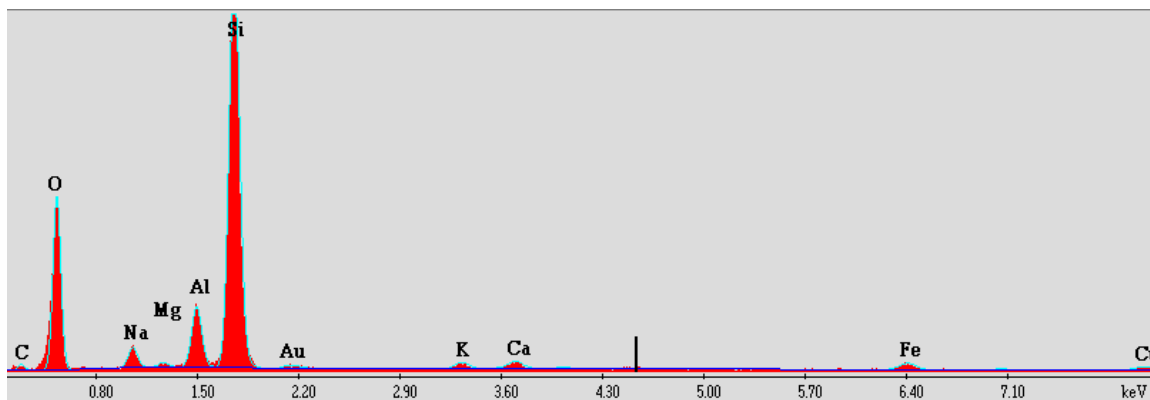
FIGURE 7-16: EDX spectrum of GP1
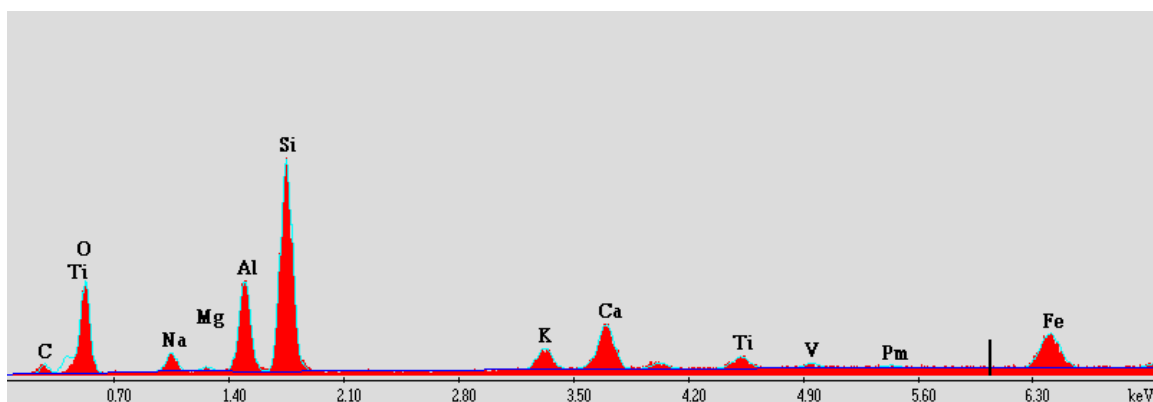
FIGURE 7-17: EDX spectrum of GP2
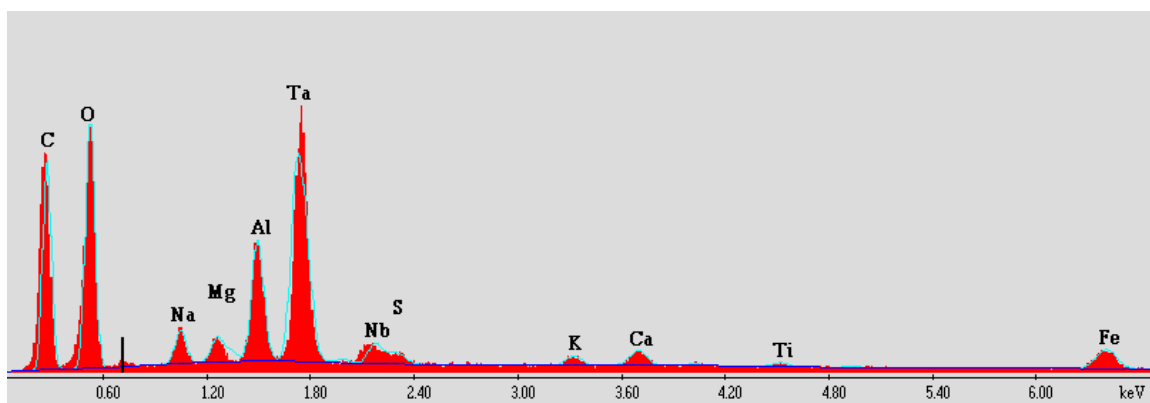
FIGURE 7-18: EDX spectrum of GP3

FIGURE 7-18 does not show the presence of Si peak in the EDX spectrum for the

GP3 geopolymer concrete. Tantalum (Ta) peak occurs instead in the spectrum which is

due to the overlap between Si-K and Ta-M peaks (Suzuki and Rohde, 2008). Si is the most probable element that belongs to the peak at 1.7 keV. After quantification of the element, the normalized bulk composition of the geopolymer concrete is presented in TABLE 7-2.

TABLE 7-2: Elemental composition of the geopolymer concretes

Elements	CFA	SF	GPC	GP1	GP2	GP3
Al	13.25	2.08	5.64	5.53	9.35	3.27
Si	18.60	28.81	29.57	33.76	19.92	
O	40.59	34.64	43.92	42.71	25.11	25.68
C	15.74	28.28	11.90	7.69	10.02	38.22
Fe	3.08		2.07	1.97	8.83	1.46
Cu	2.52	2.97	1.86	1.89	9.37	1.57
Ca	1.69		1.15	0.89	4.70	0.51
K	1.66		0.83	0.68	2.16	0.33
Ti	1.15		0.34		1.73	0.19
Mo	1.38					
Mg	0.33			0.45	0.51	0.81
Au		3.21	0.31	1.35		3.51
Na			2.41	3.08	3.05	1.46
V					0.53	
Ta*						20.22
S						0.19

*Ta presence is the result of overlap between Ta and Si peak at 1.7 KeV

7.5   Summary

The result of the XRD investigation is less satisfactory because mineral phases such as ettringite, monosulfoaluminate, CSH and calcium metalates that are considered suitable candidate for immobilizing oxyanion elements were not identified in the geopolymer concretes. This does not mean that these phases are not formed or present in the samples, the peaks of the mineral phases are most likely not successfully identified because of low peak intensity and limitation of the AMSCD database used for phase identification. On the other hand, Van Jaarsveld and Van Deventer (1999) noted that large part of geopolymer structure is amorphous to X-ray hence the absence of many crystalline phases. Therefore, the inability to identity mineral such as CSH might be due to the fact that the mineral is essentially amorphous (Gougar et al., 1996).

From the SEM analysis of the geopolymer concretes, the addition of calcium did not significantly affect the microstructure of the geopolymer. Although it is believed that the presence of extra calcium in the form of calcium hydroxide would lead to the precipitation of poorly crystalline CSH or calcium mineral phases (Temuujin et al., 2009), these minerals were not seen in the micrographs acquired from the SEM analysis.

CHAPTER 8: SPECIATION MODELING USING PHREEQC/PHREEPLOT

8.1   Background on PHREEQC/PHREEPLOT

PHREEQC is one of the most widely used speciation modeling program, which is based on the equilibrium of aqueous solutions with mineral phases, solid solutions, sorbing surfaces and gases (Parkhurst and Appelo, 1999; Halim et al., 2005). The program uses ion-association aqueous model to calculate the distribution of aqueous species in any aqueous solution and can allow the concentration of elements to be adjusted to equilibrium or a specified saturation index (SI). The ion-association model requires that before chemical equilibrium can be achieved all mass-action equations for the aqueous species must be satisfied (Parkhurst and Appelo, 1999). PHREEQC program uses information contained in the associated database and input file to calculate the distribution of species and saturation indices of mineral phases. The input file contains set of keywords that define the pH, temperature, density, chemical composition of the solution (total concentration of cations and anions) while the database file contains thermodynamic parameters such as dissociation equations and constants, mineral formation reactions, and temperature functions (Zhu and Anderson, 2002).

PHREEPLOT is a program that has the capability of using output from PHREEQC to produce high quality geochemical plots. It contains an embedded version of the PHREEQC program and has the ability to do simple looping which makes it easier to do repetitive PHREEQC calculations needed to generate a wide range of graphical

plots (Kinniburgh and Cooper, 2011). PHREEPLOT also consists of set of keywords in the input file and associated database which defines the thermodynamic data needed for the modeling. Information contained in the input file is read and processed simulation by simulation to calculate the distribution of species and saturation indices of phases. This chapter focuses on using PHREEPLOT to model the distribution of aqueous species of As, Cr and Se based on the aqueous solution input data and mineral phases identified as the solubility controlling phases.

8.1.1   The PHREEPLOT Database

Databases contain definition of chemical species, complexes and dissociation constants under specified conditions such as temperature (Charlton et al., 1997; Dhir et al., 2008). Most geochemical modeling programs come with several databases; PHREEPLOT contains more database than other geochemical modeling programs used in geochemical modeling. TABLE 8-1 present the databases associated with the PHREEPLOT program.

TABLE 8-1: Databases associated with PHREEPLOT

Database	Size	Description and key features
amm.dat	21 KB	Small entries
iso.dat	255 KB	Contains common mineral phases
minteq.dat	156 KB	Developed for the minteq program and contains organic compound, uranium minerals, arsenic minerals, metalates of Ca and other elements
minteqv4.dat	390 KB	Updated version with more entries than minteq.dat
NAPSI_290502	117 KB	

TABLE 8-1(continued)

Database	Size	Description and key features
phreeqc.dat	34 KB	Contains limited but consistent entries
phreeqd.dat	29 KB	
pitzer.dat	20 KB	
sit.dat	506 KB	Contains phases such as ettringite, monosulfoaluminate, gismondine, hydrogarnet, downeyite and CSH
wateq4f.dat	99 KB	Phreeqc.dat extended with many heavy metals included
llnl.dat	756 KB	A huge database that contains phases such as gismondine, cadmoselite, downeyite and ettringite

Most of the databases do not contain dissociation constant and dissolution equation for all the aqueous species or mineral phases needed for the simulation. Some mineral phase of interest is missing in the database, their information was manually adding into the chosen database via the input file data. These supplementary data for mineral phases were obtained from literature search and other database.

8.1.2   Description of the PHREEPLOT Input File

As discussed in section 8.1, data needed for the modeling are supplied via the input file. This input file contains set of keywords that is followed by data blocks which define the parameters needed in the modeling separated into simulations by the END keyword (Kinniburgh and Cooper, 2011). END keyword literally instructs the program to calculate. Each keyword signifies the beginning of data block and the program knows

what to do with the data that follows the keyword provided the keyword is written correctly (Zhu and Anderson, 2002). The input file is separated by the CHEMISTRY keyword. The top of the input file contains PHREEPLOT settings while the bottom contains the PHREEQC code (Kinniburgh and Cooper, 2011). The CHEMISTRY keyword is used to separate the two section of the input file i.e. it signifies the beginning of the PHREEQC input. According to Kinniburgh and Cooper (2011), PHREEPLOT input file should be kept as simple as possible and preliminary calculations should be placed at the beginning of the file.

Some of the keywords relevant for this modeling are discussed further in this section. INCLUDE is a keyword that is placed in the CHEMISTRY section which is used to call other files that contain codes needed for several calculations. Two INCLUDE files relevant for this modeling are "speciesvsph.inc" and "speciesvspht.inc". These two files are used in making the species vs pH plots; the former plots the relative concentration (in %) of all species while the later plots the overall percentage of the elements species that is in dissolved form (Kinniburgh and Cooper, 2011). The SOLUTION keyword defines the composition of the aqueous solution which includes temperature, pH and density. PHASES defines name, dissociation reactions and thermodynamic data for minerals and gases that are used in the speciation and batch-reaction calculations (Parkhurst and Appelo, 1999). EQUILIBRIUM_PHASES is used to define the combination of minerals and /or gases that react reversibly with the aqueous solution to equilibrium, prescribed saturation index (SI) or gas partial pressure (Parkhurst and Appelo, 1999; Appelo and Postma, 2005).

8.2   Procedure for the PHREEPLOT Speciation Modeling

Four different sets of simulations with PHREEPLOT are performed in this study. The pH temperature and chemical composition of the aqueous solutions from the WLT performed on the geopolymer concretes (section 6.5) were used in each simulation. Before the preparation of the input file, a suitable database was chosen that contains (1) aqueous species of the elements of interest (2) dissolution equations of mineral phases that are considered solubility controlling mineral phases (3) most accurate solubility constant (k) for the mineral phases and aqueous species. The 'llnl.dat' thermodynamic database was employed because it is the largest and contains huge amount of mineral phases that can potentially be solubility controlling phases.

The input file was then prepared by using keywords and associated data blocks. The PHREEPLOT section of the input file begins with the keyword SPECIATION and contains data blocks that define the database used, calculation type 'species', the calculation method, elements of interest, behavior of the program when an error is encountered, looping function and number of times to loop. This section also contains information on how the program handles and plots the generated data. The CHEMISTRY keyword signifies the beginning of the PHREEQC section. In this section, the solubility controlling minerals phases that are not present in the 'llnl.dat' database were manually added. TABLE 8-2 shows the manually added mineral phases, their dissolution equations and solubility constant. Compositions of the aqueous solution (TABLE 6-5 to 6-7) used in the speciation calculation are also entered in this section and the input file saved with a ".ppi" extension in a designated folder. Appendix F contains the input file for one of the simulations while the corresponding output file is in appendix G.

TABLE 8-2: Mineral phases manually added to the simulation

Phase name	Dissolution equation and log_k at $25^{\circ}C$	references[2]
Cr-ettringite	$Ca_6(Al(OH)_6)_2(CrO_4)_3:26H_2O$ $= 6Ca^{2+}+2Al^{3+}-12H^++3CrO_4^{2-}+38H_2O$ log_k 60.28	sit.dat
Se-ettringite	$Ca_6(Al(OH)_6)_2(SeO_4)_3:31.5H_2O =$ $6Ca^{2+} +2Al^{3+}+3SeO_4^{2-} -12H^+ +43.5H_2O$ log_k 61.29	(Chrysochoou and Dermatas, 2006)
Se-monosulfoaluminate	$Ca_4(Al(OH)_6)_2SeO_4:9H_2O = 4Ca^{2+}$ $+2Al^{3+} -12H^+ +SeO4^{2-} +21H_2O$ log_k 73.40	(Cornelis et al., 2008)
Monosulfoaluminate	$Ca_4Al_2(SO_4)(OH)_{12}:6H_2O = 4Ca^{2+}$ $+2Al^{3+} -12H^+ +SO_4^{2-} +18H_2O$ log_k 72.73	sit.dat
Cr-monosulfoaluminate	$Ca_4Al_2O_6(CrO_4):15H_2O=4Ca^{2+} +2Al^{3+}$ $-12H^+ +CrO_4^{2-} +21H_2O$ log_k 71.36	sit.dat
$CaSeO_4:2H_2O$	$CaSeO_4:2H_2O = Ca^{2+} +SeO_4^{2-} +2H_2O$ log_k -2.68	sit.dat
$CaSeO_3:2H_2O$	$CaSeO_3:2H_2O = Ca^{2+} +SeO_3^{2-} + 2H_2O$ log_k -4.6213	(Cornelis et al., 2008)
$CaSeO_4$	$CaSeO_4 = Ca^{2+} +SeO_4^{2-}$	

---

[2] sit.dat is a thermodynamic database in PHREEPLOT

TABLE 8-2 (continued)

Phase name	Dissolution equation and log_k at 25°C	references[2]
	log_k -3.0900	
$Ca_3(AsO_4)_2{:}3H_2O$	$Ca_3(AsO_4)_2{:}3H_2O = 3Ca^{2+} + 2AsO_4^{3-}$ $+3H_2O$ log_k -21.14	(Cornelis et al., 2008)
$CaHAsO_3$	$CaHAsO_3 = Ca^{2+} + HAsO_3^{2-}$ log_k -6.52	(Cornelis et al., 2008)
$CaCrO_4$	$CaCrO_4 = Ca^{2+} + CrO_4^{2-}$ log_k -3.15	sit.dat
$CaHAsO_4$	$CaHAsO_4 = Ca^{2+} + HAsO_4^{2-}$ Log_k -2.66	(Alexandratos et al., 2007)

8.3   Model Simulation Results and Interpretation

Plots that show the distribution of species of the three elements are discussed in this section. FIGURES 8-1 to 8-3 showed the percentage distribution of species of each element as a function of pH. It is evident from the plots that the predominant species varies across the pH range.

The simulation results of As shown in FIGURE 8-1 reveal that $HAsO_3F^-$ and AsO_3F^{2-} are the As species present in the aqueous solution from all the geopolymer concretes. $HAsO_3F^-$ is the dominant specie in the acidic pH range while AsO_3F^{2-} is more dominant in the alkaline pH. These species of As are As (5) which is less soluble and less toxic than As (3) (Moon et al., 2004). At about pH 6, the proportion of the two species in the solution is the same.
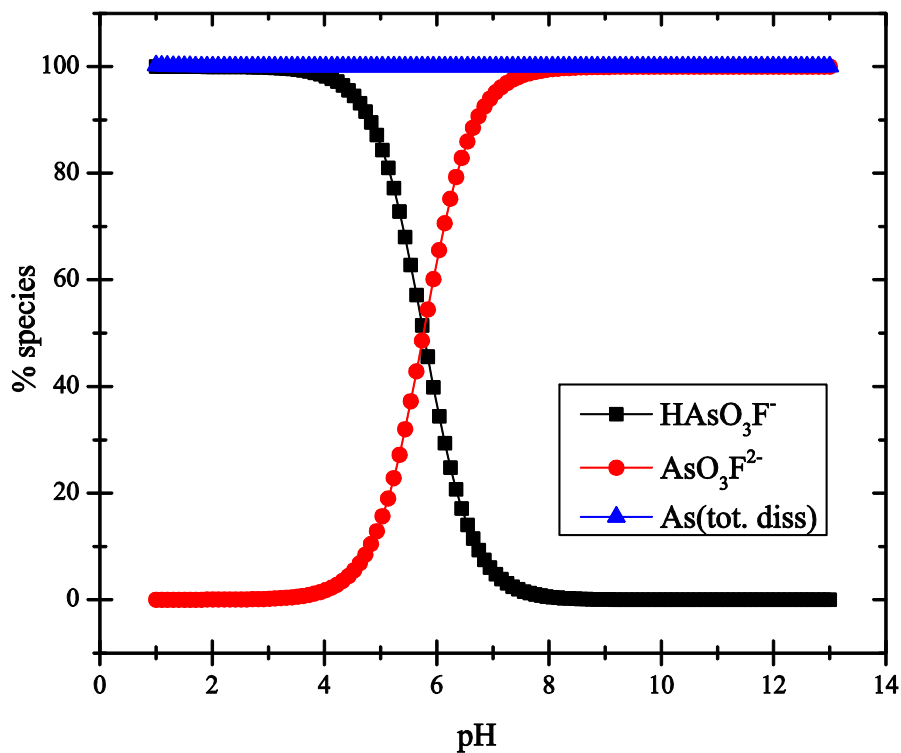
FIGURE 8-1: Typical distribution of As species from the PHREEPLOT simulation

As shown in FIGURE 8-2, SeO_4^{2-} and $HSeO_4^-$ are two species of Se (6) that are present in the aqueous solution in considerable amount. From pH 1 to pH 2, $HSeO_4^-$ is the dominant specie present in the solution and as pH increases from 2, the dominant specie changes to SeO_4^{2-}. At around pH 2, the two species have equal amount in the solution. Se (4) species such as SeO_3^{2-}, $HSeO_3^-$ and H_2SeO_3 are also present in the solution but the amount present is so small that it does not significantly contribute to the species distribution. The type of Se present in the solution in considerable amount is less toxic since Se(4) is considered to be more toxic than Se (6) (Goldberg et al., 2006).
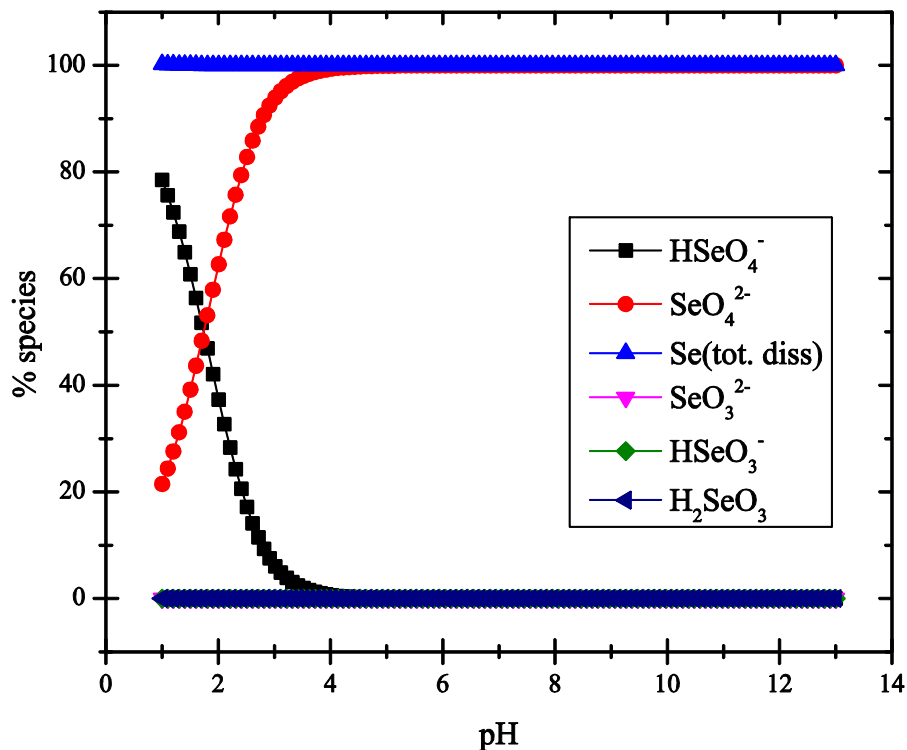
FIGURE 8-2: Typical distribution of Se species from the PHREEPLOT simulation

Both Cr (3) species: Cr^{3+}, $CrOH^{2+}$, $CrCl_2^+$ and Cr (6) species: $HCrO_4^-$, CrO_4^{2-} are responsible for the distribution of Cr in the aqueous solution. Some of these species have very low amount and therefore have insignificant contribution to the Cr distribution. The obviously dominant species are Cr^{3+}, $HCrO_4^-$ and CrO_4^{2-}. Between pH 1 and pH 1.5, Cr^{3+} is the main specie while $HCrO_4^-$ is the other specie present. Equal amount of these two species exist at pH 1.5, afterwards $HCrO_4^-$ becomes the dominant specie and Cr^{3+} reduces to zero. The amount of the $HCrO_4^-$ specie starts to diminish at around pH 5 while CrO_4^{2-} starts to increase. At around pH 7, there was equal distribution of the $HCrO_4^-$ and CrO_4^{2-} specie. In the alkaline pH range, the dominant specie is the CrO_4^{2-}. Among all the species present in the solution, the Cr(6) species are considered to be more toxic than Cr(3) species (Shtiza et al., 2009).
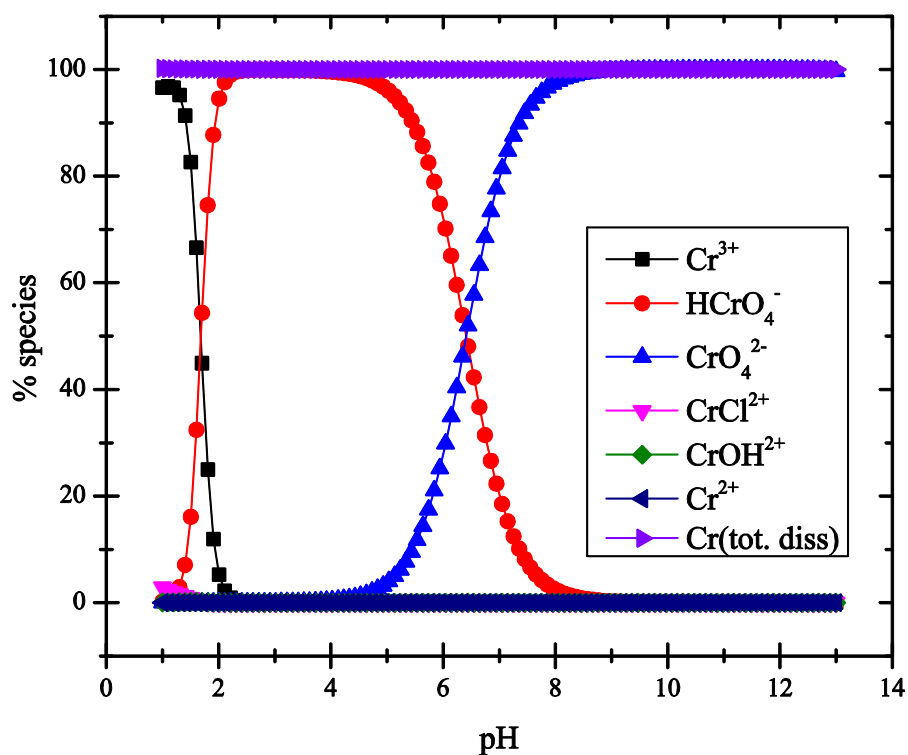
FIGURE 8-3: Typical distribution of Cr species from the PHREEPLOT simulation

8.4   Validation of the Model Output

The purpose of model validation is to check the ability of the model to correctly and realistically predict the results. Due to lack of experimental data from literature search to use for validation of the model, the validation was instead conducted by comparing the calculated molal concentration of each element (appendix G for molal concentration at pH 11.23) obtained from the simulations with the measured concentration in the aqueous solution used as input data. TABLE 8-3 contains the comparison between the measured concentration and molal concentration obtained from the modeling. Overall, the calculated concentration of As, Cr and Se from the model is relatively very close to the measured concentration from the WLT that was used as input data.

TABLE 8-3: Comparison of input and PHREEPLOT model output concentration

	Concentration (mg/l)							
	GPC		GP1		GP2		GP3	
	PHREEPLOT	WLT	PHREEPLOT	WLT	PHREEPLOT	WLT	PHREEPLOT	WLT
As	1.027	1.023	1.023	1.019	1.019	1.015	0.928	0.955
Cr	0.011	0.025	0.011	0.025	0.011	0.025	0.011	0.025
Se	0.407	0.405	0.420	0.418	0.424	0.422	0.375	0.374

8.5 Summary

The PHREEPLOT simulations showed the oxyanion elements (As, Cr, Se) are present in the leachates in As(5), Se(6), Cr(3) and Cr(6) oxidation states. The results indicated that in the alkaline pH range, As (5) exist mainly as AsO_3F^{2-}, Se(6) as SeO_4^{2-} and Cr(6) as CrO_4^{2-}. These As and Se species present in this aqueous solution are in the higher oxidation states and are less toxic than the reduced form. Cr on the other hand, exists in an oxidation state that is found in the alkaline pH range is considered to be the most toxic form. However the distribution of this higher oxidation states chromium (Cr(6)) is negligible in the alkaline pH range.

CHAPTER 9: CONCLUSIONS AND RECOMMENDATIONS

9.1   Conclusions

As stated in chapter one, the suitability of geopolymer as a safe alternative to cement in construction and waste stabilization depends on the material potential environmental impacts. There is thus a need to properly understand geopolymer leaching behavior during its service life and end of life conditions. The leaching of oxyanion forming elements such as As, Cr and Se was particularly important because these elements can exist in oxidation states that are more mobile in the alkaline pH environment that would exist in geopolymer pore solution. This dissertation was set up with the aim of understating the leaching mechanism oxyanion forming elements (As, Cr, Se) from fly ash based geopolymer concrete and investigates the effect of hydrated lime on mobility of these elements from the material and strength of the concrete. To achieve the research goals, specific objectives (Section 1.4) were set and hypothesis (Section 1.5) formulated. Several experimental tasks were designed in the course of this dissertation. The following conclusions have been made based on the results from the tasks presented in preceding chapters of this dissertation.

9.1.1   Synthesis of Geopolymer Concrete

Geopolymer concretes were synthesized using CFA, SF, CA, FA, NaOH with varying amount of hydrated lime, cured without heat at room temperature and in an oven

maintained at 75°C.   Major findings from the geopolymer concrete synthesis are summarized as follows:

- Geopolymer concretes are alkaline material with pH greater than 11 and the same bulk density as normal weight concrete (2300 kg/m^3) which is expected since aggregates determine the weight of concrete.

- The 28 days compressive strength of geopolymer concretes cured without heat is relatively lower than the strength of the concrete cured at 75°C. The average strength of the concretes cured without heat varies from 13 MPa (1937 psi) to 18 MPa (2647 psi) while the heat cured geopolymer concretes have average strength that varies from 42 MPa (6013 psi) to 56 MPa (8117psi).

- There is presence of efflorescence on the surface of the geopolymer concretes cured without heat which might indicate insufficient geopolymerization hence the lower strength of the concrete when compared with the heat cured geopolymer.

- Hydrated lime addition leads to reduction in strength of the geopolymer concretes. Geopolymer concretes made with additional hydrated lime exhibit lower compressive strength than the control geopolymer concrete that has zero hydrated lime added (GPC).

- Among the geopolymer concrete with hydrated lime, the GP2 with 1% hydrated lime have the highest strength in both the concrete cured with heat and without heat.

The lower compressive strength of the geopolymer concrete cured without heat makes it suitable for use only in low strength structural applications such as walkway, road divider and solidification of waste. The heat cured geopolymer concrete on the hand

can be used for higher strength structural applications similar to OPC concrete since it has compressive strength that exceed 41 MPa (6000 psi). It is evident from this investigation that heat curing is required in order to produce geopolymer concrete of considerable compressive strength. There is also an optimal amount of additive such as hydrated lime that can added to geopolymer concrete that would not affect the strength of the material. Part of hypothesis 5 which states that "leaching of these oxyanion forming elements can be mitigated by the addition of extra calcium in the form of lime during geopolymer synthesis, which would lead to the formation of oxyanion substituted calcium mineral phases in addition to the geopolymer phase without affecting the durability of the geopolymer" was tested in Section 5.3. The results show that even though the addition of lime lead to reduction in compressive strength of the geopolymers, the overall the minimum compressive strength of the geopolymers that contain additional lime still meets the strength requirement for concrete used in high strength structural applications.

9.1.2   Leaching of Elements from Geopolymer Concrete

The leaching tests performed on the geopolymer concretes are: pH dependence test, Dutch availability test, water leach test (WLT) on the granular form of the concretes and the tank test on the monolith form of the concretes. Hypothesis 2 which states that "oxyanion forming elements exhibit different leaching behavior than other elements that are leached from the alkaline fly ash based geopolymer" was addressed using the pH dependence test presented in Section 6.2. Results obtained from the pH dependence test indicate that all oxyanion forming elements (As, Se, Mo and V) except Cr displays higher mobility in the alkaline pH. Cr and other elements such as Al, Ca, Fe, Mg, B, Ba, Cu,

Mn, and Zn exhibit different leaching behavior with their highest mobility occurring in the acidic pH range. Elements that include Al, Si, Ca and Na have extremely high mobility from all the geopolymer concretes. The test also supported hypothesis 1 which states that "oxyanion elements (As, Cr, Se) are present in leachates from fly ash based geopolymer concrete". In both the acidic and alkaline pH range, mobility of most of the elements (As, Se, Mo, V, Si, Al, Fe, Mg, Cu, Mn and Zn) is lowest in the GP2 concrete that has 1% hydrated lime. This implies that the addition of 1% hydrated lime was able to reduce the mobility of most of the elements from the geopolymer concrete.

Hypothesis 3 which states that "standard leaching test methods conducted at a neutral pH are adequate for predicted the leaching of oxyanion forming elements" was tested in Section 3.6.2 by statistically comparing the result of the Dutch availability test conducted at neutral pH and acidic pH with result obtained from a modification of the availability test conducted at the material pH and acidic pH. No statistical difference was observed between the results from the two test methods, which signifies that the Dutch test conducted at neutral pH is adequate to predict leaching of the oxyanion forming elements (As, Cr, Se) from the alkaline fly ash based geopolymer.

The Dutch availability test used to investigate the leaching from the fly ash based geopolymer concrete under the worst case scenario showed that As and Se exhibit considerable leachability from the geopolymer concretes. As mobility varies from 8.3 mg/kg to 9.7 mg/kg while the mobility of Se range between 2.9 mg/kg to 4.5 mg/kg. The lowest amount of each element leached (As – 8.3 mg/kg, Se – 2.9 mg/kg) occurs in the GP2 sample. The amount of Cr released from all the geopolymer concrete is constant.

This results suggest that 1% hydrated lime in the geopolymer concrete may lead to reduction in mobility of As and Se.

Tank test conducted on the monolithic geopolymer concrete better represent the leaching behavior of the material during its service life. The test results showed that the release mechanisms associated with the leaching of the three elements are surface wash-off, diffusion, depletion and dissolution. Surface wash-off, diffusion and depletion are the main leaching mechanism responsible for the leaching of As and Se which have high or moderate mobility that tends to a flat plateau as the leaching duration increases. This signifies that the element is depleting in the matrix. Cumulative amount of As released from the geopolymer concretes reached a maximum of 300 mg/m^2 while that of Se reached a maximum of 130 mg/m^2. The leaching mechanisms associated with the release of Cr are surface wash-off, diffusion and dissolution with a cumulative amount of Cr released at the end of the leaching duration that reached 3 mg/m^2. It is obvious from the result that the cumulative mobility of Cr has not reached the depletion stage because the element have lower mobility rate than the other elements. Overall, the mobility of As and Se from the GP2 concrete with 1% hydrated lime is the lowest.

Hypothesis 5 which states that "leaching of these oxyanion elements can be mitigated by the addition of extra calcium in the form of lime during geopolymer synthesis" was tested using the pH dependence test (Section 6.2), Dutch availability test (Section 6.3) and the tank test (Section 6.4). The results reveal that at 1.0% lime addition there was reduction in the mobility of most of the elements including the oxyanion forming elements (As, Cr, Se).

9.1.3   XRD and SEM/EDX Analysis of the Geopolymer Concretes

Hypothesis 4 which states that "calcium containing mineral phases such as ettringite, hydrocalumite, monosulfoaluminate, calcium metalates and calcium silicate hydrates (CSH) are effective for immobilizing oxyanion forming elements via ion substitution" was tested in Section 7.2 and 7.4.   Although literature search suggested that mineral phases such as ettringite, monosulfoaluminate, CSH and precipitates of calcium are solubility controlling phases that can help reduce the mobility of the oxyanion forming elements like As, Se and Cr. Unfortunately, this hypothesis cannot be supported due to lack of identification of the mineral phases in the geopolymer concrete samples analyzed. Mineralogical analysis of the geopolymer concrete using the XRD did not reveal the presence of these solubility controlling mineral phases, but however reveals the presence of other minerals phases such as quartz, riebeckite, gypsum, bearsite, bearunite, lime, downeyite, cadmoselite, heinrichite, guyannaite and magnetite. Quartz is the only mineral that is common to all the geopolymer concretes. The mineral beraunite was found in the GP1 and GP3 concrete while the remaining minerals are found only in one geopolymer concrete sample. The inability of the mineralogical analysis to identify the solubility controlling mineral phases is most likely due to the fact that geopolymer concrete are essentially amorphous to x-ray detection or due to low peak intensity which makes their identification impossible.

Microstructural analysis of the geopolymer concrete using SEM showed that the materials have similar surface morphology. All the geopolymer concretes have homogenous featureless hydration product. It is obvious that the additional hydrated lime did not significantly affect the microstructure of the concretes.

9.1.4   Distribution of Species of As, Cr and Se

PHREEQC/PHREEPLOT simulation identified $HAsO_3F^-$ and AsO_3F^{2-} are the As species present in the aqueous solution while SeO_4^{2-} and $HSeO_4^-$ are two species of Se present in the aqueous solution in considerable amount. This species of As and Se are respectively in the As (5) and Se(6) oxidation states which are considered to be less toxic than the reduced oxidation state of the elements (As(3) and Se(4)). Dominant Cr species present in the aqueous solution include Cr^{3+}, $HCrO_4^-$ and CrO_4^{2-}. Cr^{3+} is in the Cr(3) oxidation state while $HCrO_4^-$ and CrO_4^{2-} are in Cr(6) oxidation state. Cr(6) is considered to be more toxic than Cr(3). In the alkaline pH, AsO_3F^{2-}, SeO_4^{2-}, and CrO_4^{2-} are the main species present in the aqueous solution. The closeness of the concentration of elements used in input data and the calculated concentration from PHREEQC/PHREEPLOT simulation was assessed. This comparison showed that the concentrations were very close which means that the model was able to predict the concentration of As, Cr and Se in the aqueous solution.

9.1.5   Overall Conclusions

The objectives of the research are listed below and the conclusions derived from results of various experiment conducted to meet these objectives are stated.

- To determine the release of oxyanion elements (As, Cr, Se) from fly ash based geopolymer concrete under service life (monolithic) and end of life (granular) conditions using appropriate tests.

- To determine the maximum amount of oxyanion forming elements that would be released under the worst case scenario when the material is pulverized.

The pH dependence, Dutch availability (worst case scenario) and tank (service life) test were used to determine the mobility of the elements from the fly ash based geopolymer concretes. The leaching tests reveal that As and Se leach out from the geopolymer concrete samples in the high alkaline range (pH >11) in greater amount during the service life and end of life conditions.

- To assess the potential to decrease mobility, or even total immobilization of oxyanion element (As, Cr, Se) in geopolymer concrete by means of using hydrated lime as an admixture.

  The addition of about 1% hydrated lime to geopolymer concrete led to reduction in the mobility of As and Se. The added hydrated lime also led to overall reduction in compressive strength of the geopolymer concretes but when concretes with hydrated lime additive were compared, the concrete with 1% hydrated lime result in slight increase in the compressive strength of the geopolymer concrete.

- To determine if there is formation of calcium containing mineral phases, calcium precipitates or calcium metalates in the produced geopolymer concrete.

  XRD analysis of the geopolymer concrete did not reveal the presence of these mineral phases, but minerals phases such as quartz, riebeckite, gypsum, bearsite, bearunite, lime, downeyite, cadmoselite, heinrichite, guyannaite and magnetite were identified in the geopolymer concretes.

- To identify the probable mechanisms responsible for immobilization of the oxyanion forming elements (if there is any immobilization).

Although there was observed reduction in the mobility of the oxyanion forming elements (As, Cr, Se) when 1% hydrated lime was added to the geopolymer concrete. The mechanisms responsible for the immobilization were not known due to the absence of the solubility controlling mineral phases that should immobilize the elements via ion substitution and precipitation.

- To determine the species of the oxyanion elements (As, Cr, Se) released from fly ash based geopolymer concrete and their potential environmental impacts.

  Even though there is high mobility of As and Se from the geopolymer, the species of the elements identified by geochemical modeling indicated that their mobility would not cause adverse environmental issue since these species belong to oxidation states that are less toxic, while in the case of Cr mobility results in release of low concentration of elements below the MCL.

Based on the results from this dissertation, more extensive investigation is needed on mobility of oxyanion forming elements from geopolymer concrete before deciding whether the material can be safely used in place of Portland cement concrete. However, the results suggest that the material can be used in solidification/ stabilization of waste before landfilling since the amount of oxyanion elements (As, Cr, Se) released is less than the amount specified in the TCLP test as regulatory limits.

9.2   Limitations of the Study

Although most of the research objectives and hypotheses were reached, there are some limitations and number of issues that are not properly addressed due to equipment and time constraints. First, some of the tests were performed in only duplicates. It would be advantageous to increase the number of replicates to five in order to be able to perform

proper statistical analysis of the results. Second, the free mineral phase identification software and the AMSCD mineral database is not very reliable due to the limited number of entries in the database and reduced functionality of the free software. Finally, speciation modeling is not enough in the determination of the species of oxyanion forming elements (As, Cr, Se) released from the geopolymer concretes.

9.3   Recommendations for Future Work

The following recommendations are suggested for future work:

- Leaching behavior, mineralogical and microstructural analysis of the geopolymer concrete cured without heat should be studied.

- An optimized mix design with enough additives that would ensure the formation and presence of the solubility containing mineral phases.

- More extensive XRD mineral database should be used for identification of the mineral phases present in the geopolymer concrete.

- Platinum coating can be used instead of gold before the SEM/EDX analysis in order to reduce the occurrence of charging and the ability to detect elements that are identified at high accelerating voltage.

- Speciation analysis using a combination of IC and ICP-MS should be conducted to confirm the presence of the less toxic oxidation state of As, Cr and Se.

- Accuracy of the result obtained from the PHREEPLOT modeling should be verified using the result from speciation analysis using experimental method.

- Future research should be done to establish the relationship between the strength of the geopolymer concretes and the leachability of the oxyanion forming trace elements (As, Cr, Se).

REFERENCES

ACAA. 2003. Fly ash facts for highway engineers Report No: FHWA-IF-03-019 American Coal Ash Association, Aurora, Colorado.

ACAA. 2008. Sustainable construction with coal combustion products:A primer for architects, American Coal Ash Association Educational Foundation American Coal Ash Association, Aurora, Colorado.

Alexandratos, V.G., E.J. Elzinga, and R.J. Reeder. 2007. Arsenate uptake by calcite: Macroscopic and spectroscopic characterization of adsorption and incorporation mechanisms. Geochimica et Cosmochimica Acta, 71 (17):4172-4187.

Allen, T. 2003. Powder sampling and particle size determination. Amsterdam; Boston: Elsevier.

Andrews, L.C. 2007. A geochemical analysis of aluminum hydroxides and iron oxides in little backbone creek, Shasta county, California. Bachelor of Arts, Carleton College, Northfield, Minnesota.

Appelo, C.A.J., and D. Postma. 2005. Geochemistry, groundwater and pollution. 2nd ed. Leiden, The Netherlands: A.A. Balkema publishers.

ASTM. 2003. ASTM C702 - Standard practice for reducing samples of aggregate to testing size, ASTM International, West Conshohocken, PA.

ASTM. 2006a. ASTM C136 - Standard test method for sieve analysis of fine and coarse aggregates, ASTM International, West Conshohocken, PA.

ASTM. 2006b. ASTM C207 - Standard specification for hydrated lime for masonary purposes, ASTM International, West Conshohocken, PA.

ASTM. 2006c. ASTM D3987 - Standard test method for shake extraction of solid waste with water, ASTM International, West Conshohocken, PA.

ASTM. 2008. ASTM C618 - Standard specification for coal fly ash and raw or calcined natural pozzolan for use in concrete, ASTM International, West Conshohocken, PA.

ASTM. 2010a. ASTM C39 - Standard test method for compressive strength of cylindrical concrete specimens, ASTM International, West Conshohocken, PA.

ASTM. 2010b. ASTM C1240 - Standard specification for silica fume used in cementitious mixtures, ASTM International, West Conshohocken, PA.

B'Hymer, C., and J.A. Caruso. 2006. Selenium speciation analysis using inductively coupled plasma-mass spectrometry. Journal of Chromatography A, 1114 (1):1-20.

Badur, S., and R. Chaudhary. 2008. Utilization of hazardous wastes and by-products as a green concrete material through S/S process: A review. Reviews on Advanced Materials Science, 17 (1-2):42-61.

Bankowski, P., L. Zou, and R. Hodges. 2004. Reduction of metal leaching in brown coal fly ash using geopolymers. Journal of Hazardous materials, 114 (1-3):59-67.

Barnhart, J. 1997. Occurrences, uses, and properties of chromium. Regulatory Toxicology and Pharmacology, 26 (1):S3-S7.

Baur, I., P. Keller, D. Mavrocordatos, B. Wehrli, and C.A. Johnson. 2004. Dissolution-precipitation behaviour of ettringite, monosulfate, and calcium silicate hydrate. Cement and Concrete Research, 34 (2):341-348.

Beckman Coulter. 2011. LS 13 320 Laser diffraction particle size analyzer instructions for use, Beckman Coulter, Inc, Brea, CA.

Bin-Shafique, M.S. 2002. Leaching of heavy metals from fly ash stabilized soils. PhD Dissertation, University of Wisconsin-Madison, Madison, Wisconsin.

Bond, M.M. 2000. Characterization and control of selenium releases from mining in the Idaho phosphate region. M.S Thesis, Environmental Science, Moscow, Idaho.

Bone, B.D., L.H. Barnard, D.I. Boardman, P.J. Carey, C.D. Hills, H.M. Jones, C.L. Macleod, and M. Tyrer. 2004. Review of scientific literature on the use of stabilisation/solidification for the treatment of contaminated soil, solid waste and sludges, Environment Agency, Bristol, United Kingdom.

Bremner, T. 2001. Environmental aspects of concrete: problems and solutions. 1st All-Russian Conference on Concrete and Reinforced Concrete, Moscow, Russia, 232-246

Cappuyns, V., and R. Swennen. 2008. The application of pHstat leaching tests to assess the pH-dependent release of trace metals from soils, sediments and waste materials. Journal of Hazardous materials, 158 (1):185-195.

CEN. 2006. TS 14997 - Characterization of waste. Leaching behaviour tests. Influence of pH on leaching with continuous pH-control European committee for standardization (CEN), Brussels, Belgium.

Chancey, R.T. 2008. Characterization of crystalline and amorphous phases and respective reactivities in a class F fly ash. PhD dissertation, University of Texas at Austin, Austin, Texas.

Charlton, S.R., C.L. Macklin, and D.L. Parkhurst. 1997. PHREEQCI—a graphical user interface for the geochemical computer program PHREEQC. Water Resources Investigation Report: 97-4222.

Chrysochoou, M., and D. Dermatas. 2006. Evaluation of ettringite and hydrocalumite formation for heavy metal immobilization: Literature review and experimental study. Journal of Hazardous materials, 136 (1):20-33.

Cioffi, R., L. Maffucci, and L. Santoro. 2003. Optimization of geopolymer synthesis by calcination and polycondensation of a kaolinitic residue. Resources, conservation and recycling, 40 (1):27-38.

Cornelis, G., C.A. Johnson, T.V. Gerven, and C. Vandecasteele. 2008. Leaching mechanisms of oxyanionic metalloid and metal species in alkaline solid wastes: A review. Applied Geochemistry, 23 (5):955-976.

Damtoft, J.S., J. Lukasik, D. Herfort, D. Sorrentino, and E.M. Gartner. 2008. Sustainable development and climate change initiatives. Cement and Concrete Research, 38 (2):115-127.

Das, G.P. 2008. Ash weathering controls on contaminant leachability. PhD dissertation, Infrastructure and Environmental Systems, The University of North Carolina at Charlotte, Charlotte, North Carolina.

Davidovits, J. 1991. Geopolymers : Inorganic polymeric new materials. Journal of thermal analysis, 37:1633-1656.

Dermatas, D., D.H. Moon, N. Menounou, X. Meng, and R. Hires. 2004. An evaluation of arsenic release from monolithic solids using a modified semi-dynamic leaching test. Journal of Hazardous materials, 116 (1):25-38.

Dhir, R.K., T.D. Dyer, and L.J. Csetenyi. 2008. NORA: Non-radioactive waste solidification methods and stability assessment, Concrete Technology Unit, Department of Civil Engineering, University of Dundee, Dundee, Scotland.

Diaz, E., E. Allouche, and S. Eklund. 2010. Factors affecting the suitability of fly ash as source material for geopolymers. Fuel, 89 (5):992-996.

Dogan, O., and M. Kobya. 2006. Elemental analysis of trace elements in fly ash sample of Yatağan thermal power plants using EDXRF. Journal of Quantitative Spectroscopy and Radiative Transfer, 101 (1):146-150.

Duxson, P., A. Fernâandez-Jimâenez, J. Provis, G. Lukey, A. Palomo, and J. Deventer. 2007. Geopolymer technology: the current state of the art. Journal of Materials Science, 42 (9):2917-2933.

EA. 2005a. EA NEN 7371 - The determination of the availability of inorganic components for leaching - "the maximum availability leaching test", Environment Agency, United Kingdom.

EA. 2005b. EA NEN 7375 - Determination of leaching of inorganic components with the diffusion test -The tank test, Environment Agency, United Kingdom.

Fällman, A.-M. 1997. Performance and design of the availability test for measurement of potentially leachable amounts from waste materials. Environmental Science and Technology, 31 (3):735-744.

Fernández-Jiménez, A., I. García-Lodeiro, and A. Palomo. 2007. Durability of alkali-activated fly ash cementitious materials. Journal of Materials Science, 42 (9):3055-3065.

Fernández-Jiménez, A., and A. Palomo. 2005. Composition and microstructure of alkali activated fly ash binder: Effect of the activator. Cement and Concrete Research, 35 (10):1984-1992.

Fernández-Jiménez, A., and A. Palomo. 2009. Nanostructure/microstructure of fly ash geopolymers. In Geopolymers: structure, processing, properties and industrial applications, edited by J. L. Provis and J. S. J. van Deventer. Cambridge, United Kingdom: Woodhead Publishing limited.

Finkelman, R.B., and M.E. Mrose. 1977. Downeyite, the first verified natural occurrence of SeO. American Mineralogist, 62:316-320.

Gartner, E. 2004. Industrially interesting approaches to "low-CO2" cements. Cement and Concrete Research, 34 (9):1489-1498.

Giannopoulou, I.P., and D. Panias. 2007. Structure, design and applications of geopolymeric materials. 3rd International Conference on Deformation Processing and Structure of Materials, Belgrade, Serbia,

Goldberg, S., D.A. Martens, H.S. Forster, and M. Herbel. 2006. Speciation of selenium (IV) and selenium (VI) using coupled ion chromatography—hydride generation atomic absorption spectrometry. Soil Science Society of America Journal, 70 (1):41-47.

Gougar, M., B. Scheetz, and D. Roy. 1996. Ettringite and C---S---H Portland cement phases for waste ion immobilization: A review. Waste Management, 16 (4):295-303.

Guo, X., H. Shi, L. Chen, and W.A. Dick. 2010. Alkali-activated complex binders from class C fly ash and Ca-containing admixtures. Journal of Hazardous materials, 173 (1-3):480-486.

Halim, C.E., S.A. Short, J.A. Scott, R. Amal, and G. Low. 2005. Modelling the leaching of Pb, Cd, As, and Cr from cementitious waste using PHREEQC. Journal of Hazardous materials, 125 (1-3):45-61.

Hardjito, D., and V. Rangan. 2005. Development and properties of low-calcium fly ash-based geopolymer concrete, Research Report GC 1, Curtin University of Technology, Perth, Australia.

Hardjito, D., and M. Tsen. 2008. Strength and thermal stability of fly ash based geopolymer mortar. The 3rd Asian Concrete Federation international conference ACF/VCA 2008, 11-13 November, 2008, Ho Chi Minh City, Vietnam,

Iwashita, A., T. Nakajima, H. Takanashi, A. Ohki, Y. Fujita, and T. Yamashita. 2007. Determination of trace elements in coal and coal fly ash by joint-use of ICP-AES and atomic absorption spectrometry. Talanta, 71 (1):251-257.

Izquierdo, M., and X. Querol. 2011. Leaching behaviour of elements from coal combustion fly ash: An overview. International Journal of Coal Geology.

Izquierdo, M., X. Querol, J. Davidovits, D. Antenucci, H. Nugteren, and C. Fernández-Pereira. 2009. Coal fly ash-slag-based geopolymers: Microstructure and metal leaching. Journal of Hazardous materials, 166 (1):561-566.

Izquierdo, M., X. Querol, C. Phillipart, D. Antenucci, and M. Towler. 2010. The role of open and closed curing conditions on the leaching properties of fly ash-slag-based geopolymers. Journal of Hazardous materials, 176 (1-3):623-628.

Jackson, B.P. 1998. Trace element solubility from land application of fly ash/organic waste mixtures with emphasis on arsenic and selenium speciation. PhD dissertation, University of Georgia, Athens, Georgia.

Jankowski, J., C.R. Ward, D. French, and S. Groves. 2006. Mobility of trace elements from selected Australian fly ashes and its potential impact on aquatic ecosystems. Fuel, 85 (2):243-256.

Jegadeesan, G., S.R. Al-Abed, and P. Pinto. 2008. Influence of trace metal distribution on its leachability from coal fly ash. Fuel, 87 (10):1887-1893.

Juenger, M.C.G., F. Winnefeld, J.L. Provis, and J.H. Ideker. 2010. Advances in alternative cementitious binders. Cement and Concrete Research, - Article in press.

Khale, D., and R. Chaudhary. 2007. Mechanism of geopolymerization and factors influencing its development: a review. Journal of Materials Science, 42 (3):729-746.

Kinniburgh, D., and D. Cooper. 2011. PhreePlot Guide : creating graphical output with PHREEQC. http://www.phreeplot.org/ (accessed 4th November 2011).

Klemm, W.A. 1998. Ettringite and oxyanion-substituted ettringites-- their characterization and applications in the fixation of heavy metals: A synthesis of the literature, Portland Cement Association (PCA), Stokie, Illinois.

Komnitsas, K., and D. Zaharaki. 2007. Geopolymerisation: A review and prospects for the minerals industry. Minerals Engineering, 20 (14):1261-1277.

Kong, D.L.Y., and J.G. Sanjayan. 2010. Effect of elevated temperatures on geopolymer paste, mortar and concrete. Cement and Concrete Research, 40 (2):334-339.

Kosson, D.S., H.A. van der Sloot, F. Sanchez, and A.C. Garrabrants. 2002. An integrated framework for evaluating leaching in waste management and utilization of secondary materials. Environmental Engineering Science, 19 (3):159-204.

Lloyd, N.A., and B.V. Rangan. 2010. Geopolymer concrete with fly ash. 2nd International Conference on Sustainable Construction Materials and Technologies, Ancona, Italy,

Magalhães, M.C.F. 2002. Arsenic. An environmental problem limited by solubility. Pure and Applied Chemistry, 74 (10):1843-1850.

Mehta, P.K., and P.J.M. Monteiro. 2006. Concrete : microstructure, properties, and materials. New York: McGraw-Hill.

Min, J.H. 1997. Removal of arsenic, selenium and chromium from wastewater using Fe(III) doped alginate gel sorbent. PhD dissertation, Civil Engineering, University of California, Los Angeles, California.

Miyano, T., and C. Klein. 1983. Conditions of riebeckite formation in the iron-formation of the Dales Gorge Member, Hamersley Group, Western Australia. American Mineralogist, 68 (5-6):517.

Moon, D.H., D. Dermatas, and N. Menounou. 2004. Arsenic immobilization by calcium-arsenic precipitates in lime treated soils. Science of the Total Environment, 330 (1-3):171-185.

NAS. 1977. Arsenic - medical and biological effects of environmental pollutants. Washington, DC: The National Research Council, National Academy of Sciences.

Nazari, A., A. Bagheri, and S. Riahi. 2011. Properties of geopolmer with seeded fly ash and rice husk bark ash. Materials Science and Engineering A, - Article In press.

Nordtest. 1995. NT ENVIR 003 - Solid waste, granular inorganic material : Availability test, Nordtest, Espoo, Finland.

OEWRI. 2008. Standard operating procedure for: LS 13 320 laser diffraction particle size analyzer operation, Missouri State University and Ozarks Environmental and Water Resources Institute (OEWRI), Springfield, MO.

Ogunro, V., and O. Sanusi. 2010. Short-term mobility of elements from fly ash based geopolymer paste. 11th International symposium on environmental geotechnology and sustainable development (ISEG 2010), Beijing, China,

Pacheco-Torgal, F., J. Castro-Gomes, and S. Jalali. 2008a. Alkali-activated binders: A review. Part 2. About materials and binders manufacture. Construction & building materials., 22 (7):1315-1322.

Pacheco-Torgal, F., J. Castro-Gomes, and S. Jalali. 2008b. Alkali-activated binders: A review:Part 1. Historical background, terminology, reaction mechanisms and hydration products. Construction and Building Materials, 22 (7):1305-1314.

Panagiotopoulou, C., E. Kontori, T. Perraki, and G. Kakali. 2007. Dissolution of aluminosilicate minerals and by-products in alkaline media. Journal of Materials Science, 42 (9):2967-2973.

Paoletti, F. 2002. Behavior of oxyanions forming heavy metals in municipal solid waste incineration. PhD dissertation, Institute for Technical Chemistry (Institut für Technische Chemie), Karlsruhe Institute of Technology (KIT) formerly Forschungszentrum Karlsruhe, Karlsruhe, Germany.

Pariatamby, A., C. Subramaniam, S. Mizutani, and H. Takatsuki. 2006. Solidification and stabilization of fly ash from mixed hazardous waste incinerator using ordinary Portland cement. Environmental Sciences, 13:8-13.

Parkhurst, D.L., and C.A.J. Appelo. 1999. User's guide to PHREEQC (Version 2): A computer program for speciation, batch-reaction, one-dimensional transport, and inverse geochemical calculations. Denver, Colorado: United States Geological Survey.

PCA. Concrete technology - what causes efflorescence and how can it be avoided? Portland Cement Asssociation (PCA) 2012. Available from http://www.cement.org/tech/faq_efflorescence.asp.

Perera, D.S., O. Uchida, E.R. Vance, and K.S. Finnie. 2007. Influence of curing schedule on the integrity of geopolymers. Journal of Materials Science, 42 (9):3099-3106.

Provis, J.L., P. Duxson, R.M. Harrex, C.-Z. Yong, and J.S.J. van Deventer. 2009. Valorisation of fly ashes by geopolymerisation. Global NEST Journal, 11 (2):147-154.

Provis, J.L., and J. van Deventer. 2009. Introduction to geopolymers. In Geopolymers: Structure, Processing, Properties and Industrial Applications, edited by J. L. Provis and J. S. J. van Deventer. Cambridge, United Kingdom: Woodhead Publ. Limited.

Quiroga, P.N., and D.W. Fowler. 2004. The effects of aggregates characteristics on the performance of Portland cement concrete. Austin, TX: International Center for Aggregates Research, University of Texas at Austin.

Rangan, B.V. 2008. Low calcium fly ash based geopolymer concrete. In Concrete Construction Engineering Handbook, edited by E. G. Nawy. Boca Raton, Florida: Taylor & Francis Ltd.

Rangan, B.V. 2009. Engineering properties of geopolymer concrete. In Geopolymers: structure, processing , properties and industrial applications, edited by J. L. Provis and J. S. J. Van Deventer. Cambridge, United Kingdom.

Rattanasak, U., and P. Chindaprasirt. 2009. Influence of NaOH solution on the synthesis of fly ash geopolymer. Minerals Engineering, 22 (12):1073-1078.

Roy, D.M. 1999. Alkali-activated cements opportunities and challenges. Cement and Concrete Research, 29 (2):249-254.

Saikia, N., S. Kato, and T. Kojima. 2006. Behavior of B, Cr, Se, As, Pb, Cd, and Mo present in waste leachates generated from combustion residues during the formation of ettringite. Environmental Toxicology and Chemistry, 25 (7):1710-1719.

Sakulich, A.R. 2009. Characterization of environmentally-friendly alkali activated slag cements and ancient building materials. PhD dissertation, Drexel University, Philadelphia, PA.

Sanusi, O., and V. Ogunro. 2009. Assessment of oxyanions trace elements leaching from fly ash-based geopolymer. 10th International Symposium on Environmental Geotechnology and Sustainable Development, Bochum, Germany,

Sanusi, O., and V. Ogunro. 2011a. Influence of calcium on strength and mobility of elements from monolithic fly ash based geopolymer paste - submitted manuscript, University of North Carolina at Charlotte.

Sanusi, O., and V. Ogunro. 2011b. Predicting the leaching of oxyanion forming trace elements from fly ash based geopolymer paste using the availability test - unpublished manuscript, University of North Carolina at Charlotte.

Sanusi, O., B. Tempest, and V.O. Ogunro. 2011. Mitigating leachability from fly ash based geopolymer concrete using recycled concrete aggregate (RCA). Geotechnical special publication of American Society of Civil Engineers, 2 (211):1315-1324.

Schiopu, N., L. Tiruta-Barna, E. Jayr, J. Méhu, and P. Moszkowicz. 2009. Modelling and simulation of concrete leaching under outdoor exposure conditions. Science of the Total Environment, 407 (5):1613-1630.

Schuwirth, N., and T. Hofmann. 2006. Comparability of and alternatives to leaching tests for the assessment of the emission of inorganic soil contamination Journal of Soils and Sediments, 6 (2):102-112.

Schwantes, J.M., and B. Batchelor. 2006. Simulated infinite-dilution leach test. Environmental Engineering Science, 23 (1):4-13.

Sear, L.K.A. 2001. Properties and use of coal fly ash : a valuable industrial by-product. London: Thomas Telford.

Shtiza, A., R. Swennen, V. Cappuyns, and A. Tashko. 2009. ANC, BNC and mobilization of Cr from polluted sediments in function of pH changes. Environmental Geology, 56 (8):1663-1678.

Škvára, F. 2007. Alkali activated materials or geopolymers? Ceramics- Silikáty, 51 (3):173-177.

Soco, E., and J. Kalembkiewicz. 2009. Investigations on Cr mobility from coal fly ash. Fuel, 88 (8):1513-1519.

Somna, K., C. Jaturapitakkul, P. Kajitvichyanukul, and P. Chindaprasirt. 2011. NaOH-activated ground fly ash geopolymer cured at ambient temperature. Fuel, 90 (6):2118-2124.

Struble, L., and J. Godfrey. 2004. How sustainable is concrete? Proceedings of the International Workshop on Sustainable Development and Concrete Technology Beijing, China,

Subaer. 2004. Influence of aggregate on the microstructure of geopolymer. PhD Dissertation, Deparment of Applied Physics, Curtin University of Technology, Perth, Western Australia.

Sun, P. 2005. Fly ash based inorganic polymeric building material. PhD Dissertation, Civil Engineering, Wayne State University, Detroit, Michigan.

Suzuki, M., and D. Rohde. 2008. Resolving overlapping peak problems with NORAN system 7 spectral imaging software, Thermo Fisher scientific, Madison, WI.

Tempest, B. 2010. Engineering characterization of waste derived geopolymer cement concrete for structural applications. Ph.D Dissertation, Infrastructure and Environmental Systems, The University of North Carolina at Charlotte, Charlotte, North Carolina.

Temuujin, J., A. van Riessen, and R. Williams. 2009. Influence of calcium compounds on the mechanical properties of fly ash geopolymer pastes. Journal of Hazardous materials, 167 (1-3):82-88.

USEPA. 1986. Method 1320 - Multiple extraction procedure (MEP), United States Environmental Protection Agency.

USEPA. 1994. Method 1312 - Synthetic precipitation leaching procedure (SPLP), United States Environmental Protection Agency.

USEPA. 2009a. National primary drinking water regulations, United States Environmental Protection Agency.

USEPA. 2009b. Preliminary method 1313 - Liquid - solid partitioning as a function of extract pH for constituents in solid materials using a parallel batch extraction, United States Environmental Protection Agency.

USEPA. 2009c. Preliminary method 1315 - Mass transfer in monolithic or compacted granular materials using a semi-dynamic leaching procedure, United States Environmental Protection Agency.

USEPA. 2012. Regional screening table -user's guide 2012 [cited 30th October 2012]. Available from http://www.epa.gov/reg3hwmd/risk/human/rb-concentration_table/usersguide.htm.

USGS. 2012. Change in nitric acid preservative for trace element samples. United States Geological Survey (USGS) 1998 [cited 19th July 2012]. Available from http://water.usgs.gov/admin/memo/QW/qw98.06.html.

Van der Sloot, H., and D. Kosson. 2003. A unified approach for the judgement of environmental properties of construction materials (cement-based, asphaltic, unbound aggregates, soil) in different stages of their life cycle. WASCON 2003 conference, San Sebastian, Spain,

Van Jaarsveld, J., and J. Van Deventer. 1999. The effect of metal contaminants on the formation and properties of waste-based geopolymers. Cement and Concrete Research, 29 (8):1189-1200.

van Oss, H., and A.C. Padovani. 2002. Cement manufacture and the environment, part I: chemistry and technology. Journal of Industrial Ecology, 6 (1):89-105.

van Oss, H.G., and A.C. Padovani. 2003. Cement manufacture and the environment, part II: environmental challenges and opportunities. Journal of Industrial Ecology, 7 (1):93-126.

Wang, T. 2007. The leaching behavior of arsenic, selenium and other trace elements in coal fly ash. PhD dissertation, Civil Engineering, University of Missouri-Rolla, Rolla, Missouri.

Wang, T., T. Su, J. Wang, and K. Ladwig. 2007. Calcium effect on asernic (v) adsorption onto coal fly ash. World of Coal Ash conference (WOCA 2007), Lexington, Kentucky,

Xu, H., and J.S.J. Van Deventer. 2000. The geopolymerisation of alumino-silicate minerals. International Journal of Mineral Processing, 59 (3):247-266.

Xu, J., Y. Zhou, Q. Chang, and H. Qu. 2006. Study on the factors of affecting the immobilization of heavy metals in fly ash-based geopolymers. Materials Letters, 60 (6):820-822.

Yao, X., Z. Zhang, H. Zhu, and Y. Chen. 2009. Geopolymerization process of alkali-metakaolinite characterized by isothermal calorimetry. Thermochimica Acta, 493 (1-2):49-54.

Yip, C., G. Lukey, and J. Van Deventer. 2005. The coexistence of geopolymeric gel and calcium silicate hydrate at the early stage of alkaline activation. Cement and Concrete Research, 35 (9):1688-1697.

Yip, C., and J. van Deventer. 2003. Microanalysis of calcium silicate hydrate gel formed within a geopolymeric binder. Journal of Materials Science, 38 (18):3851-3860.

Zhang, J., J.L. Provis, D. Feng, and J.S. van Deventer. 2008. Geopolymers for immobilization of Cr(6+), Cd(2+), and Pb(2+). Journal of Hazardous materials, 157 (2-3):2-3.

Zhang, M. 2000. Incorporation of oxyanionic boron, chromium, molybdenum, and selenium into hydrocalumite and ettringite: Application to cementitious systems. PhD dissertation, Earth Science, Waterloo, Ontario, CanadaUniversity of Waterloo.

Zhang, M., and E.J. Reardon. 2003. Removal of B, Cr, Mo, and Se from wastewater by incorporation into hydrocalumite and ettringite. Environmental science & technology, 37 (13):2947-2952.

Zhang, M., and E.J. Reardon. 2005. Chromate and selenate hydrocalumite solid solutions and their applications in waste treatment. Science in China Series C: Life Sciences, 48:165-173.

Zhang, Y., W. Sun, and Z. Li. 2009. Preparation and microstructure characterization of poly-sialate-disiloxo type of geopolymeric cement. Journal of Central South University of Technology, 16 (6):906-913.

Zheng, L., C. Wang, W. Wang, Y. Shi, and X. Gao. 2011. Immobilization of MSWI fly ash through geopolymerization: Effects of water-wash. Waste Management, 31 (2):311-317.

Zhu, C. 2009. Geochemical modeling of reaction paths and geochemical reaction networks. Reviews in Mineralogy and Geochemistry, 70 (1):533.

Zhu, C., and G.M. Anderson. 2002. Environmental applications of geochemical modeling. Cambridge, United Kingdom: Cambridge University Press.

Zhu, Y.N., X.H. Zhang, Q.L. Xie, D.Q. Wang, and G.W. Cheng. 2006. Solubility and stability of calcium arsenates at 25 C. Water, Air, & Soil Pollution, 169 (1):221-238.

APPENDIX A: MIX DESIGN FOR THE GEOPOLYMER CONCRETE

TABLE A-1: Mix design for the geopolymer concrete (kg/m^3)

Mix	HL(%)	HL (kg)	CFA(kg)	FA (kg)	CA (kg)	SF (kg)	NaOH (kg)	H$_2$O (kg)	w/c
GPC	0.000	0.000	483.437	773.371	774.012	36.202	48.376	206.959	0.364
GP1	0.530	2.563	483.437	773.371	774.012	36.202	48.376	206.959	0.363
GP2	0.994	4.806	483.437	773.371	774.012	36.202	48.376	206.959	0.361
GP3	1.988	9.611	483.437	773.371	774.012	36.202	48.376	206.959	0.358

TABLE A-2: Percentage of each component in the geopolymer concrete (%)

Aggregates*	CFA	SF	HL	NaOH	H$_2$O	Total
67	20.8	1.6	0.0	2.1	8.9	100.0
67	20.8	1.6	0.1	2.1	8.9	100.0
66	20.8	1.6	0.2	2.1	8.9	100.0
66	20.7	1.6	0.4	2.1	8.9	100.0

*Aggregates = FA + CA

TABLE A-3: Explanation of notations used in mix design

HL	Hydrated lime
CFA	Coal fly ash
FA	Fine agregate
CA	Coarse aggregate
SF	Silica fume
NaOH	Sodium hydroxide
H$_2$O	water

APPENDIX B: COMPRESSIVE STRENGTH MEASUREMENTS FOR THE
GEOPOLYMER CONCRETE MIXES

TABLE B-1: Compressive strength of the geopolymer concrete (psi)

	7d_wo*	28d_wo	7d_w**	28d_w
GPC	951.9	3155.772	7542.79	7811.404
GPC	974.11	3121.392	7472.34	8330.362
GPC	973.26	1664.686	5344.46	8209.819
GP1	1008.065	1898.557	5286.786	5894.171
GP1	1050.792	2065.507	5563.667	5768.251
GP1	1075.41	1950.764	5440.719	6377.9
GP2	1194.963	1968.874	6530.702	7520.939
GP2	1177.985	2246.604	6264.431	7231.749
GP2	1211.658	2146.576	6363.894	7209.536
GP3	1378.183	1867.148	6579.938	7066.638
GP3	1437.323	1942.841	5539.191	6934.776
GP3	1182.654	2000.849	6218.308	4607.668

TABLE B-2: Compressive strength of geopolymer
concrete (MPa)

	7d_wo*	28d_wo	7d_w**	28d_w
GPC	6.56	21.76	52.01	53.86
GPC	6.72	21.52	51.51	57.43
GPC	6.71	11.48	36.85	56.61
GP1	6.95	13.09	36.45	40.64
GP1	7.25	14.25	38.36	39.77
GP1	7.41	13.45	37.51	43.97
GP2	8.24	13.58	45.03	51.86
GP2	8.12	15.49	43.19	49.86
GP2	8.36	14.8	43.88	49.7
GP3	9.5	12.87	45.37	48.72
GP3	9.91	13.4	38.19	47.82
GP3	8.16	13.8	42.87	31.77

*Geopolymer concrete cured without heat
**Geopolymer concrete cured at 75°C

APPENDIX C: STATISTICAL ANALYSIS OF THE GEOPOLYMER CONCRETE COMPRESSIVE STRENGTH

APPENDIX C1: 7 DAYS COMPRRESIVE STRENGTH FOR GEOPOLYMER CONCRETE CURED WITHOUT HEAT
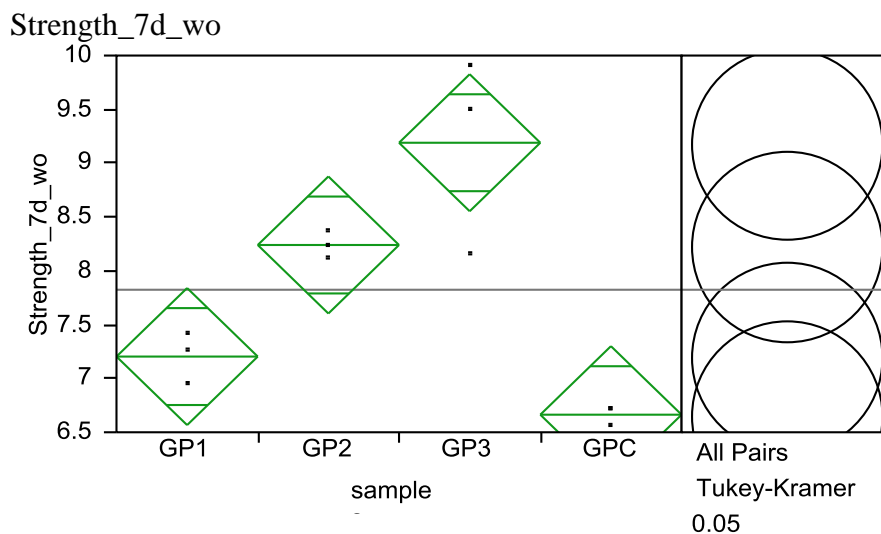
Strength_7d_wo

Wilcoxon / Kruskal-Wallis Tests (Rank Sums)

Level	Count	Score Sum	Expected Score	Score Mean	(Mean-Mean0)/Std0
GP1	3	15.000	19.500	5.0000	-0.740
GP2	3	26.000	19.500	8.6667	1.109
GP3	3	31.000	19.500	10.3333	2.034
GPC	3	6.000	19.500	2.0000	-2.404

1-way Test, ChiSquare Approximation

ChiSquare	DF	Prob>ChiSq
9.6667	3	0.0216 *

Small sample sizes. Refer to statistical tables for tests, rather than large-sample approximations.

Comparisons for all pairs using Tukey-Kramer HSD

q*	Alpha
3.20234	0.05

Abs(Dif)-HSD

	GP3	GP2	GP1	GPC
GP3	-1.2503	-0.3003	0.7363	1.2763
GP2	-0.3003	-1.2503	-0.2137	0.3263
GP1	0.7363	-0.2137	-1.2503	-0.7103
GPC	1.2763	0.3263	-0.7103	-1.2503

Positive values show pairs of means that are significantly different.

Level		Mean
GP3	A	9.1900000
GP2	A B	8.2400000
GP1	B C	7.2033333
GPC	C	6.6633333

Levels not connected by same letter are significantly different.

Level	- Level	Difference	Std Err Dif	Lower CL	Upper CL	p-Value
GP3	GPC	2.526667	0.3904413	1.27634	3.776994	0.0009 *
GP3	GP1	1.986667	0.3904413	0.73634	3.236994	0.0042 *
GP2	GPC	1.576667	0.3904413	0.32634	2.826994	0.0158 *
GP2	GP1	1.036667	0.3904413	-0.21366	2.286994	0.1082
GP3	GP2	0.950000	0.3904413	-0.30033	2.200328	0.1475
GP1	GPC	0.540000	0.3904413	-0.71033	1.790328	0.5421
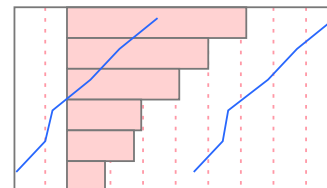
APPENDIX C2: 28 DAYS COMPRRESIVE STRENGTH FOR GEOPOLYMER
CONCRETE CURED WITHOUT HEAT
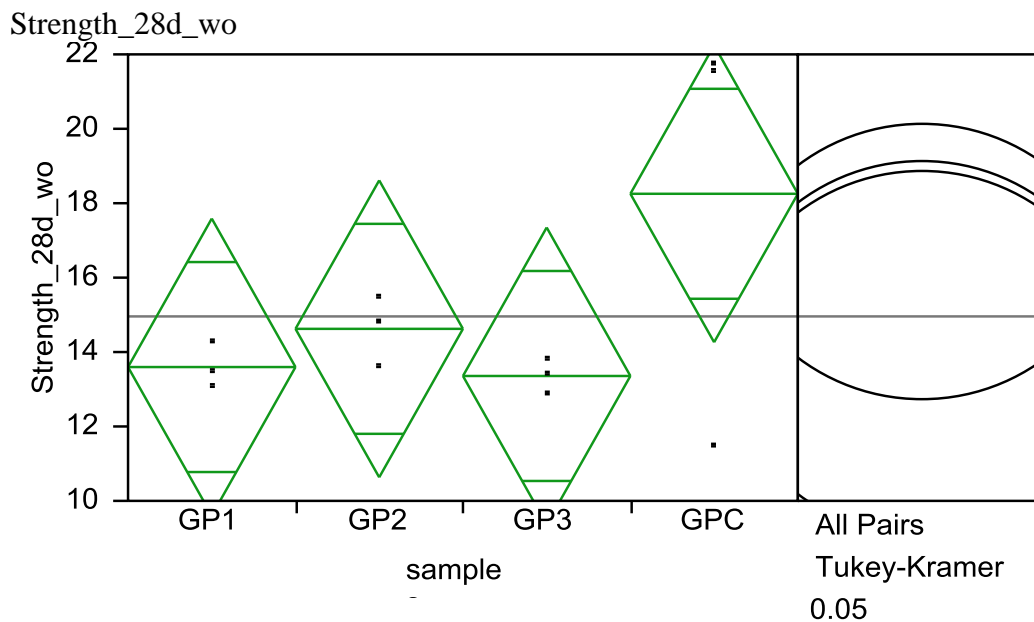
Strength_28d_wo

Wilcoxon / Kruskal-Wallis Tests (Rank Sums)

Level	Count	Score Sum	Expected Score	Score Mean	(Mean-Mean0)/Std0
GP1	3	16.000	19.500	5.33333	-0.555
GP2	3	25.000	19.500	8.33333	0.925
GP3	3	13.000	19.500	4.33333	-1.109
GPC	3	24.000	19.500	8.00000	0.740

1-way Test, ChiSquare Approximation

ChiSquare	DF	Prob>ChiSq
2.6923	3	0.4415

Small sample sizes. Refer to statistical tables for tests, rather than
large-sample approximations.

Comparisons for all pairs using Tukey-Kramer HSD

q*	Alpha
3.20234	0.05

Abs(Dif)-HSD

	GPC	GP2	GP1	GP3
GPC	-7.8363	-4.2063	-3.1797	-2.9397
GP2	-4.2063	-7.8363	-6.8097	-6.5697
GP1	-3.1797	-6.8097	-7.8363	-7.5963
GP3	-2.9397	-6.5697	-7.5963	-7.8363

Positive values show pairs of means that are significantly different.

Level		Mean
GPC	A	18.253333
GP2	A	14.623333
GP1	A	13.596667
GP3	A	13.356667

Levels not connected by same letter are significantly different.

Level	- Level	Difference	Std Err Dif	Lower CL	Upper CL	p-Value
GPC	GP3	4.896667	2.447057	-2.93965	12.73299	0.2637
GPC	GP1	4.656667	2.447057	-3.17965	12.49299	0.2989
GPC	GP2	3.630000	2.447057	-4.20632	11.46632	0.4886
GP2	GP3	1.266667	2.447057	-6.56965	9.10299	0.9525
GP2	GP1	1.026667	2.447057	-6.80965	8.86299	0.9735
GP1	GP3	0.240000	2.447057	-7.59632	8.07632	0.9996
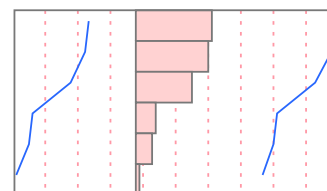
APPENDIX C3: 7 DAYS COMPRRESIVE STRENGTH FOR GEOPOLYMER
CONCRETE CURED WITH HEAT
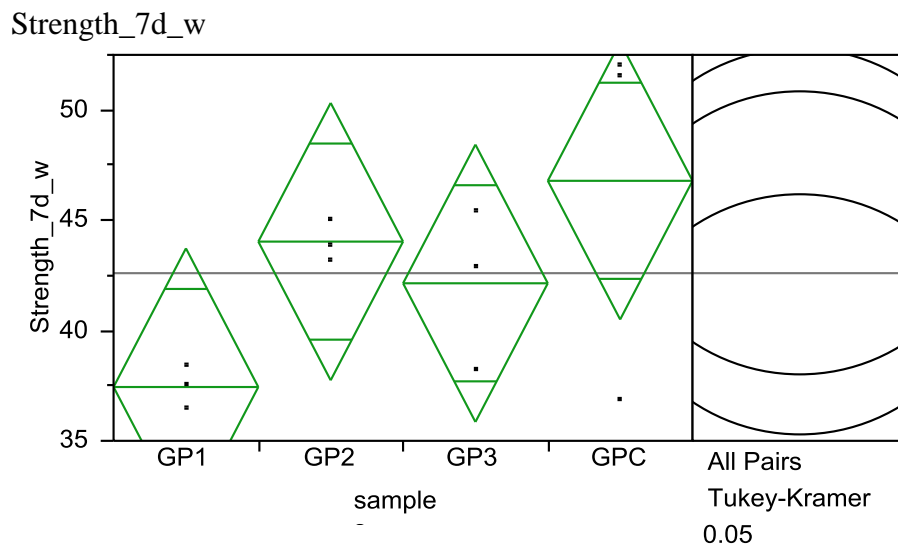
Strength_7d_w

Wilcoxon / Kruskal-Wallis Tests (Rank Sums)

Level	Count	Score Sum	Expected Score	Score Mean	(Mean-Mean0)/Std0
GP1	3	9.000	19.500	3.00000	-1.849
GP2	3	24.000	19.500	8.00000	0.740
GP3	3	20.000	19.500	6.66667	0.000
GPC	3	25.000	19.500	8.33333	0.925

1-way Test, ChiSquare Approximation

ChiSquare	DF	Prob>ChiSq
4.1282	3	0.2479

Small sample sizes. Refer to statistical tables for tests, rather than
large-sample approximations.

Comparisons for all pairs using Tukey-Kramer HSD

q*	Alpha
3.20234	0.05

Abs(Dif)-HSD

	GPC	GP2	GP3	GP1
GPC	-12.349	-9.593	-7.703	-2.999
GP2	-9.593	-12.349	-10.459	-5.756
GP3	-7.703	-10.459	-12.349	-7.646
GP1	-2.999	-5.756	-7.646	-12.349

Positive values show pairs of means that are significantly different

Level		Mean
GPC	A	46.790000
GP2	A	44.033333
GP3	A	42.143333
GP1	A	37.440000

Levels not connected by same letter are significantly different

Level	- Level	Difference	Std Err Dif	Lower CL	Upper CL	p-Value
GPC	GP1	9.350000	3.856360	-2.9994	21.69939	0.1492
GP2	GP1	6.593333	3.856360	-5.7561	18.94272	0.3787
GP3	GP1	4.703333	3.856360	-7.6461	17.05272	0.6326
GPC	GP3	4.646667	3.856360	-7.7027	16.99606	0.6409
GPC	GP2	2.756667	3.856360	-9.5927	15.10606	0.8885
GP2	GP3	1.890000	3.856360	-10.4594	14.23939	0.9591
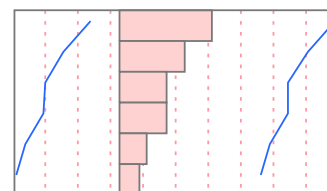
APPENDIX C4: 28 DAYS COMPRRESIVE STRENGTH FOR GEOPOLYMER
CONCRETE CURED WITH HEAT
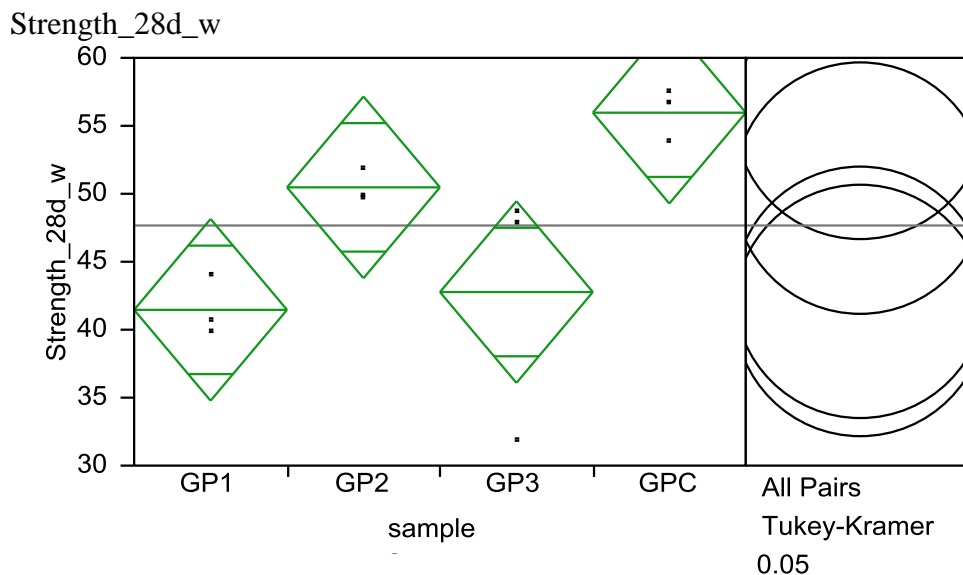
Strength_28d_w

Wilcoxon / Kruskal-Wallis Tests (Rank Sums)

Level	Count	Score Sum	Expected Score	Score Mean	(Mean-Mean0)/Std0
GP1	3	9.000	19.500	3.0000	-1.849
GP2	3	24.000	19.500	8.0000	0.740
GP3	3	12.000	19.500	4.0000	-1.294
GPC	3	33.000	19.500	11.0000	2.404

1-way Test, ChiSquare Approximation

ChiSquare	DF	Prob>ChiSq
9.4615	3	0.0237 *

Small sample sizes. Refer to statistical tables for tests, rather than
large-sample approximations.

Comparisons for all pairs using Tukey-Kramer HSD

q*	Alpha
3.20234	0.05

Abs(Dif)-HSD

	GPC	GP2	GP3	GP1
GPC	-13.126	-7.633	0.070	1.380
GP2	-7.633	-13.126	-5.423	-4.113
GP3	0.070	-5.423	-13.126	-11.816
GP1	1.380	-4.113	-11.816	-13.126

Positive values show pairs of means that are significantly different.

Level		Mean
GPC	A	55.966667
GP2	A B	50.473333
GP3	B	42.770000
GP1	B	41.460000

Levels not connected by same letter are significantly different.

Level	- Level	Difference	Std Err Dif	Lower CL	Upper CL	p-Value	
GPC	GP1	14.50667	4.099024	1.3802	27.63315	0.0312	*
GPC	GP3	13.19667	4.099024	0.0702	26.32315	0.0488	*
GP2	GP1	9.01333	4.099024	-4.1132	22.13982	0.2031	
GP2	GP3	7.70333	4.099024	-5.4232	20.82982	0.3079	
GPC	GP2	5.49333	4.099024	-7.6332	18.61982	0.5655	
GP3	GP1	1.31000	4.099024	-11.8165	14.43648	0.9879	
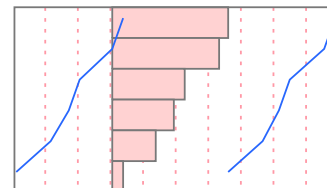
APPENDIX D: PH DEPENDENCE LEACHING TEST RESULTS FOR OTHER ELEMENTS
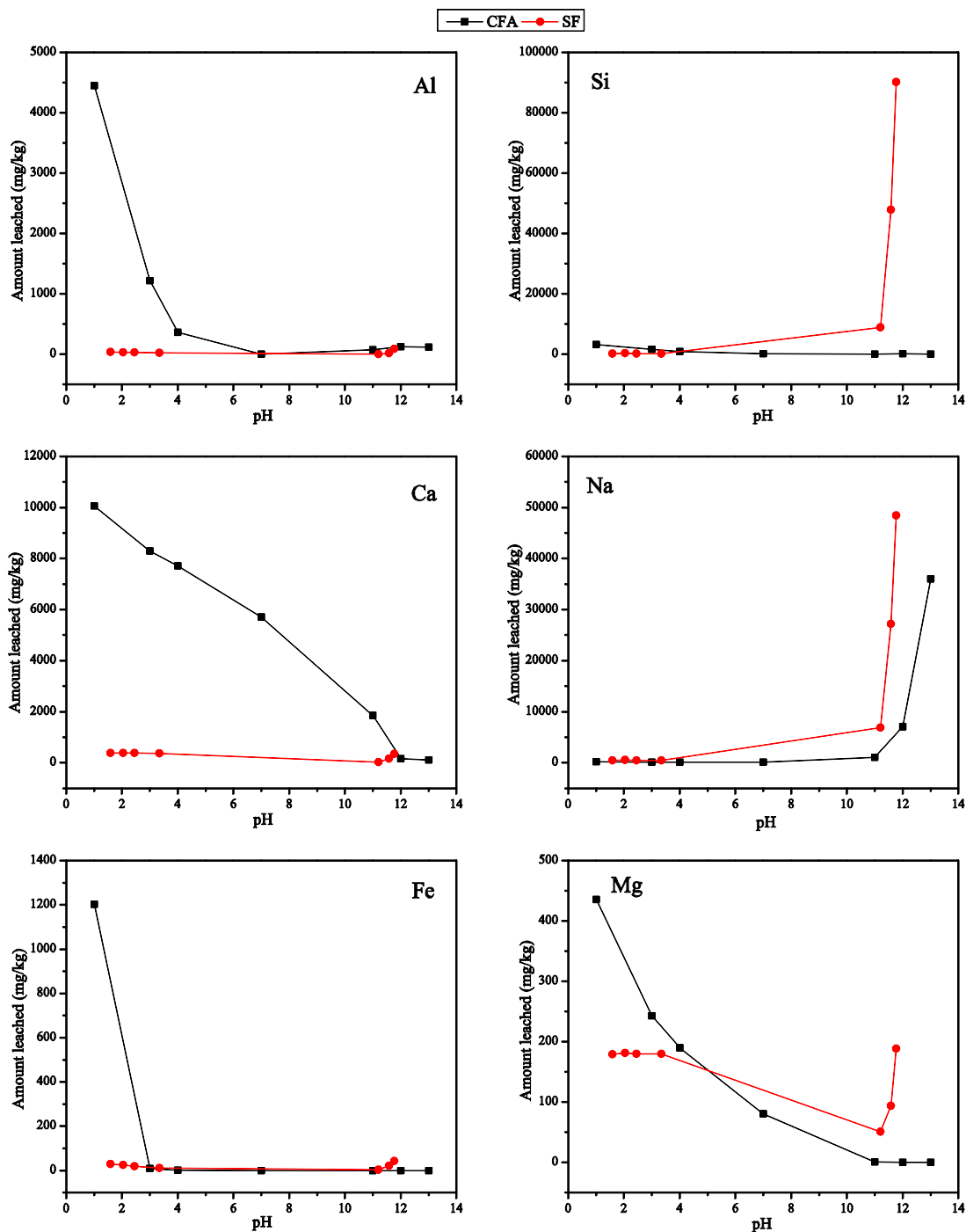
FIGURE D-1: pH dependence mobility of elements from CFA and SF
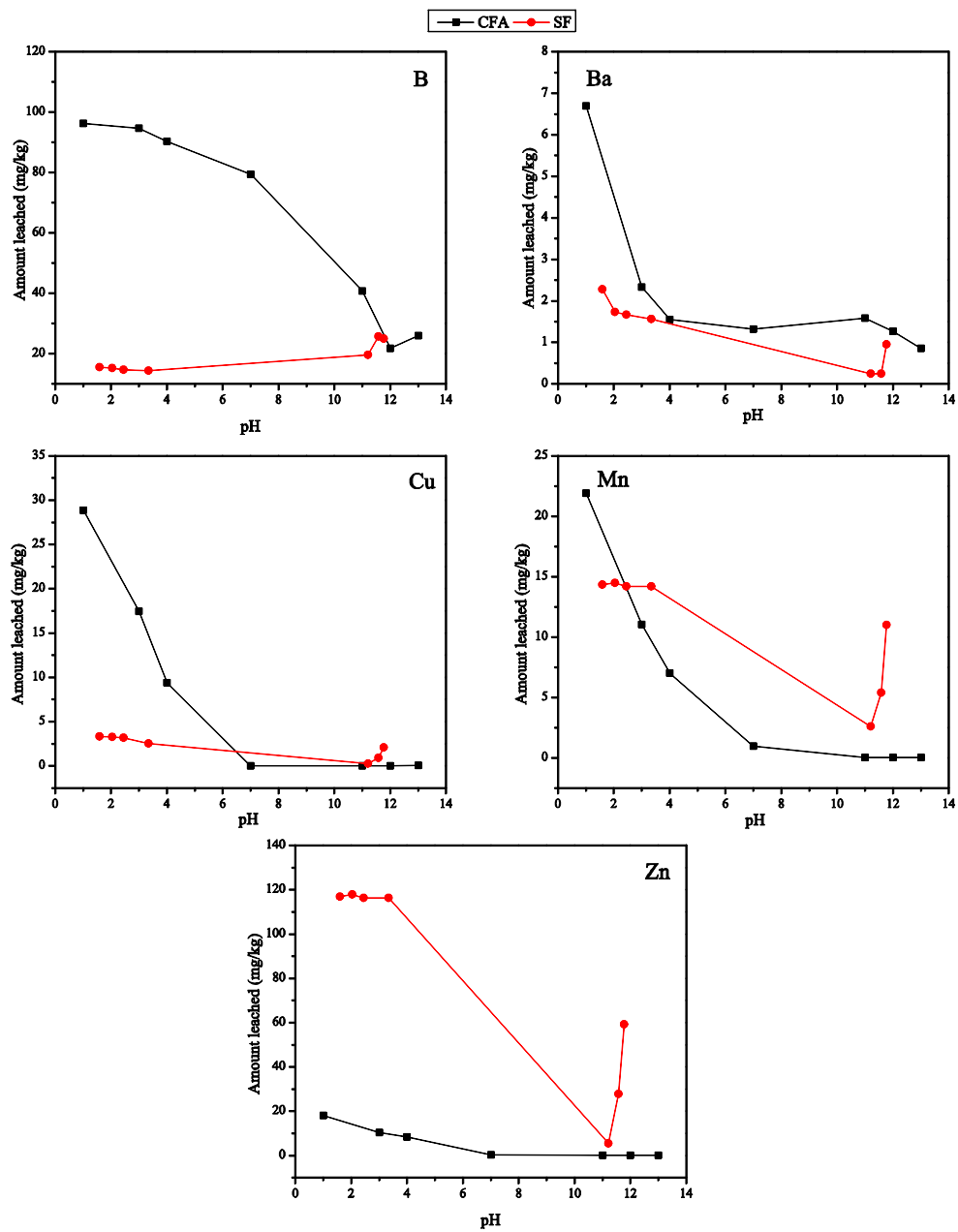
FIGURE D-2: pH dependence mobility of elements from CFA and SF
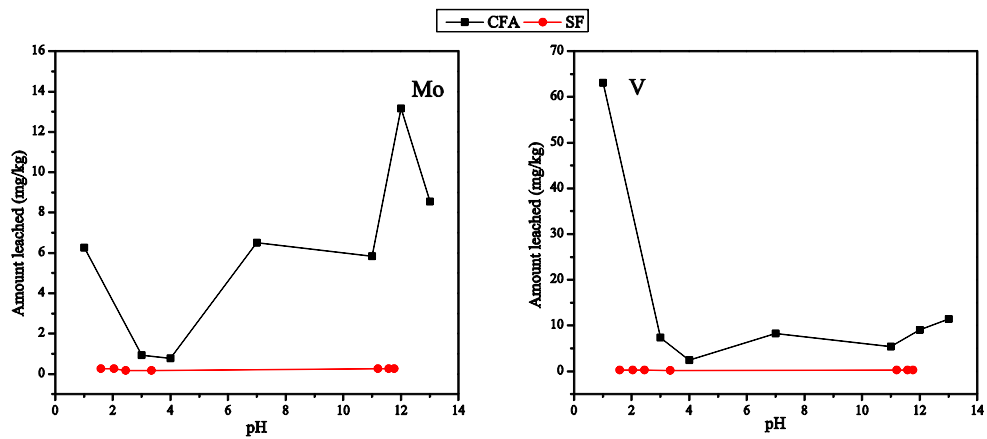
FIGURE D-3: pH dependence mobility of Mo and V from the CFA and SF
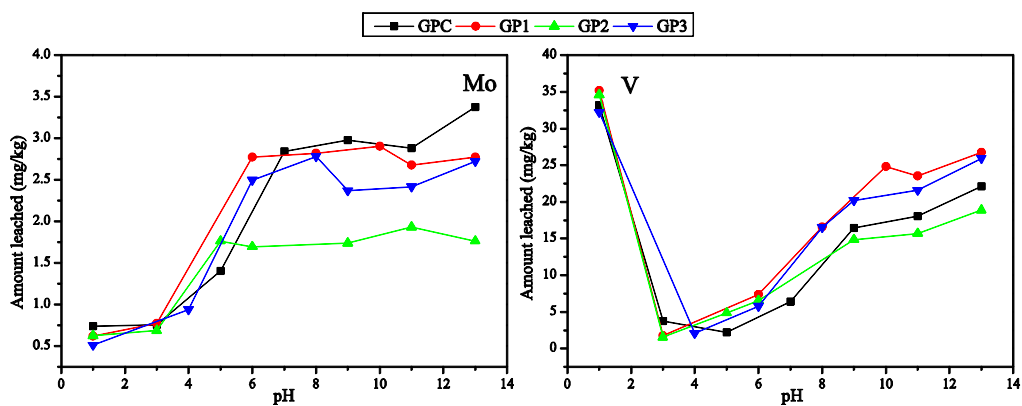
FIGURE D-4: pH dependence mobility of Mo and V from the geopolymer concretes
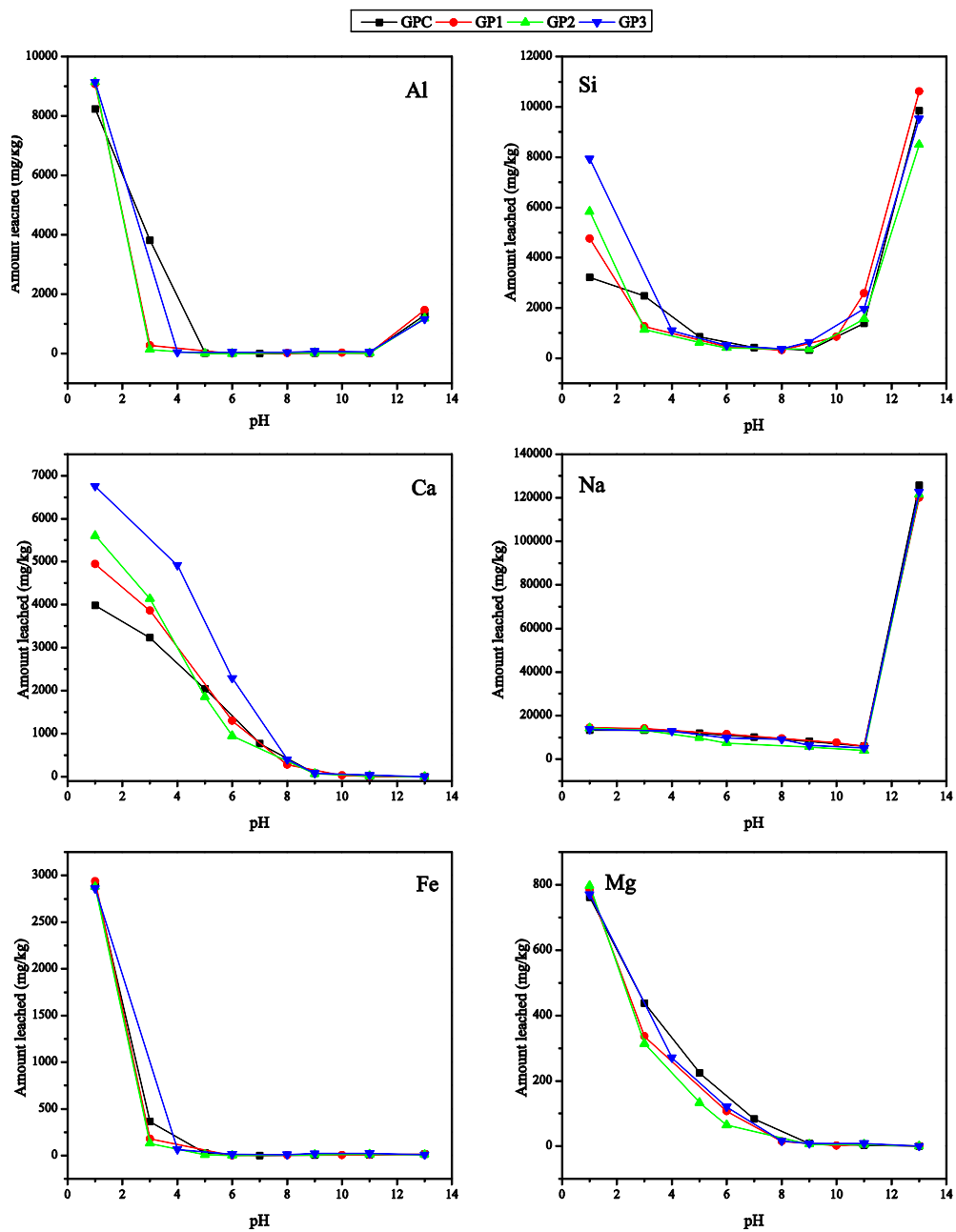
FIGURE D-5: pH dependence mobility of elements from the geopolymer concretes
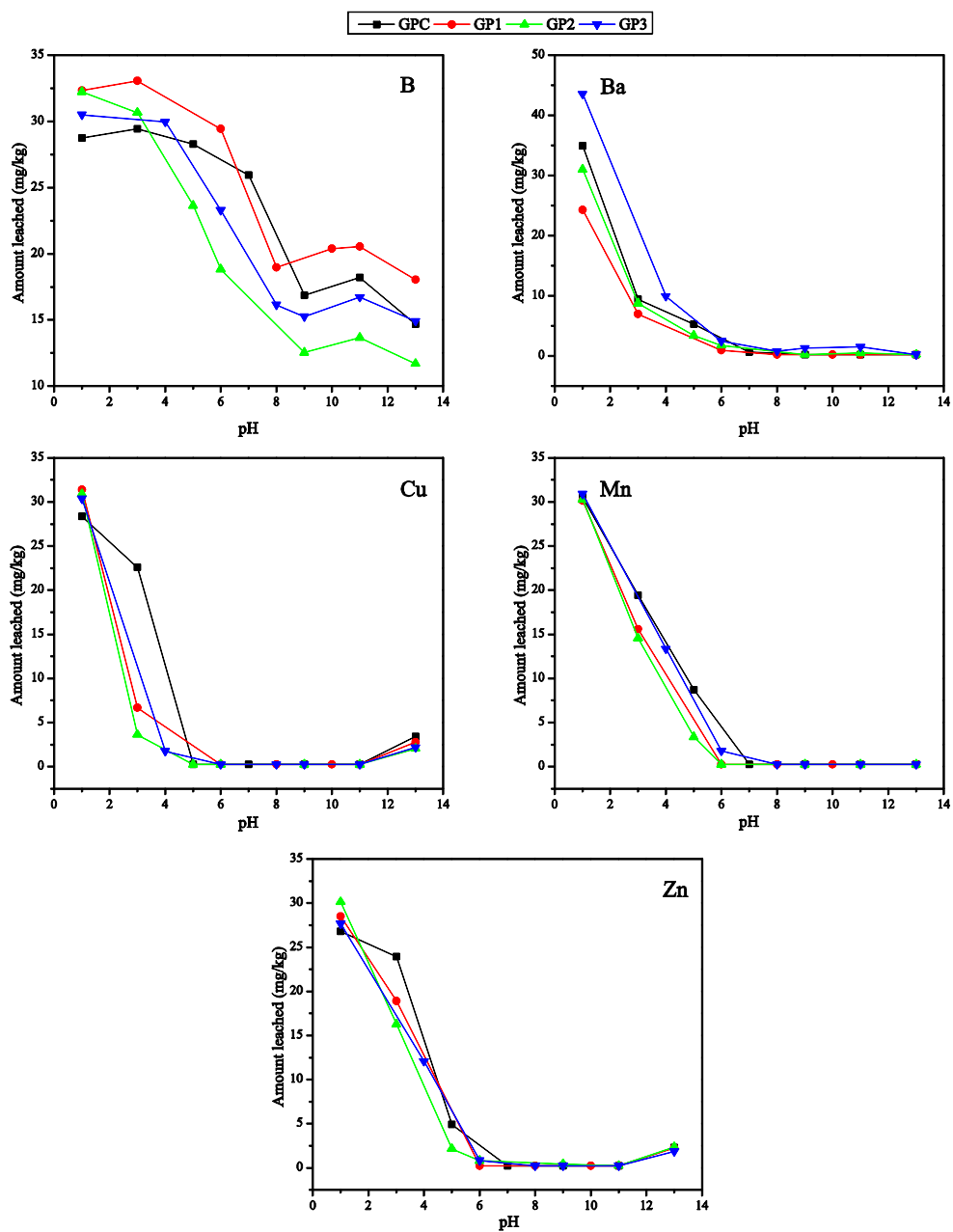
FIGURE D-6: pH dependence mobility of elements from the geopolymer concretes

APPENDIX E: ENLARGED CUMULATIVE PLOT OF THE ELEMENTS
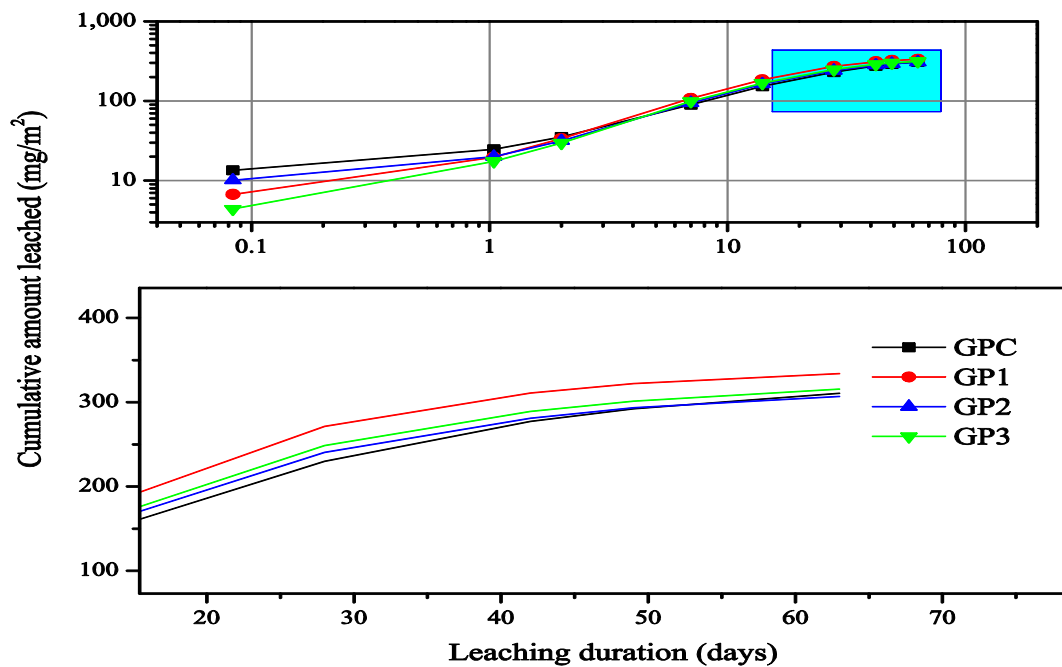
FIGURE E-1: Plot showing enlarged cumulative release of As
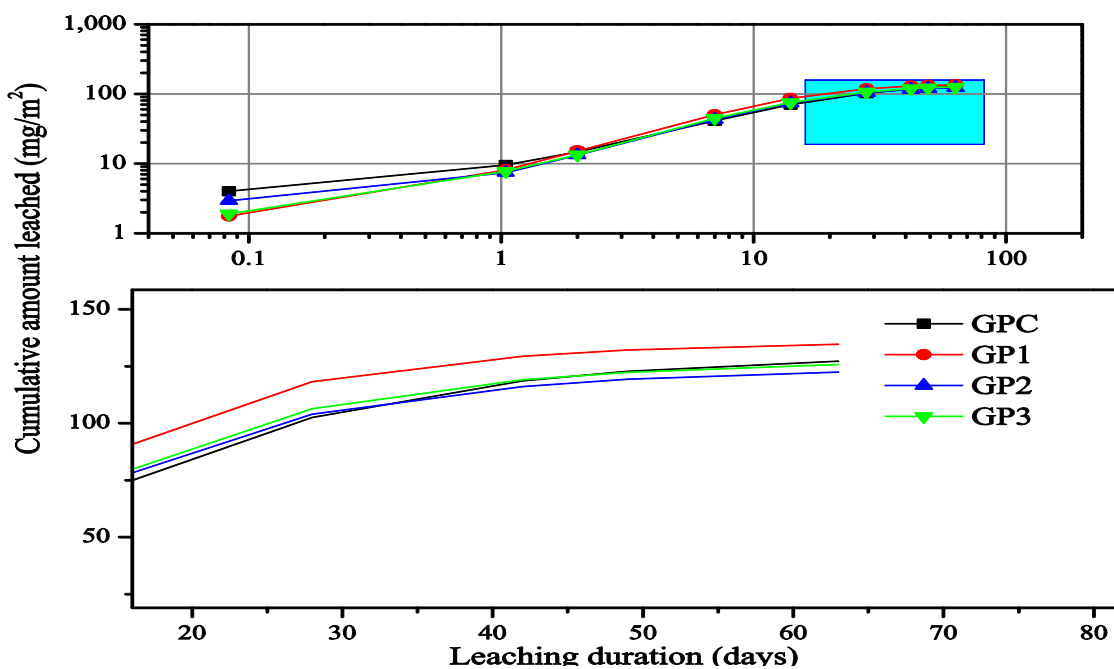
FIGURE E-2: Plot showing enlarged cumulative release of Se
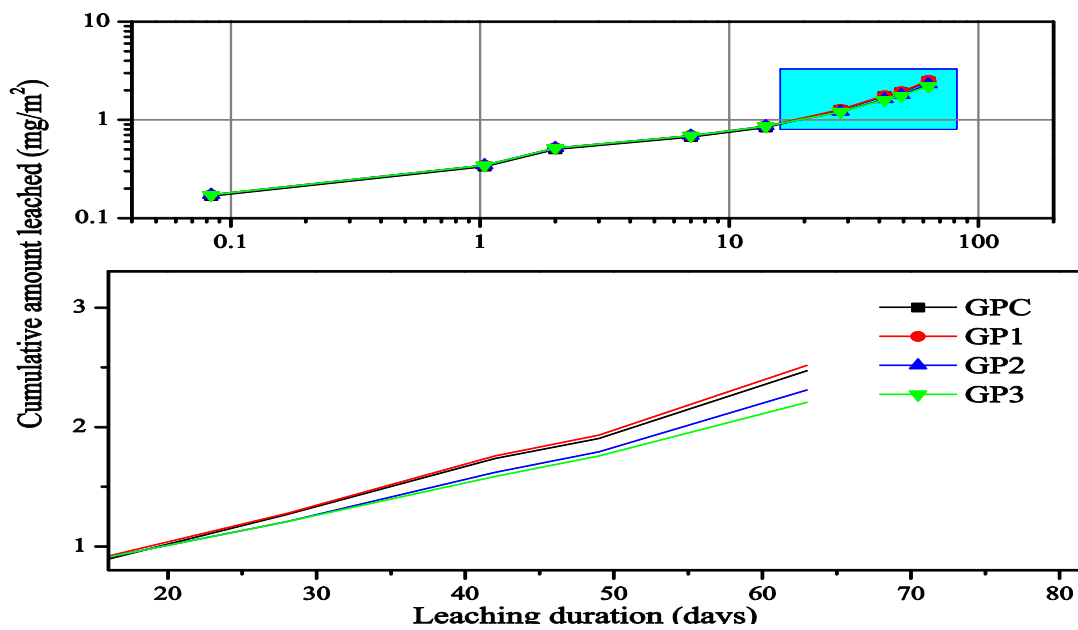
FIGURE E-3: Plot showing enlarged cumulative release of Cr

APPENDIX F: INPUT FILE FOR PHREEQC/PHREEPLOT

Input file – GPC composition used in this file

```
SPECIATION
  jobTitle      "Speciation of oxyanion forming elements (As, Cr, amd Se) vs pH"
  database      llnl.dat  # this is a larger database (750kB) contains over 1155 minerals
  calculationType    species      # plot %C species vs pH
  calculationMethod  1 # Full set of speciation calculation done
  mainSpecies      As Cr Se  # produce species plot for these  elements
  xmin             1    # controls the range of pH plotted - min pH
  xmax             13   # max pH
  resolution       120     # (13-1)/120 = 0.1 pH division
  debug       2     #create the phreeqcall.out that conatisn the accumulated phreeqc.out

PLOT
  plotTitle               "Speciation of oxyanion forming elements"
  xtitle            pH
  ytitle            " % species"
  multipageFile         True  # put all the plots into a single file

CHEMISTRY

# first simulation - initial solution calculation only calculated once
# speciation modeling section -osanusi

include        'speciesvspht.inc'    # calculates % species and plot it against the pH

PRINT
  -reset       true          #  Output initial solution calculation
  -equilibrium_phases true   # output the equilibrium phases
  -species            TRUE   #output the species

SELECTED_OUTPUT
  reset            false
  high_precision   true

PHASES                 # temporarily add this to the database
Fix_H+
  H+ = H+
  log_K 0.0

CaSeO3:2H2O
      CaSeO3:2H2O  =  + 1.0000 Ca++ + 1.0000 SeO3-- + 2.0000 H2O
       log_k         -4.6213
       -delta_H      -14.1963       kJ/mol # Calculated enthalpy of reaction
       CaSeO3:2H2O   #       Enthalpy of formation: -384.741 kcal/mol
       -analytic -4.1771e+001 -2.0735e-002 9.7870e+002 1.6180e+001 1.6634e+00
#       -Range:  0-200

CaSeO3:H2O                                          # Cornelis et al. 2008
      CaSeO3:H2O =  + 1.0000 Ca++ + 1.0000 SeO3-- + 1.0000 H2O
      log_k            -6.84

CaSeO4
      CaSeO4  =  + 1.0000 Ca++ + 1.0000 SeO4--
       log_k         -3.0900
       -delta_H      0             # Not possible to calculate enthalpy of reaction
       CaSeO4     #  Enthalpy of formation: 0 kcal/mol

Ca3(AsO4)2:3H2O                          #Cornelis et al 2008
      Ca3(AsO4)2:3H2O = + 3.0000 Ca+2 + 2.000 AsO4-3 + 3.0000 H2O
      log_k  -21.14

CaHAsO4                   #Weilite source: Alexandratos et al. 2007
      CaHAsO4 = +1.0000Ca++ +1.0000HAsO4--
      log_k       -2.66
CaHAsO4:H2O                      #Haidingerite source: Alexandratos et al. 2007
      CaHAsO4:H2O = +1.0000Ca++ +1.0000HAsO4-- +1.0000H2O
```

```
      log_k           -4.79

CaCrO4                          # from sit.dat
      CaCrO4 = +1.000Ca+2     +1.000CrO4-2
      log_k  -3.15            #03DEA
      delta_h -22.814         kJ/mol         #
      # Enthalpy of formation:              -1399.186   kJ/mol


Ca3(AsO4)2:10H2O                #Phaunouvite source:Cornelis etal. 2008
      Ca3(AsO4)2:10H2O = +3.0000Ca++ +2.0000AsO4--- +10.0000H2O
      log_k          -21.21

Ca5(AsO4)3(OH)
      Ca5(AsO4)3(OH) = +5.0000Ca++ +3.0000AsO4--- +1.0000OH-
      log_k          -40.12

Cr-ettringite                   # from sit.dat
Ca6(Al(OH)6)2(CrO4)3:26H2O = +6.000Ca+2     +2.000Al+3     -12.000H+     +3.000CrO4-2
+38.000H2O
      log_k    60.28           #00PER/PAL
      delta_h -509.59          kJ/mol         #00PER/PAL
      # Enthalpy of formation:              -17323.75   kJ/mol

Se-ettringite                   # Chrysochoou and Dermatas 2006
Ca6(Al(OH)6)2(SeO4)3:31.5H2O = +6.000Ca+2 +2.000Al+3 +3.000SeO4-2 -12.000H+ +43.500H2O
      log_k    61.29

Se-monosulfoaluminate           # Cornelis et al 2008
Ca4(Al(OH)6)2SeO4:9H2O = +4.000Ca+2 +2.000Al+3 -12.000H+ +1.000SeO4-2 +21.000H2O
      log_k    73.40

Monosulfoaluminate              # Cornelis et al. 2008
Ca4Al2(SO4)(OH)12:13H2O = +4.000Ca+2     +2.000Al+3     -12.000H+     +1.000SO4-2
+25.000H2O
      log_k    72.57           #07BLA/BOU
      delta_h -522.63          kJ/mol         #
      # Enthalpy of formation:              -8780.45    kJ/mol       82WAG/EVA

Cr-monosulfoaluminate           #Cornelis et al. 2008
Ca4Al2(OH)12(CrO4):9H2O = +4.000Ca+2     +2.000Al+3     -12.000H+     +1.000CrO4-2
+21.000H2O
      log_k    71.36           #01PER/PAL
      delta_h -545.98          kJ/mol         #01PER/PAL
      # Enthalpy of formation:              -9584.25    kJ/mol

#CSH1.6                         # from sit.dat
#Ca1.6SiO3.6:2.58H2O = +1.600Ca+2     -3.200H+     +1.000H4(SiO4)     +2.180H2O
 #    log_k   -28             #07BLA/BOU
  #   delta_h -133.314        kJ/mol         #
      # Enthalpy of formation:              -2819.79    kJ/mol       07BLA/BOU


#CSH1.2                         # sit.dat
#Ca1.2SiO3.2:2.06H2O = +1.200Ca+2     -2.400H+     +1.000H4(SiO4)     +1.260H2O
 #    log_k   -19.3           #07BLA/BOU
  #   delta_h -88.6           kJ/mol         #
      # Enthalpy of formation:              -2384.34    kJ/mol       07BLA/BOU

#CSH0.8                         #sit.dat
#Ca0.8SiO2.8:1.54H2O = +0.800Ca+2     -1.600H+     +1.000H4(SiO4)     +0.340H2O
 #    log_k   -11.05          #07BLA/BOU
  #   delta_h -47.646         kJ/mol         #
      # Enthalpy of formation:              -1945.13    kJ/mol       07BLA/BOU

CaSeO4:2H2O            # from sit.dat
CaSeO4:2H2O = +1.000Ca+2     +1.000SeO4-2     +2.000H2O
      log_k   -2.68           #05OLI/NOL
      delta_h -9.16           kJ/mol         #
      # Enthalpy of formation:              -1709       kJ/mol       05OLI/NOL
```

```
 # The concentration measured from the WLT was used as solution composition
SOLUTION 1             # Composition of the aqueous solution obtained from the tests
  temp                25                # Temperature in C
  pH                  11.23             # Material ph or pH at zero acid and base addition
  units               mg/L
  density             0.997                        #kg/l
  Na                  564.50
  Si                  160.00
  V                   1.685
  Al                  0.4485
  As                  1.0231
  B                   1.78
  Ca                  0.644
  Fe                  0.329                                  # total Fe
  Mg                  0.164
  Mo                  0.265
  Se                  0.405
  Cr                  0.025
  Cl                  1.20     Charge
  F                   0.395
  N(5)                0.195
  P                   31.50
  S(6)                155.00


# no reaction so no need to SAVE solution 1

END

# second (final) simulation - the final simulation is iterated many times as required by
the speciation procedure
# batch reaction modeling - osanusi

USE solution 1
EQUILIBRIUM_PHASES 1
  Fix_H+      -<x_axis>      NaOH
    -force_equality   true
     Halite   -12    10      # maintains Na in the system for functioning of fix_H+ when
it goes -ve

  # Include possible As, Cr and Se solubility controlling minerals

  Cr-ettringite                     0.5     0
  Se-ettringite                     0.5     0
  Cr-monosulfoaluminate     0.5     0
  Se-monosulfoaluminate     0.5     0
  CaHAsO4                           0.5     0
  Ettringite                0.0     0
  Monosulfoaluminate        0.0     0
  CaHAsO4:H2O               0.5     0
  Ca3(AsO4)2:10H2O          0.5     0
  Ca5(AsO4)3(OH)                    0.5     0
  CaSeO4                            0.5     0
  CaSeO4:2H2O               0.5     0
  Ca3(AsO4)2:10H2O          0.5     0
  CaSeO3:2H2O               0.5     0
  CaCrO4                            0.5     0


END
```

APPENDIX G: OUTPUT FILE FOR PHREEQC/PHREEPLOT

Output file – obtained from simulation performed using GPC composition

```
----------------------------------
Reading input data for simulation 1.
----------------------------------

        PRINT
        reset false
        equilibrium_phases    true
        species               TRUE
        SELECTED_OUTPUT
        reset                 false
        high_precision        true
        PHASES
        Fix_H+
        H+ = H+
        log_K 0.0
        CaSeO3:2H2O
        CaSeO3:2H2O  =  + 1.0000 Ca++ + 1.0000 SeO3-- + 2.0000 H2O
        log_k          -4.6213
             delta_h -14.1963       kJ/mol
        analytical_expression   -4.1771e+001   -2.0735e-002   9.7870e+002   1.6180e+001
1.6634e+001
        CaSeO3:H2O
             CaSeO3:H2O =  + 1.0000 Ca++ + 1.0000 SeO3-- + 1.0000 H2O
             log_k                -6.84
        CaSeO4
        CaSeO4  =  + 1.0000 Ca++ + 1.0000 SeO4--
        log_k         -3.0900
             delta_h 0
        Ca3(AsO4)2:3H2O
             Ca3(AsO4)2:3H2O = + 3.0000 Ca+2 + 2.000 AsO4-3 + 3.0000 H2O
             log_k   -21.14
        CaHAsO4
             CaHAsO4 = +1.0000Ca++ +1.0000HAsO4--
             log_k          -2.66
        CaHAsO4:H2O
             CaHAsO4:H2O = +1.0000Ca++ +1.0000HAsO4-- +1.0000H2O
             log_k          -4.79
        CaCrO4
             CaCrO4 = +1.000Ca+2      +1.000CrO4-2
        log_k    -3.15
        delta_h  -22.814       kJ/mol
        Ca3(AsO4)2:10H2O
             Ca3(AsO4)2:10H2O = +3.0000Ca++ +2.0000AsO4--- +10.0000H2O
             log_k          -21.21
        Ca5(AsO4)3(OH)
             Ca5(AsO4)3(OH) = +5.0000Ca++ +3.0000AsO4--- +1.0000OH-
             log_k          -40.12
        Cr-ettringite
        Ca6(Al(OH)6)2(CrO4)3:26H2O  =  +6.000Ca+2        +2.000Al+3        -12.000H+
+3.000CrO4-2     +38.000H2O
        log_k    60.28
        delta_h  -509.59       kJ/mol
        Se-ettringite
        Ca6(Al(OH)6)2(SeO4)3:31.5H2O  =  +6.000Ca+2  +2.000Al+3  +3.000SeO4-2  -12.000H+
+43.500H2O
        log_k  61.29
        Se-monosulfoaluminate
        Ca4(Al(OH)6)2SeO4:9H2O = +4.000Ca+2 +2.000Al+3 -12.000H+ +1.000SeO4-2 +21.000H2O
        log_k  73.40
        Monosulfoaluminate
```

```
        Ca4Al2(SO4)(OH)12:13H2O = +4.000Ca+2      +2.000Al+3      -12.000H+      +1.000SO4-2
+25.000H2O
        log_k      72.57
        delta_h  -522.63          kJ/mol
        Cr-monosulfoaluminate
        Ca4Al2(OH)12(CrO4):9H2O = +4.000Ca+2      +2.000Al+3      -12.000H+      +1.000CrO4-2
+21.000H2O
        log_k      71.36
        delta_h  -545.98          kJ/mol
        CaSeO4:2H2O
        CaSeO4:2H2O = +1.000Ca+2      +1.000SeO4-2      +2.000H2O
        log_k    -2.68
        delta_h  -9.16            kJ/mol

        SOLUTION 1
        temp                  25
        pH                    11.23
        units                 mg/L
        density               0.997
        Na                         564.50
        Si                         160.00
        V                          1.685
        Al                         0.4485
        As                         1.0231
        B                          1.78
        Ca                         0.644
        Fe                         0.329
        Mg                         0.164
        Mo                         0.265
        Se                         0.405
        Cr                         0.025
        Cl                         1.20    Charge
        F                          0.395
        N(5)                       0.195
        P                          31.50
        S(6)                       155.00
        END
----------------------------------------
Beginning of initial solution calculations.
----------------------------------------

Initial solution 1.

WARNING: USER_PUNCH: Headings count doesn't match number of calls to PUNCH.

----------------------------Solution composition-----------------------------

        Elements         Molality        Moles

        Al            1.669e-005  1.669e-005
        As            1.371e-005  1.371e-005
        B             1.653e-004  1.653e-004
        Ca            1.613e-005  1.613e-005
        Cl            1.437e-002  1.437e-002  Charge balance
        Cr            2.164e-007  2.164e-007
        F             2.087e-005  2.087e-005
        Fe            5.914e-006  5.914e-006
        Mg            6.774e-006  6.774e-006
        Mo            2.773e-006  2.773e-006
        N(5)          1.398e-005  1.398e-005
        Na            2.465e-002  2.465e-002
        P             1.021e-003  1.021e-003
        S(6)          1.620e-003  1.620e-003
        Se            5.149e-006  5.149e-006
        Si            2.674e-003  2.674e-003
        V             3.321e-005  3.321e-005

---------------------------Description of solution---------------------------

                                pH  =  11.230
                                pe  =   4.000
```

```
                    Activity of water  =   0.999
                      Ionic strength  =  2.602e-002
                  Mass of water (kg)  =  1.000e+000
              Total alkalinity (eq/kg) =  7.107e-003
                 Total carbon (mol/kg) =  0.000e+000
                   Total CO2 (mol/kg) =  0.000e+000
                  Temperature (deg C) =  25.000
              Electrical balance (eq) =  1.261e-018
 Percent error, 100*(Cat-|An|)/(Cat+|An|) =   0.00
                          Iterations =  50
                             Total H = 1.110562e+002
                             Total O = 5.554645e+001


--------------------------Distribution of species--------------------------

                                              Log       Log       Log
         Species          Molality   Activity Molality  Activity  Gamma

         OH-              1.914e-003 1.635e-003  -2.718   -2.786   -0.069
         H+               6.680e-012 5.888e-012 -11.175  -11.230   -0.055
         H2O              5.553e+001 9.992e-001   1.744   -0.000    0.000
Al              1.669e-005
         AlO2-            1.663e-005 1.426e-005  -4.779   -4.846   -0.067
         NaAlO2           5.418e-008 5.418e-008  -7.266   -7.266    0.000
         HAlO2            2.451e-010 2.451e-010  -9.611   -9.611    0.000
         Al(OH)2+         1.157e-015 9.915e-016 -14.937  -15.004   -0.067
         AlOH+2           4.635e-021 2.516e-021 -20.334  -20.599   -0.265
         AlHPO4+          1.631e-023 1.398e-023 -22.788  -22.855   -0.067
         AlF2+            2.293e-025 1.965e-025 -24.640  -24.707   -0.067
         AlF+2            1.489e-025 8.084e-026 -24.827  -25.092   -0.265
         AlF3             1.511e-026 1.511e-026 -25.821  -25.821    0.000
         Al+3             4.200e-027 1.324e-027 -26.377  -26.878   -0.501
         AlSO4+           1.267e-027 1.086e-027 -26.897  -26.964   -0.067
         Al(SO4)2-        7.888e-029 6.760e-029 -28.103  -28.170   -0.067
         AlF4-            2.705e-029 2.318e-029 -28.568  -28.635   -0.067
         Al2(OH)2+4       1.080e-038 1.030e-039 -37.967  -38.987   -1.021
         AlH2PO4+2        7.599e-039 4.125e-039 -38.119  -38.385   -0.265
         Al3(OH)4+5       0.000e+000 0.000e+000 -48.033  -49.596   -1.563
         Al13O4(OH)24+7   0.000e+000 0.000e+000 -85.731  -88.796   -3.065
As(-3)          0.000e+000
         AsH3             0.000e+000 0.000e+000 -156.444 -156.444   0.000
As(3)           0.000e+000
         AsO2OH-2         0.000e+000 0.000e+000 -57.669  -57.940   -0.271
         H2AsO3-          0.000e+000 0.000e+000 -58.093  -58.160   -0.067
         AsO2-            0.000e+000 0.000e+000 -58.112  -58.179   -0.067
         HAsO2            0.000e+000 0.000e+000 -60.117  -60.117    0.000
         As(OH)3          0.000e+000 0.000e+000 -60.176  -60.176    0.000
As(5)           1.371e-005
         AsO3F-2          1.371e-005 7.343e-006  -4.863   -5.134   -0.271
         HAsO3F-          3.746e-011 3.210e-011 -10.426  -10.493   -0.067
         HAsO4-2          3.596e-036 1.926e-036 -35.444  -35.715   -0.271
         AsO4-3           3.430e-036 8.392e-037 -35.465  -36.076   -0.611
         H2AsO4-          0.000e+000 0.000e+000 -40.098  -40.165   -0.067
         H3AsO4           0.000e+000 0.000e+000 -49.150  -49.150    0.000
B(-5)           0.000e+000
         BH4-             0.000e+000 0.000e+000 -181.463 -181.530  -0.067
B(3)            1.653e-004
         BO2-             1.585e-004 1.358e-004  -3.800   -3.867   -0.067
         NaB(OH)4         5.349e-006 5.349e-006  -5.272   -5.272    0.000
         B(OH)3           1.490e-006 1.490e-006  -5.827   -5.827    0.000
         CaB(OH)4+        1.543e-009 1.323e-009  -8.812   -8.879   -0.067
         MgB(OH)4+        5.752e-010 4.930e-010  -9.240   -9.307   -0.067
         B2O(OH)5-        9.086e-020 7.787e-020 -19.042  -19.109   -0.067
         BF2(OH)2-        1.584e-021 1.357e-021 -20.800  -20.867   -0.067
         BF3OH-           2.431e-031 2.084e-031 -30.614  -30.681   -0.067
         BF4-             0.000e+000 0.000e+000 -42.237  -42.304   -0.067
Ca              1.613e-005
         CaPO4-           1.583e-005 1.357e-005  -4.800   -4.867   -0.067
         Ca+2             2.454e-007 1.383e-007  -6.610   -6.859   -0.249
         CaHPO4           3.194e-008 3.194e-008  -7.496   -7.496    0.000
         CaSO4            1.620e-008 1.620e-008  -7.791   -7.791    0.000
```

```
        CaOH+                3.867e-009  3.314e-009   -8.413    -8.480   -0.067
        CaB(OH)4+            1.543e-009  1.323e-009   -8.812    -8.879   -0.067
        CaCl+                4.170e-010  3.574e-010   -9.380    -9.447   -0.067
        CaP2O7-2             5.166e-011  2.767e-011  -10.287   -10.558   -0.271
        CaNO3+               9.616e-012  8.242e-012  -11.017   -11.084   -0.067
        CaCl2                5.126e-012  5.126e-012  -11.290   -11.290    0.000
        CaF+                 5.008e-012  4.292e-012  -11.300   -11.367   -0.067
        CaH2PO4+             1.003e-020  8.597e-021  -19.999   -20.066   -0.067
Cl(-1)          1.437e-002
        Cl-                  1.433e-002  1.220e-002   -1.844    -1.914   -0.070
        NaCl                 4.270e-005  4.270e-005   -4.370    -4.370    0.000
        MgCl+                4.812e-010  4.124e-010   -9.318    -9.385   -0.067
        CaCl+                4.170e-010  3.574e-010   -9.380    -9.447   -0.067
        CaCl2                5.126e-012  5.126e-012  -11.290   -11.290    0.000
        HCl                  1.613e-014  1.613e-014  -13.792   -13.792    0.000
        FeCl+                2.579e-022  2.211e-022  -21.589   -21.655   -0.067
        CrO3Cl-              2.199e-024  1.884e-024  -23.658   -23.725   -0.067
        FeCl2                1.447e-026  1.447e-026  -25.840   -25.840    0.000
        FeCl4-2              1.161e-029  6.217e-030  -28.935   -29.206   -0.271
        FeCl2+               5.584e-031  4.786e-031  -30.253   -30.320   -0.067
        FeCl+2               8.930e-032  4.848e-032  -31.049   -31.314   -0.265
        FeCl4-               9.985e-038  8.558e-038  -37.001   -37.068   -0.067
        CrCl+2               2.229e-038  1.210e-038  -37.652   -37.917   -0.265
        CrCl2+               3.786e-040  3.245e-040  -39.422   -39.489   -0.067
Cl(1)           3.195e-030
        ClO-                 3.194e-030  2.738e-030  -29.496   -29.563   -0.067
        HClO                 5.978e-034  5.978e-034  -33.223   -33.223    0.000
Cl(3)           0.000e+000
        ClO2-                0.000e+000  0.000e+000  -50.039   -50.106   -0.067
        HClO2                0.000e+000  0.000e+000  -58.166   -58.166    0.000
Cl(5)           0.000e+000
        ClO3-                0.000e+000  0.000e+000  -56.729   -56.797   -0.069
Cl(7)           0.000e+000
        ClO4-                0.000e+000  0.000e+000  -67.722   -67.790   -0.069
Cr(2)           0.000e+000
        Cr+2                 0.000e+000  0.000e+000  -48.108   -48.373   -0.265
Cr(3)           5.454e-019
        Cr(OH)4-             5.386e-019  4.616e-019  -18.269   -18.336   -0.067
        Cr(OH)3              6.833e-021  6.833e-021  -20.165   -20.165    0.000
        Cr(OH)2+             9.374e-024  8.034e-024  -23.028   -23.095   -0.067
        CrOH+2               4.371e-029  2.373e-029  -28.359   -28.625   -0.265
        Cr+3                 4.437e-036  1.398e-036  -35.353   -35.854   -0.501
        CrCl+2               2.229e-038  1.210e-038  -37.652   -37.917   -0.265
        CrCl2+               3.786e-040  3.245e-040  -39.422   -39.489   -0.067
        Cr2(OH)2+4           0.000e+000  0.000e+000  -53.289   -54.309   -1.021
        Cr3(OH)4+5           0.000e+000  0.000e+000  -69.231   -70.795   -1.563
Cr(5)           2.502e-009
        CrO4-3               2.502e-009  6.123e-010   -8.602    -9.213   -0.611
Cr(6)           2.139e-007
        CrO4-2               2.139e-007  1.146e-007   -6.670    -6.941   -0.271
        HCrO4-               2.617e-012  2.243e-012  -11.582   -11.649   -0.067
        Cr2O7-2              3.139e-022  1.681e-022  -21.503   -21.774   -0.271
        CrO3Cl-              2.199e-024  1.884e-024  -23.658   -23.725   -0.067
        H2CrO4               6.038e-025  6.038e-025  -24.219   -24.219    0.000
F               2.087e-005
        AsO3F-2              1.371e-005  7.343e-006   -4.863    -5.134   -0.271
        F-                   7.151e-006  6.107e-006   -5.146    -5.214   -0.069
        NaF                  1.301e-008  1.301e-008   -7.886    -7.886    0.000
        HAsO3F-              3.746e-011  3.210e-011  -10.426   -10.493   -0.067
        MgF+                 7.449e-012  6.384e-012  -11.128   -11.195   -0.067
        CaF+                 5.008e-012  4.292e-012  -11.300   -11.367   -0.067
        PO3F-2               4.470e-013  2.394e-013  -12.350   -12.621   -0.271
        HF                   5.521e-014  5.521e-014  -13.258   -13.258    0.000
        HF2-                 9.529e-020  8.167e-020  -19.021   -19.088   -0.067
        HPO3F-               2.068e-020  1.773e-020  -19.684   -19.751   -0.067
        BF2(OH)2-            1.584e-021  1.357e-021  -20.800   -20.867   -0.067
        FeF+                 4.062e-024  3.481e-024  -23.391   -23.458   -0.067
        AlF2+                2.293e-025  1.965e-025  -24.640   -24.707   -0.067
        AlF+2                1.489e-025  8.084e-026  -24.827   -25.092   -0.265
        AlF3                 1.511e-026  1.511e-026  -25.821   -25.821    0.000
        H2F2                 7.580e-027  7.580e-027  -26.120   -26.120    0.000
```

```
        VO2F                    6.951e-027   6.951e-027   -26.158   -26.158    0.000
        AlF4-                   2.705e-029   2.318e-029   -28.568   -28.635   -0.067
        VO2F2-                  1.428e-029   1.224e-029   -28.845   -28.912   -0.067
        FeF+2                   4.025e-030   2.185e-030   -29.395   -29.661   -0.265
        H2PO3F                  6.676e-031   6.676e-031   -30.175   -30.175    0.000
        FeF2+                   2.519e-031   2.159e-031   -30.599   -30.666   -0.067
        BF3OH-                  2.431e-031   2.084e-031   -30.614   -30.681   -0.067
        VOF+                    1.033e-035   8.851e-036   -34.986   -35.053   -0.067
        VOF2                    3.257e-038   3.257e-038   -37.487   -37.487    0.000
        BF4-                    0.000e+000   0.000e+000   -42.237   -42.304   -0.067
        SiF6-2                  0.000e+000   0.000e+000   -53.747   -54.018   -0.271
Fe(2)           1.017e-016
        FePO4-                  8.408e-017   7.206e-017   -16.075   -16.142   -0.067
        Fe(OH)3-                1.419e-017   1.216e-017   -16.848   -16.915   -0.067
        Fe(OH)2                 1.800e-018   1.800e-018   -17.745   -17.745    0.000
        FeOH+                   1.558e-018   1.335e-018   -17.807   -17.874   -0.067
        Fe+2                    4.417e-020   2.488e-020   -19.355   -19.604   -0.249
        FeHPO4                  4.164e-020   4.164e-020   -19.380   -19.380    0.000
        Fe(OH)4-2               3.852e-021   2.063e-021   -20.414   -20.685   -0.271
        FeSO4                   3.162e-021   3.162e-021   -20.500   -20.500    0.000
        FeCl+                   2.579e-022   2.211e-022   -21.589   -21.655   -0.067
        FeF+                    4.062e-024   3.481e-024   -23.391   -23.458   -0.067
        FeCl2                   1.447e-026   1.447e-026   -25.840   -25.840    0.000
        FeCl4-2                 1.161e-029   6.217e-030   -28.935   -29.206   -0.271
        FeH2PO4+                3.602e-032   3.087e-032   -31.443   -31.510   -0.067
Fe(3)           5.914e-006
        Fe(OH)4-                5.798e-006   4.969e-006    -5.237    -5.304   -0.067
        Fe(OH)3                 1.166e-007   1.166e-007    -6.933    -6.933    0.000
        Fe(OH)2+                1.714e-012   1.469e-012   -11.766   -11.833   -0.067
        FeOH+2                  4.815e-020   2.614e-020   -19.317   -19.583   -0.265
        FeHPO4+                 1.771e-022   1.518e-022   -21.752   -21.819   -0.067
        Fe+3                    7.570e-029   2.386e-029   -28.121   -28.622   -0.501
        FeF+2                   4.025e-030   2.185e-030   -29.395   -29.661   -0.265
        FeSO4+                  2.159e-030   1.851e-030   -29.666   -29.733   -0.067
        FeCl2+                  5.584e-031   4.786e-031   -30.253   -30.320   -0.067
        FeF2+                   2.519e-031   2.159e-031   -30.599   -30.666   -0.067
        FeCl+2                  8.930e-032   4.848e-032   -31.049   -31.314   -0.265
        Fe(SO4)2-               2.927e-032   2.509e-032   -31.534   -31.601   -0.067
        FeNO3+2                 5.227e-033   2.837e-033   -32.282   -32.547   -0.265
        Fe2(OH)2+4              1.929e-037   1.839e-038   -36.715   -37.735   -1.021
        FeCl4-                  9.985e-038   8.558e-038   -37.001   -37.068   -0.067
        FeH2PO4+2               1.609e-039   8.735e-040   -38.793   -39.059   -0.265
        Fe3(OH)4+5              0.000e+000   0.000e+000   -45.685   -47.249   -1.563
H(0)            5.468e-034
        H2                      2.734e-034   2.751e-034   -33.563   -33.560    0.003
Mg              6.774e-006
        MgPO4-                  6.675e-006   5.721e-006    -5.176    -5.243   -0.067
        Mg+2                    7.366e-008   4.332e-008    -7.133    -7.363   -0.231
        MgHPO4                  1.480e-008   1.480e-008    -7.830    -7.830    0.000
        MgSO4                   9.275e-009   9.275e-009    -8.033    -8.033    0.000
        MgB(OH)4+               5.752e-010   4.930e-010    -9.240    -9.307   -0.067
        MgCl+                   4.812e-010   4.124e-010    -9.318    -9.385   -0.067
        MgP2O7-2                4.793e-011   2.567e-011   -10.319   -10.591   -0.271
        MgF+                    7.449e-012   6.384e-012   -11.128   -11.195   -0.067
        MgH2PO4+                5.718e-021   4.901e-021   -20.243   -20.310   -0.067
        Mg4(OH)4+4              5.444e-024   5.191e-025   -23.264   -24.285   -1.021
Mo              2.773e-006
        MoO4-2                  2.773e-006   1.505e-006    -5.557    -5.822   -0.265
N(5)            1.398e-005
        NO3-                    1.398e-005   1.189e-005    -4.855    -4.925   -0.070
        CaNO3+                  9.616e-012   8.242e-012   -11.017   -11.084   -0.067
        HNO3                    3.663e-018   3.663e-018   -17.436   -17.436    0.000
        FeNO3+2                 5.227e-033   2.837e-033   -32.282   -32.547   -0.265
Na              2.465e-002
        Na+                     2.325e-002   1.992e-002    -1.634    -1.701   -0.067
        NaHSiO3                 1.147e-003   1.147e-003    -2.940    -2.940    0.000
        NaSO4-                  1.231e-004   1.055e-004    -3.910    -3.977   -0.067
        NaHPO4-                 8.128e-005   6.966e-005    -4.090    -4.157   -0.067
        NaCl                    4.270e-005   4.270e-005    -4.370    -4.370    0.000
        NaOH                    5.620e-006   5.620e-006    -5.250    -5.250    0.000
        NaB(OH)4                5.349e-006   5.349e-006    -5.272    -5.272    0.000
```

```
      NaAlO2                  5.418e-008  5.418e-008    -7.266    -7.266    0.000
      NaF                     1.301e-008  1.301e-008    -7.886    -7.886    0.000
      NaP2O7-3                5.036e-010  1.232e-010    -9.298    -9.909   -0.611
      Na2P2O7-2               3.641e-010  1.950e-010    -9.439    -9.710   -0.271
      NaHP2O7-2               2.741e-013  1.468e-013   -12.562   -12.833   -0.271
O(0)            1.669e-025
      O2                      8.347e-026  8.400e-026   -25.078   -25.076    0.003
P(-3)           0.000e+000
      PH4+                    0.000e+000  0.000e+000  -199.589  -199.656   -0.067
P(5)            1.021e-003
      HPO4-2                  7.849e-004  4.204e-004    -3.105    -3.376   -0.271
      PO4-3                   1.322e-004  3.236e-005    -3.879    -4.490   -0.611
      NaHPO4-                 8.128e-005  6.966e-005    -4.090    -4.157   -0.067
      CaPO4-                  1.583e-005  1.357e-005    -4.800    -4.867   -0.067
      MgPO4-                  6.675e-006  5.721e-006    -5.176    -5.243   -0.067
      H2PO4-                  4.884e-008  4.186e-008    -7.311    -7.378   -0.067
      CaHPO4                  3.194e-008  3.194e-008    -7.496    -7.496    0.000
      MgHPO4                  1.480e-008  1.480e-008    -7.830    -7.830    0.000
      NaP2O7-3                5.036e-010  1.232e-010    -9.298    -9.909   -0.611
      P2O7-4                  4.202e-010  3.433e-011    -9.377   -10.464   -1.088
      Na2P2O7-2               3.641e-010  1.950e-010    -9.439    -9.710   -0.271
      CaP2O7-2                5.166e-011  2.767e-011   -10.287   -10.558   -0.271
      MgP2O7-2                4.793e-011  2.567e-011   -10.319   -10.591   -0.271
      HP2O7-3                 1.349e-012  3.300e-013   -11.870   -12.481   -0.611
      PO3F-2                  4.470e-013  2.394e-013   -12.350   -12.621   -0.271
      NaHP2O7-2               2.741e-013  1.468e-013   -12.562   -12.833   -0.271
      FePO4-                  8.408e-017  7.206e-017   -16.075   -16.142   -0.067
      H3PO4                   3.798e-017  3.798e-017   -16.420   -16.420    0.000
      H2P2O7-2                1.501e-017  8.037e-018   -16.824   -17.095   -0.271
      FeHPO4                  4.164e-020  4.164e-020   -19.380   -19.380    0.000
      HPO3F-                  2.068e-020  1.773e-020   -19.684   -19.751   -0.067
      CaH2PO4+                1.003e-020  8.597e-021   -19.999   -20.066   -0.067
      MgH2PO4+                5.718e-021  4.901e-021   -20.243   -20.310   -0.067
      FeHPO4+                 1.771e-022  1.518e-022   -21.752   -21.819   -0.067
      VO2HPO4-                1.686e-022  1.445e-022   -21.773   -21.840   -0.067
      VO2(HPO4)2-3            1.462e-022  3.577e-023   -21.835   -22.447   -0.611
      AlHPO4+                 1.631e-023  1.398e-023   -22.788   -22.855   -0.067
      H3P2O7-                 1.269e-026  1.088e-026   -25.897   -25.963   -0.067
      H2PO3F                  6.676e-031  6.676e-031   -30.175   -30.175    0.000
      FeH2PO4+                3.602e-032  3.087e-032   -31.443   -31.510   -0.067
      H4P2O7                  1.882e-036  1.882e-036   -35.725   -35.725    0.000
      VO2H2PO4                6.024e-038  6.024e-038   -37.220   -37.220    0.000
      AlH2PO4+2               7.599e-039  4.125e-039   -38.119   -38.385   -0.265
      FeH2PO4+2               1.609e-039  8.735e-040   -38.793   -39.059   -0.265
S(6)            1.620e-003
      SO4-2                   1.497e-003  8.018e-004    -2.825    -3.096   -0.271
      NaSO4-                  1.231e-004  1.055e-004    -3.910    -3.977   -0.067
      CaSO4                   1.620e-008  1.620e-008    -7.791    -7.791    0.000
      MgSO4                   9.275e-009  9.275e-009    -8.033    -8.033    0.000
      HSO4-                   5.565e-013  4.769e-013   -12.255   -12.322   -0.067
      FeSO4                   3.162e-021  3.162e-021   -20.500   -20.500    0.000
      VO2SO4-                 1.808e-026  1.550e-026   -25.743   -25.810   -0.067
      H2SO4                   2.650e-027  2.650e-027   -26.577   -26.577    0.000
      AlSO4+                  1.267e-027  1.086e-027   -26.897   -26.964   -0.067
      Al(SO4)2-               7.888e-029  6.760e-029   -28.103   -28.170   -0.067
      FeSO4+                  2.159e-030  1.851e-030   -29.666   -29.733   -0.067
      Fe(SO4)2-               2.927e-032  2.509e-032   -31.534   -31.601   -0.067
      VOSO4                   3.510e-035  3.510e-035   -34.455   -34.455    0.000
      VSO4+                   0.000e+000  0.000e+000   -54.201   -54.268   -0.067
Se(-2)          0.000e+000
      HSe-                    0.000e+000  0.000e+000   -57.377   -57.444   -0.067
      Se-2                    0.000e+000  0.000e+000   -60.889   -61.160   -0.271
      H2Se                    0.000e+000  0.000e+000   -64.852   -64.852    0.000
Se(4)           1.791e-007
      SeO3-2                  1.791e-007  9.593e-008    -6.747    -7.018   -0.271
      HSeO3-                  1.355e-011  1.161e-011   -10.868   -10.935   -0.067
      H2SeO3                  2.597e-020  2.597e-020   -19.586   -19.586    0.000
Se(6)           4.970e-006
      SeO4-2                  4.970e-006  2.662e-006    -5.304    -5.575   -0.271
      HSeO4-                  1.556e-015  1.333e-015   -14.808   -14.875   -0.067
Si              2.674e-003
```

```
    HSiO3-                   1.426e-003  1.222e-003    -2.846    -2.913   -0.067
    NaHSiO3                  1.147e-003  1.147e-003    -2.940    -2.940    0.000
    SiO2                     6.305e-005  6.305e-005    -4.200    -4.200    0.000
    H2SiO4-2                 3.717e-005  1.991e-005    -4.430    -4.701   -0.271
    H4(H2SiO4)4-4            1.835e-007  1.500e-008    -6.736    -7.824   -1.088
    H6(H2SiO4)4-2            1.937e-008  1.037e-008    -7.713    -7.984   -0.271
    SiF6-2                   0.000e+000  0.000e+000   -53.747   -54.018   -0.271
V(3)          1.272e-038
    V(OH)2+                  1.272e-038  1.090e-038   -37.895   -37.962   -0.067
    VOH+2                    0.000e+000  0.000e+000   -45.267   -45.533   -0.265
    V+3                      0.000e+000  0.000e+000   -53.917   -54.502   -0.586
    VSO4+                    0.000e+000  0.000e+000   -54.201   -54.268   -0.067
    V2(OH)2+4                0.000e+000  0.000e+000   -89.325   -90.346   -1.021
V(4)          6.135e-029
    VOOH+                    6.135e-029  5.258e-029   -28.212   -28.279   -0.067
    VO+2                     2.670e-034  1.449e-034   -33.574   -33.839   -0.265
    VOSO4                    3.510e-035  3.510e-035   -34.455   -34.455    0.000
    VOF+                     1.033e-035  8.851e-036   -34.986   -35.053   -0.067
    VOF2                     3.257e-038  3.257e-038   -37.487   -37.487    0.000
    (VO)2(OH)2+2             0.000e+000  0.000e+000   -51.623   -51.888   -0.265
V(5)          3.321e-005
    VO3OH-2                  3.014e-005  1.615e-005    -4.521    -4.792   -0.271
    HVO4-2                   3.001e-006  1.607e-006    -5.523    -5.794   -0.271
    VO4-3                    6.158e-008  1.507e-008    -7.211    -7.822   -0.611
    H2VO4-                   1.340e-009  1.149e-009    -8.873    -8.940   -0.067
    VO2(OH)2-                8.561e-010  7.337e-010    -9.067    -9.134   -0.067
    VO(OH)3                  4.321e-017  4.321e-017   -16.364   -16.364    0.000
    VO2HPO4-                 1.686e-022  1.445e-022   -21.773   -21.840   -0.067
    VO2(HPO4)2-3            1.462e-022  3.577e-023   -21.835   -22.447   -0.611
    VO2+                     5.932e-025  5.084e-025   -24.227   -24.294   -0.067
    VO2SO4-                  1.808e-026  1.550e-026   -25.743   -25.810   -0.067
    VO2F                     6.951e-027  6.951e-027   -26.158   -26.158    0.000
    VO2F2-                   1.428e-029  1.224e-029   -28.845   -28.912   -0.067
    VO2H2PO4                 6.024e-038  6.024e-038   -37.220   -37.220    0.000


----------------------------Saturation indices-----------------------------

        Phase             SI  log IAP   log KT

        (VO)3(PO4)2      -134.60   -85.81    48.79   (VO)3(PO4)2
        Afwillite         -21.56    38.40    59.96   Ca3Si2O4(OH)6
        Akermanite         -7.33    37.90    45.23   Ca2MgSi2O7
        Al               -124.30    25.62   149.91   Al
        Al(g)            -175.00    25.62   200.62   Al
        Al2(SO4)3         -81.94   -63.04    18.90   Al2(SO4)3
        Al2(SO4)3:6H2O    -64.60   -63.05     1.56   Al2(SO4)3:6H2O
        Albite              1.08     3.74     2.66   NaAlSi3O8
        Albite_high        -0.24     3.74     3.98   NaAlSi3O8
        Albite_low          1.08     3.74     2.66   NaAlSi3O8
        AlF3              -25.26   -42.52   -17.27   AlF3
        Amesite-14A         3.95    79.23    75.27   Mg4Al4Si2O10(OH)8
        Analcime            1.06     7.12     6.06   Na.96Al.96Si2.04O6:H2O
        Analcime-dehy      -5.30     7.12    12.42   Na.96Al.96Si2.04O6
        Andalusite         -6.46     9.42    15.88   Al2SiO5
        Andradite          11.15    44.33    33.19   Ca3Fe2(SiO4)3
        Anhydrite          -5.61    -9.96    -4.35   CaSO4
        Anorthite          -5.65    20.82    26.48   CaAl2(SiO4)2
        Antarcticite      -14.78   -10.69     4.09   CaCl2:6H2O
        Anthophyllite       5.59    72.07    66.48   Mg7Si8O22(OH)2
        Antigorite        106.17   581.80   475.63   Mg48Si34O85(OH)62
        Arsenolite       -118.94  -138.78   -19.84   As2O3
        As                -93.27   -50.58    42.68   As
        As2O5            -104.93  -102.79     2.14   As2O5
        As4O6(cubi)      -237.73  -277.56   -39.82   As4O6
        As4O6(mono)      -237.51  -277.56   -40.05   As4O6
        B                 -96.58    12.98   109.56   B
        B(g)             -187.86    12.98   200.84   B
        B2O3              -17.20   -11.65     5.55   B2O3
        Bassanite          -6.25    -9.96    -3.71   CaSO4:0.5H2O
        Beidellite-Ca      -2.41     3.03     5.44   Ca.165Al2.33Si3.67O10(OH)2
        Beidellite-H       -4.03     0.45     4.49   H.33Al2.33Si3.67O10(OH)2
```

```
Beidellite-Mg   -2.46    2.95    5.41  Mg.165Al2.33Si3.67O10(OH)2
Beidellite-Na   -1.90    3.60    5.50  Na.33Al2.33Si3.67O10(OH)2
Berlinite      -11.76  -19.02   -7.27  AlPO4
BF3(g)         -52.18  -55.16   -2.98  BF3
Bischofite     -15.59  -11.19    4.39  MgCl2:6H2O
Bloedite       -14.48  -16.96   -2.48  Na2Mg(SO4)2:4H2O
Boehmite        -0.74    6.81    7.55  AlO2H
Borax          -16.29   -4.25   12.04  Na2(B4O5(OH)4):8H2O
Boric_acid      -5.67   -5.83   -0.16  B(OH)3
Brucite         -1.19   15.10   16.28  Mg(OH)2
Brushite       -16.79  -10.24    6.55  CaHPO4:2H2O
Ca            -111.69   28.14  139.83  Ca
Ca(g)         -136.93   28.14  165.07  Ca
Ca-Al_Pyroxene -10.88   25.02   35.90  CaAl2SiO6
Ca2Al2O5:8H2O  -14.75   44.82   59.57  Ca2Al2O5:8H2O
Ca2Cl2(OH)2:H2O -21.38    4.91   26.29  Ca2Cl2(OH)2:H2O
Ca2V2O7        -12.11  -51.82  -39.71  Ca2V2O7
Ca3(AsO4)2     -73.79  -55.99   17.80  Ca3(AsO4)2
Ca3(AsO4)2:10H2O -71.52 -92.73  -21.21  Ca3(AsO4)2:10H2O
Ca3(AsO4)2:3H2O -71.59 -92.73  -21.14  Ca3(AsO4)2:3H2O
Ca3Al2O6       -52.61   60.42  113.03  Ca3Al2O6
Ca3V2O8        -17.90  -36.22  -18.32  Ca3V2O8
Ca4Al2Fe2O10   -54.32   86.16  140.48  Ca4Al2Fe2O10
Ca4Al2O7:13H2O -31.23   76.02  107.25  Ca4Al2O7:13H2O
Ca4Al2O7:19H2O -27.66   76.02  103.68  Ca4Al2O7:19H2O
Ca4Cl2(OH)6:13H2O -32.22  36.11   68.33  Ca4Cl2(OH)6:13H2O
Ca5(AsO4)3(OH) -105.19 -145.31 -40.12  Ca5(AsO4)3(OH)
CaAl2O4        -17.69   29.22   46.91  CaAl2O4
CaAl2O4:10H2O   -8.77   29.22   37.99  CaAl2O4:10H2O
CaAl4O7        -25.75   42.85   68.59  CaAl4O7
CaCrO4         -10.65  -13.80   -3.15  CaCrO4
CaHAsO4        -39.91  -42.57   -2.66  CaHAsO4
CaHAsO4:H2O    -37.78  -42.57   -4.79  CaHAsO4:H2O
CaSeO3:2H2O     -9.24  -13.88   -4.63  CaSeO3:2H2O
CaSeO3:H2O      -7.04  -13.88   -6.84  CaSeO3:H2O
CaSeO4          -9.34  -12.43   -3.09  CaSeO4
CaSeO4:2H2O     -9.75  -12.43   -2.68  CaSeO4:2H2O
CaSO4:0.5H2O(beta)  -6.42   -9.96   -3.54  CaSO4:0.5H2O
CaV2O6         -16.06  -67.42  -51.36  CaV2O6
Chalcedony      -0.44   -4.20   -3.76  SiO2
Chamosite-7A   -17.62   15.13   32.76  Fe2Al2SiO5(OH)4
Chloromagnesite -33.01  -11.19   21.82  MgCl2
Chromite       -16.63   -1.47   15.16  FeCr2O4
Chrysotile       5.86   36.89   31.03  Mg3Si2O5(OH)4
Cl2(g)         -41.82  -38.83    2.99  Cl2
Claudetite    -118.98 -138.78  -19.80  As2O3
Clinochlore-14A   9.45   76.50   67.05  Mg5Al2Si3O10(OH)8
Clinochlore-7A    6.08   76.50   70.42  Mg5Al2Si3O10(OH)8
Clinoptilolite-Ca          -2.90           -10.42              -7.52
Ca1.7335Al3.45Fe.017Si14.533O36:10.922H2O
Clinoptilolite-dehy-Ca -38.56 -10.42   28.14  Ca1.7335Al3.45Fe.017Si14.533O36
Clinoptilolite-dehy-Na -32.43  -4.42   28.01  Na3.467Al3.45Fe.017Si14.533O36
Clinoptilolite-hy-Ca       -2.90           -10.42              -7.52
Ca1.7335Al3.45Fe.017Si14.533O36:11.645H2O
Clinoptilolite-hy-Na        3.22            -4.42              -7.65
Na3.467Al3.45Fe.017Si14.533O36:10.877H2O
Clinoptilolite-Na   3.22   -4.42   -7.64  Na3.467Al3.45Fe.017Si14.533O36:10.922H2O
Clinozoisite    -4.07   39.03   43.10  Ca2Al3Si3O12(OH)
Coesite         -0.98   -4.20   -3.22  SiO2
Colemanite     -25.27   -3.76   21.51  Ca2B6O11:5H2O
Cordierite_anhyd -15.63   36.44   52.07  Mg2Al4Si5O18
Cordierite_hydr -13.15   36.44   49.59  Mg2Al4Si5O18:H2O
Corundum        -4.67   13.62   18.29  Al2O3
Cr             -82.03   16.64   98.67  Cr
Cr-ettringite  -41.27   19.01   60.28  Ca6(Al(OH)6)2(CrO4)3:26H2O
Cr-monosulfoaluminate -24.74  46.62   71.36  Ca4Al2(OH)12(CrO4):9H2O
CrCl3          -59.52  -41.60   17.92  CrCl3
CrF3           -42.86  -51.50   -8.64  CrF3
CrF4           -81.10  -93.43  -12.34  CrF4
Cristobalite(alpha) -0.72   -4.20   -3.48  SiO2
Cristobalite(beta)  -1.17   -4.20   -3.03  SiO2
```

```
CrO2              -8.52  -27.66  -19.14  CrO2
CrO3             -25.84  -29.40   -3.56  CrO3
Cronstedtite-7A   -4.53   11.64   16.18  Fe2Fe2SiO5(OH)4
Daphnite-14A     -36.80   15.30   52.10  Fe5AlAlSi3O10(OH)8
Daphnite-7A      -40.18   15.30   55.48  Fe5AlAlSi3O10(OH)8
Diaspore          -0.34    6.81    7.15  AlHO2
Dicalcium_silicate -10.13 27.00   37.13  Ca2SiO4
Diopside           1.41   22.30   20.89  CaMgSi2O6
Downeyite        -22.69  -29.48   -6.79  SeO2
Enstatite         -0.39   10.90   11.29  MgSiO3
Epidote            4.52   37.29   32.77  Ca2FeAl2Si3O12OH
Epidote-ord        4.52   37.29   32.76  FeCa2Al2(OH)(SiO4)3
Epsomite          -8.50  -10.46   -1.96  MgSO4:7H2O
Eskolaite        -11.97  -21.19   -9.22  Cr2O3
Ettringite       -31.92   30.55   62.46  Ca6Al2(SO4)3(OH)12:26H2O
F2(g)           -101.14  -45.43   55.71  F2
Fayalite         -17.55    1.51   19.06  Fe2SiO4
Fe               -43.62   15.39   59.02  Fe
Fe(OH)2          -11.04    2.86   13.89  Fe(OH)2
Fe(OH)3           -0.57    5.07    5.64  Fe(OH)3
Fe2(SO4)3        -69.58  -66.53    3.05  Fe2(SO4)3
FeF2             -27.61  -30.03   -2.42  FeF2
FeF3             -25.01  -44.26  -19.26  FeF3
FeO              -10.67    2.86   13.52  FeO
Ferrite-Ca         4.24   25.73   21.50  CaFe2O4
Ferrite-Dicalcium -15.46  41.33   56.80  Ca2Fe2O5
Ferrite-Mg         4.21   25.23   21.02  MgFe2O4
Ferroselite      -87.62 -168.44  -80.82  FeSe2
Ferrosilite       -8.75   -1.34    7.41  FeSiO3
FeSO4            -25.31  -22.70    2.61  FeSO4
FeV2O4          -319.33  -38.77  280.56  FeV2O4
Fix_H+           -11.23  -11.23    0.00  H+
Fluorapatite       9.21  -15.95  -25.16  Ca5(PO4)3F
Fluorite          -7.22  -17.29  -10.07  CaF2
Forsterite        -1.82   25.99   27.81  Mg2SiO4
Foshagite        -16.00   49.80   65.80  Ca4Si3O9(OH)2:0.5H2O
Gehlenite        -15.60   40.62   56.22  Ca2Al2SiO7
Gibbsite          -0.93    6.81    7.74  Al(OH)3
Gismondine        -0.08   41.64   41.72  Ca2Al4Si4O16:9H2O
Glauberite       -10.98  -16.45   -5.47  Na2Ca(SO4)2
Goethite           4.54    5.07    0.53  FeOOH
Greenalite       -22.42    0.17   22.58  Fe3Si2O5(OH)4
Grossular         -3.95   47.82   51.78  Ca3Al2(SiO4)3
Gypsum            -5.42   -9.96   -4.53  CaSO4:2H2O
Gyrolite          -4.20   18.60   22.80  Ca2Si3O7(OH)2:1.5H2O
H2(g)            -30.46  -33.56   -3.10  H2
H2O(g)            -1.59   -0.00    1.59  H2O
Halite            -5.18   -3.61    1.56  NaCl
Hatrurite        -30.75   42.60   73.35  Ca3SiO5
HCl(g)           -19.45  -13.14    6.30  HCl
Hedenbergite      -9.47   10.06   19.53  CaFe(SiO3)2
Hematite          10.06   10.13    0.08  Fe2O3
Hercynite        -12.32   16.48   28.80  FeAl2O4
Hexahydrite       -8.73  -10.46   -1.73  MgSO4:6H2O
Hillebrandite     -9.77   27.00   36.77  Ca2SiO3(OH)2:0.17H2O
Hydroboracite    -24.63   -4.26   20.36  MgCaB6O11:6H2O
Hydrophilite     -22.43  -10.69   11.75  CaCl2
Hydroxylapatite    3.72    0.49   -3.22  Ca5(OH)(PO4)3
Ice               -0.14   -0.00    0.14  H2O
Jadeite           -0.37    7.94    8.31  NaAl(SiO3)2
Jarosite-Na      -20.93  -26.38   -5.45  NaFe3(SO4)2(OH)6
Kaolinite         -1.50    5.22    6.72  Al2Si2O5(OH)4
Karelianite      -51.57  -41.63    9.95  V2O3
Katoite          -18.52   60.42   78.94  Ca3Al2H12O12
Kieserite        -10.19  -10.46   -0.27  MgSO4:H2O
Kyanite           -6.19    9.42   15.61  Al2SiO5
Larnite          -11.42   27.00   38.42  Ca2SiO4
Laumontite        -1.09   12.42   13.51  CaAl2Si4O12:4H2O
Lawrencite       -32.49  -23.43    9.05  FeCl2
Lawsonite         -1.28   20.82   22.11  CaAl2Si2O7(OH)2:H2O
Lime             -16.97   15.60   32.57  CaO
```

```
Magnesiochromite -10.92   10.77   21.69  MgCr2O4
Magnetite         2.57   12.99   10.42  Fe3O4
Margarite        -6.48   34.44   40.93  CaAl4Si2O10(OH)2
Mayenite       -211.59  282.56  494.15  Ca12Al14O33
Melanterite     -20.30  -22.70   -2.40  FeSO4:7H2O
Merwinite       -14.91   53.50   68.41  MgCa3(SiO4)2
Mesolite          4.11   17.60   13.49  Na.676Ca.657Al1.99Si3.01O10:2.647H2O
Mg              -94.89   27.63  122.52  Mg
Mg(g)          -114.61   27.63  142.25  Mg
Mg1.25SO4(OH)0.5:0.5H2O -11.88   -6.69    5.20  Mg1.25SO4(OH)0.5:0.5H2O
Mg1.5SO4(OH)    -12.12   -2.91    9.21  Mg1.5SO4(OH)
Mg2V2O7         -21.93  -52.83  -30.90  Mg2V2O7
MgCl2:2H2O      -23.92  -11.19   12.73  MgCl2:2H2O
MgCl2:4H2O      -18.49  -11.19    7.30  MgCl2:4H2O
MgCl2:H2O       -27.26  -11.19   16.07  MgCl2:H2O
MgOHCl          -13.94    1.95   15.89  MgOHCl
MgSeO3          -16.05  -14.38    1.67  MgSeO3
MgSeO3:6H2O     -10.95  -14.38   -3.44  MgSeO3:6H2O
MgSO4           -15.29  -10.46    4.83  MgSO4
MgV2O6          -22.08  -67.93  -45.85  MgV2O6
Minnesotaite    -22.07   -8.24   13.83  Fe3Si4O10(OH)2
Mirabilite       -5.35   -6.50   -1.15  Na2SO4:10H2O
Mo              -99.94    9.33  109.27  Mo
Molysite        -47.83  -34.36   13.47  FeCl3
Monosulfoaluminate -22.11   50.46   72.57  Ca4Al2(SO4)(OH)12:13H2O
Monticellite     -3.03   26.50   29.53  CaMgSiO4
Montmor-Ca       -0.22    2.13    2.34  Ca.165Mg.33Al1.67Si4O10(OH)2
Montmor-Mg       -0.19    2.05    2.23  Mg.495Al1.67Si4O10(OH)2
Montmor-Na        0.37    2.70    2.33  Na.33Mg.33Al1.67Si4O10(OH)2
Mordenite        -1.53   -6.90   -5.36  Ca.2895Na.361Al.94Si5.06O12:3.468H2O
Mordenite-dehy  -16.66   -6.89    9.77  Ca.2895Na.361Al.94Si5.06O12
MoSe2          -127.86 -182.98  -55.12  MoSe2
Na              -51.57   15.80   67.37  Na
Na(g)           -65.06   15.80   80.86  Na
Na2Cr2O7        -29.56  -39.74  -10.18  Na2Cr2O7
Na2CrO4         -13.24  -10.34    2.90  Na2CrO4
Na2O            -48.36   19.06   67.42  Na2O
Na2Se           -76.39  -64.56   11.83  Na2Se
Na2Se2          -99.36 -160.72  -61.35  Na2Se2
Na2SiO3          -7.34   14.86   22.20  Na2SiO3
Na3H(SO4)2      -21.63  -22.52   -0.89  Na3H(SO4)2
Na4Ca(SO4)3:2H2O -17.06  -22.95   -5.89  Na4Ca(SO4)3:2H2O
Na4SiO4         -36.68   33.92   70.60  Na4SiO4
Na6Si2O7        -52.76   48.77  101.53  Na6Si2O7
NaFeO2           -5.29   14.60   19.88  NaFeO2
Natrolite         1.69   20.08   18.39  Na2Al2Si3O10:2H2O
Natrosilite      -7.41   10.66   18.07  Na2Si2O5
Nepheline        -1.61   12.14   13.75  NaAlSiO4
NO2(g)          -18.23   -9.89    8.35  NO2
Nontronite-Ca    11.27   -0.46  -11.73  Ca.165Fe2Al.33Si3.67H2O12
Nontronite-H      9.66   -3.03  -12.69  H.33Fe2Al.33Si3.67H2O12
Nontronite-Mg    11.23   -0.54  -11.77  Mg.165Fe2Al.33Si3.67H2O12
Nontronite-Na    11.79    0.11  -11.68  Na.33Fe2Al.33Si3.67H2O12
O2(g)           -22.18  -25.08   -2.89  O2
Okenite          -3.11    7.20   10.31  CaSi2O4(OH)2:H2O
Oxychloride-Mg   -8.78   17.05   25.83  Mg2Cl(OH)3:4H2O
P              -126.54    5.51  132.05  P
Paragonite       -0.02   17.36   17.38  NaAl3Si3O10(OH)2
Pargasite        -5.35   96.35  101.70  NaCa2Al3Mg4Si6O22(OH)2
Pentahydrite     -9.07  -10.46   -1.39  MgSO4:5H2O
Periclase        -6.23   15.10   21.33  MgO
Portlandite      -6.95   15.60   22.55  Ca(OH)2
Prehnite         -0.57   32.22   32.79  Ca2Al2Si3O10(OH)2
Pseudowollastonite -2.56   11.40   13.96  CaSiO3
Pyrophyllite     -3.47   -3.18    0.29  Al2Si4O10(OH)2
Quartz           -0.17   -4.20   -4.03  SiO2
Rankinite       -13.42   38.40   51.82  Ca3Si2O7
Ripidolite-14A   -8.76   52.02   60.78  Mg3Fe2Al2Si3O10(OH)8
Ripidolite-7A   -12.14   52.02   64.16  Mg3Fe2Al2Si3O10(OH)8
Saponite-Ca       8.55   34.70   26.14  Ca.165Mg3Al.33Si3.67O10(OH)2
Saponite-H        6.94   32.12   25.18  H.33Mg3Al.33Si3.67O10(OH)2
```

```
Saponite-Mg        8.51   34.61   26.10  Mg3.165Al.33Si3.67O10(OH)2
Saponite-Na        9.07   35.27   26.20  Na.33Mg3Al.33Si3.67O10(OH)2
Scolecite          0.88   16.62   15.75  CaAl2Si3O10:3H2O
Se               -30.50   -4.40   26.10  Se
Se-ettringite    -38.18   23.11   61.29  Ca6(Al(OH)6)2(SeO4)3:31.5H2O
Se-monosulfoaluminate -25.42  47.98  73.40  Ca4(Al(OH)6)2SeO4:9H2O
Se2O5            -67.00  -57.51    9.49  Se2O5
SeCl4            -96.39  -82.05   14.33  SeCl4
Sellaite          -8.35  -17.79   -9.44  MgF2
SeO3             -47.20  -28.03   19.16  SeO3
Sepiolite          4.96   35.18   30.22  Mg4Si6O15(OH)2:6H2O
Shcherbinaite    -24.68  -26.13   -1.45  V2O5
Si              -127.99   20.88  148.86  Si
Si(g)           -199.06   20.88  219.94  Si
SiF4(g)          -54.74  -69.98  -15.24  SiF4
Sillimanite       -6.82    9.42   16.24  Al2SiO5
SiO2(am)          -1.46   -4.20   -2.74  SiO2
Spinel            -8.89   28.72   37.61  Al2MgO4
Starkeyite        -9.46  -10.46   -1.00  MgSO4:4H2O
Strengite         -9.38  -20.77  -11.39  FePO4:2H2O
Tachyhydrite     -50.22  -33.07   17.14  Mg2CaCl6:12H2O
Talc               7.50   28.49   20.99  Mg3Si4O10(OH)2
Thenardite        -6.14   -6.50   -0.36  Na2SO4
Tobermorite-11A  -12.59   52.80   65.39  Ca5Si6H11O22.5
Tobermorite-14A  -10.81   52.80   63.61  Ca5Si6H21O27.5
Tobermorite-9A   -16.06   52.80   68.86  Ca5Si6H6O20
Tremolite         12.15   73.08   60.93  Ca2Mg5Si8O22(OH)2
Tridymite         -0.36   -4.20   -3.84  SiO2
V               -108.95   -2.01  106.94  V
V2O4             -31.32  -22.76    8.56  V2O4
V3O5             -66.43  -53.01   13.43  V3O5
V4O7             -83.18  -64.38   18.80  V4O7
Vivianite        -38.38  -43.11   -4.72  Fe3(PO4)2:8H2O
Wairakite         -5.50   12.42   17.92  CaAl2Si4O10(OH)4
Whitlockite       -0.55   -4.87   -4.32  Ca3(PO4)2
Wollastonite      -2.32   11.40   13.72  CaSiO3
Wustite           -9.46    2.94   12.40  Fe.947O
Xonotlite        -23.34   68.40   91.74  Ca6Si6O17(OH)2
Zoisite           -4.10   39.03   43.14  Ca2Al3(SiO4)3OH
```

```
-----------------
End of simulation.
-----------------
```

APPENDIX H: MOLAL CONCENTRATION OF ELEMENTS OBTAINED FROM THE MODEL

TABLE H-1: Molal concentration from simulation at pH 11.588

		GPC	GP1	GP2	GP3
As(5)	mol/l	1.371E-05	1.365E-05	1.360E-05	1.239E-05
	mg/l	1.027	1.023	1.019	0.928
Cr(3)	mol/l	3.863E-28	5.440E-28	3.776E-28	4.268E-28
	mg/l	2.008E-23	2.828E-23	1.963E-23	2.219E-23
Cr(5)	mol/l	5.570E-12	6.254E-12	5.566E-12	5.479E-12
	mg/l	2.896E-07	3.251E-07	2.894E-07	2.849E-07
Cr(6)	mol/l	2.164E-07	2.164E-07	2.164E-07	2.164E-07
	mg/l	0.011	0.011	0.011	0.011
Se(4)	mol/l	2.386E-13	3.096E-13	2.455E-13	2.313E-13
	mg/l	1.884E-08	2.445E-08	1.938E-08	1.826E-08
Se(6)	mol/l	5.149E-06	5.315E-06	5.366E-06	4.749E-06
	mg/l	0.407	0.420	0.424	0.375